

---

# **A Role for Improved Angular Observations in Geosynchronous Orbit Determination**

**Dr. Chris Sabol**

**September 1998**

**Final Report**

**APPROVED FOR PUBLIC RELEASE; DISTRIBUTION IS UNLIMITED.**



**AIR FORCE RESEARCH LABORATORY  
Space Vehicles Directorate  
3550 Aberdeen Ave SE  
AIR FORCE MATERIEL COMMAND  
KIRTLAND AIR FORCE BASE, NM 87117-5776**

---


Using Government drawings, specifications, or other data included in this document for any purpose other than Government procurement does not in any way obligate the U.S. Government. The fact that the Government formulated or supplied the drawings, specifications, or other data, does not license the holder or any other person or corporation; or convey any rights or permission to manufacture, use, or sell any patented invention that may relate to them.


This report has been reviewed by Public Affairs Office and is releasable to the National Technical Information Service (NTIS). At NTIS, it will be available to the general public, including foreign nationals.

If you change your address, wish to be removed from this mailing list, or your organization no longer employs the addressee, please notify AFRL/DEBI, 3550 Aberdeen Ave SE, Kirtland AFB, NM 87117-5776.

Do not return copies of this report unless contractual obligations or notice on specific document requires its return.

This report has been approved for publication.

  
CHRIS SABOL, Ph.D. for  
Project Manager

  
DAVID L. DINWIDDIE, DR-IV, DAF  
Chief, Advanced Optics and Imaging Division

  
L. BRUCE SIMPSON, SES  
Director, Directed Energy Directorate

REPORT DOCUMENTATION PAGE			Form Approved OMB No. 0704-0188		
Public reporting burden for this collection of information is estimated to average 1 hour per response, including the time for reviewing instructions, searching existing data sources, gathering and maintaining the data needed, and completing and reviewing this collection of information. Send comments regarding this burden estimate or any other aspect of this collection of information, including suggestions for reducing this burden to Department of Defense, Washington Headquarters Services, Directorate for Information Operations and Reports (0704-0188), 1215 Jefferson Davis Highway, Suite 1204, Arlington, VA 22202-4302. Respondents should be aware that notwithstanding any other provision of law, no person shall be subject to any penalty for failing to comply with a collection of information if it does not display a currently valid OMB control number. <b>PLEASE DO NOT RETURN YOUR FORM TO THE ABOVE ADDRESS.</b>					
1. REPORT DATE (DD-MM-YYYY) 30-09-1998		2. REPORT TYPE Final		3. DATES COVERED (From - To) 1993 - 1998	
4. TITLE AND SUBTITLE A Role for Improved Angular Observations in Geosynchronous Orbit Determination			5a. CONTRACT NUMBER IN-HOUSE		
			5b. GRANT NUMBER N/A		
			5c. PROGRAM ELEMENT NUMBER N/A		
6. AUTHOR(S) Dr. Chris Sabol			5d. PROJECT NUMBER 8809		
			5e. TASK NUMBER TA		
			5f. WORK UNIT NUMBER 01		
7. PERFORMING ORGANIZATION NAME(S) AND ADDRESS(ES)  Det 15 535 Lapoi Parkway Ste 200 Kihei Maui HI 96753			8. PERFORMING ORGANIZATION REPORT NUMBER		
9. SPONSORING / MONITORING AGENCY NAME(S) AND ADDRESS(ES) AFRL/DEBI (Det 15) 3550 Aberdeen Ave SE Kirtland AFB, NM 87117-5776			10. SPONSOR/MONITOR'S ACRONYM(S)		
			11. SPONSOR/MONITOR'S REPORT NUMBER(S) AFRL-VS-PS-TR-1998-1085		
12. DISTRIBUTION / AVAILABILITY STATEMENT  APPROVED FOR PUBLIC RELEASE; DISTRIBUTION IS UNLIMITED.					
13. SUPPLEMENTARY NOTES					
14. ABSTRACT The goal of this thesis showed improved angular observations aided the determination of satellite position and velocity in the geosynchronous orbit regime. Raven was a sensor developed by U. S. Air Force Research Laboratory which allowed for angular observations of satellites to be made with a standard deviation of 1 arcsecond (which maps into approximately 170 meters at geosynchronous altitude); this was an order of magnitude improvement over traditional angular observation techniques and represented state of the art accuracy of angular observations for geosynchronous orbit determination work. Studies showed these angular observations could be used in the orbit determination process both as the only tracking data source and as a supplement to other tracking data sources such as radar and radio transponder ranges. Results from the radio transponder range analysis were extended to cover Satellite Laser Ranging (SLR) and Global Positioning System (GPS) observation types as well. The studies targeted both space surveillance and owner/operator mission support aspects of orbit determination although the emphasis was on mission support satellite operations. Parameters varied in the simulation studies included the number of observing stations, density of the angular observations, and number of nights of optical tracking.					
15. SUBJECT TERMS Raven, Geosynchronous Orbit Regime, Orbit Determination, Radar, Perturbation Methods, GPS Studies, GTDS,					
16. SECURITY CLASSIFICATION OF:			17. LIMITATION OF ABSTRACT	18. NUMBER OF PAGES	19a. NAME OF RESPONSIBLE PERSON
a. REPORT UNCLASSIFIED	b. ABSTRACT UNCLASSIFIED	c. THIS PAGE UNCLASSIFIED	Unlimited	167	Chris Sabol
					19b. TELEPHONE NUMBER (include area code) 808-874-1594

**[This page intentionally left blank]**

## CONTENTS

### Chapter

1. INTRODUCTION .....	1
1.1 The Geosynchronous Orbit Regime .....	2
1.2 The Role of Orbit Determination .....	3
1.2.1 Mission Support .....	4
1.2.2 Space Surveillance .....	6
1.3 Sensors and Observation Types .....	8
1.3.1 Optical Sensors .....	9
1.3.1.1 GEODSS .....	10
1.3.1.2 MSX .....	10
1.3.1.3 Raven .....	11
1.3.2 RADAR .....	11
1.3.3 Radio Transponders .....	12
1.3.4 SLR .....	13
1.3.5 GPS .....	14
1.4 Orbital Theory .....	17
1.4.1 Perturbations .....	18
1.4.1.1 Central Nonspherical Gravity .....	18
1.4.1.1 Third Body Gravity .....	21
1.4.1.2 Solar Radiation Pressure .....	22
1.4.1.3 Other Perturbations Acting on a Geosynchronous Satellite .....	23
1.4.2 Solution Methods .....	23
1.4.2.1 Special Perturbation Methods .....	24
1.4.2.2 General Perturbation Methods .....	24
1.4.2.3 Semianalytic Methods .....	25

1.5 Methods of Orbit Determination .....	26
1.5.1 Batch Least Squares Estimation .....	27
1.5.2 Filters .....	28
1.5.3 Solve-for and Consider Parameters .....	29
1.6 Orbit Determination for Geosynchronous Satellites .....	31
1.6.1 Challenges of Geosynchronous Orbit Determination .....	31
1.6.2 Current Practices and Relevant Research .....	32
1.6.2.1 Optical Orbit Determination .....	32
1.6.2.2 Transponder Based Practices .....	33
1.6.2.3 GPS Studies .....	34
1.6.3 The Value of Improved Accuracy .....	36
1.6.4 A Role for Improved Angular Observations .....	37
1.7 Thesis Overview .....	38
2. APPROACH .....	39
2.1 Orbit Determination Scenarios .....	40
2.1.1 Mission Support Scenarios .....	40
2.1.2 Space Surveillance Scenarios .....	41
2.2 Analysis Tools .....	42
2.2.1 GIPSY/OASIS II .....	43
2.2.2 Ops GTDS .....	44
2.2.3 Draper GTDS .....	44
2.3 Force Model Assessment .....	45
2.4 Available Real Data .....	48
2.4.1 Mission Support Data .....	48
2.4.1.1 Radio Transponder Data .....	48
2.4.1.2 Raven Data .....	50

2.4.1.3 Raven Data Accuracy Assessment .....	51
2.4.2 Space Surveillance Data .....	55
2.4.2.1 Radio Transponder Data .....	56
2.4.2.2 Radar Data .....	56
2.4.2.3 Raven Data .....	57
2.5 Analysis Methodology .....	58
2.5.1 Data Simulation Approach .....	59
2.5.2 Validation of the Data Simulation Approach .....	60
 3. RESULTS ..	65
3.1 Mission Support Analysis and Results .....	66
3.1.1 Range-Only .....	66
3.1.1.1 Variable Fit Span .....	68
3.1.1.2 Observability at Lower Inclinations .....	68
3.1.1.3 A Station Bias Not Estimated .....	70
3.1.1.4 Summary .....	71
3.1.2 Extensive Range and Angles .....	72
3.1.2.1 Number of Optical Sensors .....	76
3.1.2.2 Optical Observation Density .....	77
3.1.2.3 Nights Tracking Optically .....	78
3.1.2.4 Lower Inclinations .....	79
3.1.2.5 Shorter Fit Spans .....	80
3.1.2.6 Summary .....	81
3.1.3 Limited Range and Angles .....	82
3.1.3.1 Range-Only .....	82
3.1.3.2 Range and Angles .....	84
3.1.3.3 Single Site Range and Angles .....	85

3.1.3.4	Angles-Only .....	86
3.1.3.5	Summary .....	88
3.1.4	Extension to Other Data Types .....	89
3.1.4.1	SLR .....	89
3.1.4.2	GPS .....	90
3.2	Space Surveillance Analysis and Results .....	91
3.2.1	Angles-Only .....	93
3.2.1.1	Traditional Angular Observations .....	94
3.2.1.2	Improved Angular Observations .....	97
3.2.1.3	Number of Stations .....	102
3.2.1.4	Summary .....	103
3.2.2	Range and Angles .....	104
3.2.2.1	Traditional Angular Observations .....	104
3.2.2.2	Improved Angular Observations .....	107
3.2.2.3	A Second Range Pass .....	108
3.2.2.4	Summary .....	111
3.2.3	Real Data Analysis .....	111
4.	CONCLUSIONS AND FUTURE WORK .....	117
4.1	Conclusions .....	118
4.1.1	Mission Support .....	118
4.2.2	Space Surveillance .....	120
4.2	Future Work .....	122
4.2.1	Further Simulation Studies .....	122
4.2.2	Raven Development .....	123
4.2.3	Real Data Analysis .....	124
4.2.4	GPS Studies .....	125



BIBLIOGRAPHY , 126

APPENDIX .....	136
A. GPS to GEO Observability .....	137
B. IGS GPS Precise Orbit Ephemerides .....	143
C. Software Modified and Developed .....	146
C.1 DGTDS Modifications .....	146
C.1.1 OUTTLE Card .....	146
C.1.2 Optical Data Types in Data Simulation Program .....	146
C.1.3 GPS Observation Simulation and Processing Models .....	147
C.1.4 PHLUID4 GTDS .....	147
C.2 Stand-alone Utilities .....	148
C.2.1 CONIGS .....	148
C.2.2 CORNXO .....	148
C.2.3 GEOOBS .....	148
C.2.4 GPSCAL .....	149
C.2.5 GPSGUESS .....	149
C.2.6 GPSTIME .....	149
C.2.7 GOA2GTDS .....	149
C.2.8 OSCON .....	150
C.2.9 RAVROT .....	150
C.2.10 SP32GTDS .....	150

## FIGURES

### Figure

1.1	Typical Satellite Orbit Regimes .....	3
1.2	The Shapes Produced by Tesseral Harmonics of Degree 8, Order 6, 7, and 8 .....	20
2.1	Radio Transponder Observation Distribution .....	49
2.2	Raven Observations Compared to Range Based Reference Orbit .....	52
2.3	Raven Observations Compared to GPS Reference Orbit .....	53
2.4	Short Arc Raven Observations .....	54
2.5	GOES-10 Observation Distribution .....	57
2.6	Data Simulation Validation Procedure .....	63
3.1	Best Range-Only Orbit Solution Errors .....	67
3.2	Along-Track Error as a Function of a Single Station Unestimated Bias Error .....	71
3.3	Primary Range and Angles Orbit Solution Errors .....	74
3.4	Along-Track Accuracy as a Function of Optical Station Number .....	77
3.5	Along-Track Accuracy as a Function of Optical Data Density .....	78
3.6	Along-Track Errors as a Function of Nights of Optical Tracking .....	79
3.7	Two Day Fit Orbital Errors .....	81
3.8	Three Station Range-Only Orbital Errors .....	83
3.9	Three Range Station Plus Single Optical Station Orbital Errors .....	84
3.10	Single Site Range and Angles Orbit Determination Errors .....	86
3.11	Two Station Angles-Only Orbit Determination Errors .....	87
3.12	Traditional Angles-Only Space Surveillance Cowell Orbital Errors .....	95
3.13	Traditional Angles-Only Space Surveillance DSST Orbital Errors .....	96
3.14	Traditional Angles-Only Space Surveillance SGP4 Orbital Errors .....	97
3.15	Improved Angles-Only Space Surveillance Cowell Orbital Errors .....	99
3.16	Improved Angles-Only Space Surveillance DSST Orbital Errors .....	100

3.17	Improved Angles-Only Space Surveillance SGP4 Orbital Errors .....	101
3.18	Range and Traditional Angles Space Surveillance Cowell Orbital Errors .....	105
3.19	Range and Traditional Angles Space Surveillance DSST Orbital Errors .....	106
3.20	Additional Range and Traditional Angles Space Surveillance DSST Orbital Errors .....	109
3.21	Additional Range and Improved Angles Space Surveillance DSST Orbital Errors .....	110
3.22	Case 1 Orbit Differences to GSFC GOES-10 Reference Orbit .....	113
3.23	Case 2 Orbit Differences to GSFC GOES-10 Reference Orbit .....	114
3.24	Case 3 Orbit Differences to GSFC GOES-10 Reference Orbit .....	114
3.25	Case 4 Orbit Differences to GSFC GOES-10 Reference Orbit .....	115
A.1	GPS to GEO Geometry .....	137
A.2	GPS to GEO Observability Constraint Geometry 1.....	138
A.3	GPS to GEO Observability Constraint Geometry 2.....	139
A.4	Average GPS to GEO Observability for an Atmosphere Radius of 6,700 km .....	141
A.5	Average GPS to GEO Observability for an Atmosphere Radius of 8,000 km .....	141
A.6	GPS to 0 Degree GEO Observability for an Atmosphere Radius of 6,700 km .....	142
A.7	GPS to 0 Degree GEO Observability for an Atmosphere Radius of 8,000 km .....	142

## TABLES

### Table

1.1	Orbital Elements for a Typical Geosynchronous Orbit .....	2
2.1	Radio Transponder Ground Stations .....	49
2.2	Mission Support Raven Data Summary .....	50
2.3	Space Surveillance Raven Data Summary .....	58
2.4	Mission Support Orbit Generator Models .....	61
2.5	Real Data Range Bias Differences .....	61
2.6	Real Data and Simulated Data Comparisons .....	63
2.7	Simulated Data Range Bias Differences .....	64
3.1	Real Range Data Bias Solution Standard Deviations .....	68
3.2	Bias Errors for Range-Only Inclination Cases .....	69
3.3	Orbit Errors for Range-Only Inclination Cases .....	69
3.4	Single Station Bias and Resulting Along-Track Errors .....	71
3.5	Range and Angles Range Bias Errors .....	74
3.6	Range and Range and Angles Orbit Errors .....	74
3.7	Number of Optical Stations and Orbital Errors .....	76
3.8	Along-Track Error as a Function of Optical Density .....	77
3.9	Orbit Errors for Range and Angles Inclination Cases .....	80
3.10	Limited Range-Only Orbital Errors .....	83
3.11	Three Range Station Plus Angles Orbit Errors .....	85
3.12	Single Site Range and Angles Orbit Errors .....	86
3.13	Angles-Only Orbit Errors .....	87
3.14	Space Surveillance Dynamic Models .....	93
3.15	Traditional Angles-Only Space Surveillance Orbital Errors .....	94
3.16	Improved Angles-Only Space Surveillance Orbital Errors .....	98
3.17	Dynamic Modelling and Maximum Along-Track Errors .....	98

3.18	Number of Stations and Angles-Only Space Surveillance Orbital Errors .....	102
3.19	Range and Traditional Angles Space Surveillance Orbital Errors .....	104
3.20	Range and Improved Angles Space Surveillance Orbital Errors .....	107
3.21	Additional Range and Angles Space Surveillance DSST Orbital Errors .....	108
3.22	GOES-10 Orbit Determination Data Cases .....	112
3.23	Orbit Differences from GSFC GOES-10 Reference Orbit .....	113
A.1	Average Number of GPS satellites Visible to the Geostationary Ring .....	140

## Summary

The goal of this thesis is to show that improved angular observations can aid in the determination of satellite position and velocity in the geosynchronous orbit regime. Raven is a new sensor being developed by the U. S. Air Force Research Laboratory which should allow for angular observations of satellites to be made with a standard deviation of 1 arcsecond (which maps into approximately 170 meters at geosynchronous altitude); this is an order of magnitude improvement over traditional angular observation techniques and represents state of the art accuracy of angular observations for geosynchronous orbit determination work. Simulation studies are undertaken to show that these angular observations can be used in the orbit determination process both as the only tracking data source and as a supplement to other tracking data sources such as radar and radio transponder ranges. Results from the radio transponder range analysis are extended to cover Satellite Laser Ranging (SLR) and Global Positioning System (GPS) observation types as well. The studies target both space surveillance and owner/operator mission support aspects of orbit determination although the emphasis will be on mission support satellite operations. Parameters varied in the simulation studies include the number of observing stations, the density of the angular observations, and the number of nights of optical tracking. The data simulations are calibrated based on real data results from a geosynchronous satellite to ensure the integrity of the simulations and the accuracy of the results. The studies show that including the improved angular observations with traditional high accuracy range observations produces a significant improvement in orbit determination accuracy over the range observations alone. The studies also show single site geosynchronous orbit determination is an attractive alternative when combining improved angular and high accuracy range observations.

## ACKNOWLEDGMENTS

The author would like to thank his Doctoral Committee members headed by Prof. Bob Culp. Thanks to Dr. David Spencer for his support and leadership of the Air Force Research Laboratory Astrodynamics Group's orbit determination research. Dr. Paul Cefola of Draper Laboratory has continued to serve in an advisory capacity even though his duties require him elsewhere; for that I am always grateful. Prof. George Born and Dr. Kenn Gold for their comments helpful in shaping the direction of this research. Thanks to Capt. Scott Wallace, Rich Burns and Capt. Scott Carter for providing support from Phillips. Capt. Wallace spearheaded the Raven acquisition effort. Much appreciation goes to the Raven teams in Albuquerque (Lt. Megan Bir, Lt. Tiffany Montague, Lt. Eric Beck, Capt. Nate Devilbus) and Maui (Daron Nishimoto, Paul Sydney). The author would also like to thank the people and organizations that provided us with the radio transponder data and information which allowed us to produce these studies. LtC. David Vallado (AFRL), Dr. Ron Proulx (Draper), Col. Sal Alfano (USSPACECOM), Dr. George Davis (Orbital Sciences), Steve Casali (ITT), and Craig McLaughlin (AFRL, CCAR) as well as those mentioned above have all been meaningful resources of orbit determination information and insight. David Harris (SAIC), Kira Jorgensen (CCAR), Dr. Kristine Larson (CCAR), Carey Noll (NASA/CDDIS), Tim Springer (CODE), Jim Zumberge (JPL), Capt. Mike Violet (USAF/FAFB), Dave Monet (USNO), Patrick Wallace (Rutherford Appleton Laboratory Starlink Project), Ron Roehrich (USSPACECOM), and Bob Defazio (GSFC) all contributed their knowledge to my understanding of the various data sources. Thanks to Joe Toth and the NASA/Goddard Flight Dynamics Division for their delivery and support of the Ops GTDS software and to David Chart of CCAR for his PC support. And most of all, thanks to K. Kim Luu of AFRL/Astro and CCAR for her patience and understanding.

Finally, thanks to the USAF Palace Knight Program, AFRL, CCAR, and the University of Colorado for allowing my education to continue in this manner with special thanks to Pat, Lori and Nancy.

[This page intentionally left blank]



## **Chapter 1: Introduction**

## 1.1 The Geosynchronous Orbit Regime

Satellites have many different applications and the application dictates the type of orbit the satellite is launched into. Typical orbit types are:

- geosynchronous orbits
- highly eccentric orbits
- low Earth orbits
- medium Earth orbits

These are broad classifications but many classes of satellite systems can be readily associated with each type. Figure 1.1 demonstrates the typical orbit shapes and sizes associated with each.

In the early 1960's, the first experimental satellites were launched into low Earth orbits but as technology grew, the emergence of communications satellites shifted emphasis to geosynchronous orbits.

Geosynchronous Earth Orbits (or GEO's) are orbits with approximately 24 hour (one sidereal day) periods and are usually near circular with low inclination. Thus, the satellite "rotates" with the Earth. If the satellite is at zero eccentricity and inclination, it appears to be fixed above a point on the equator; this is a geostationary orbit. Geosynchronous orbits are still most widely used in communications, mostly for broadcast purposes, and weather satellites. Early Warning and Nuclear Detection Systems are also mission types suited for satellites in geosynchronous orbits [1]. The main advantages of GEO's include the large coverage area (almost 42% of the Earth [2]) and simple tracking requirements (Earth station antennas may be directional and fixed) [3].

Table 1.1 gives a set of orbital elements for a typical geosynchronous orbit.

Table 1.1: Orbital Elements for a Typical Geosynchronous Orbit

Semimajor Axis	42164 km
Eccentricity	0.0
Inclination	0° - 15°

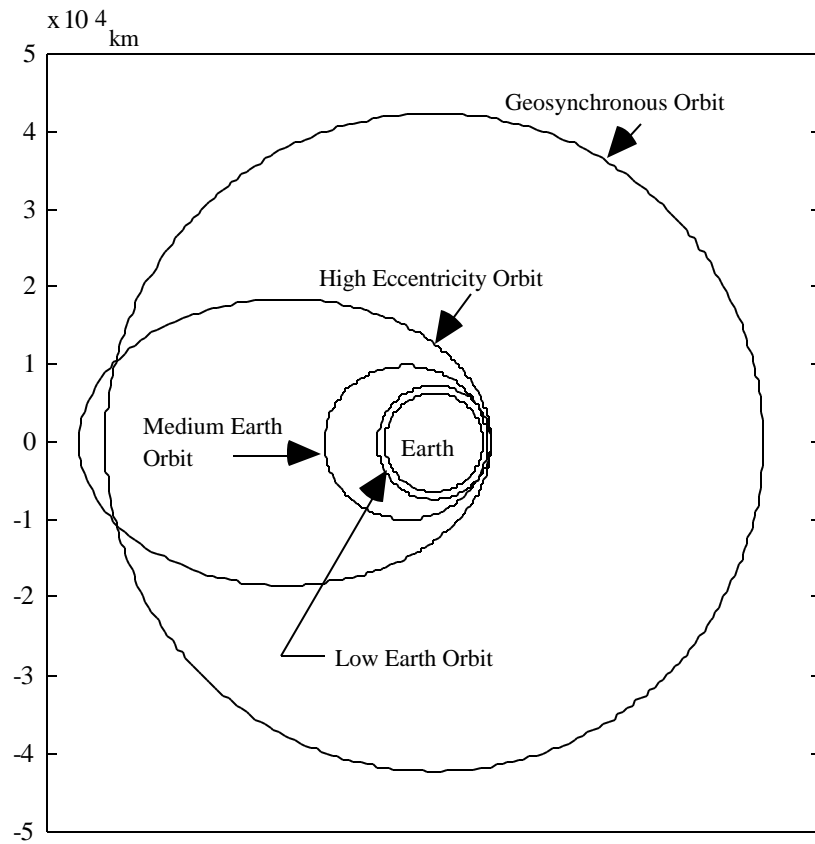


Figure 1.1: Typical Satellite Orbit Regimes

In 1995, there were 545 tracked space objects in the geosynchronous orbit regime with a near linear growth trend of 30 objects per year [4,5]. Most of these resident objects are, however, nonoperational (either dead satellites, rocket bodies, or other forms of space debris).

## 1.2 The Role of Orbit Determination

Orbit determination can be described as a process used to estimate a satellite's state (position, velocity, and any other parameters governing the motion of the satellite) as a function of time based on observations of that satellite. This process requires models to describe the motion of the satellite as a function of time and also to relate the observations to this trajectory. Given perfect models, one could

assume the state of the satellite was known at some point, propagate that solution to any time in the future or past, and always have the proper solution. Or, given perfect observations, one could just observe the satellite at the time of interest and know what the state is exactly. Models of orbital motion are not perfect, however, and the observations always contain some error; thus, the orbit determination process is nontrivial.

Orbit determination is generally performed on satellites for one of two reasons:

- mission support
- space surveillance

The goal for each is different. The particular role of the orbit determination dictates how the process is structured from the models to the observations. In this section, the role of orbit determination and how it influences the orbit determination process will be discussed.

### **1.2.1 Mission Support**

Mission support refers to satellite operations (including orbit determination) performed by the owner/operators of a satellite or group of satellites in order to meet and maintain mission requirements. References 6 and 68 describe how the orbit determination process fits into the overall flight dynamics system for the RADARSAT and Canadian Telesat satellites, respectively. Since the owner/operators have specific mission requirements, they can tailor their orbit determination approach to meet their needs. The owner/operators can choose:

- the extent of the dynamic modeling
- the type and number of observations
- the amount of time devoted to processing and analysis

Orbit determination accuracy goals vary with mission requirements, but the common factor in mission support is that the systems used are design for individual satellites.

If high precision orbit determination is required, the dynamic models can include specific details about the design of the spacecraft. For instance, mission support orbit determination practices for the TOPEX and GPS spacecraft include detailed solar radiation and thermal models [7,8]. These models include details regarding the specific shape, size, material properties, and attitude of the spacecraft. A study for the precise orbit determination of the EOS Altimeter Satellite (EOS ALT/GLAS) experimented with "tuning" the gravity field to improve their orbit determination accuracy [9]. These are examples of tailored dynamic models used to meet high precision accuracy requirements (error on the order of centimeters).

Owner/operators also have the ability to communicate with their spacecraft. They usually know when maneuvers and momentum dumps occur and can utilize that knowledge in their orbit determination. They can use forms of cooperative tracking where communications with the satellite helps provide observations. GPS and radio transponder data are examples of cooperative tracking (observation types will be discussed in a later section).

Since the owner/operators are only concerned with their particular mission, mission support orbit determination also allows for dedicated or heavy tracking. This means that an adequate number of observations are available for use in the orbit determination process. The tracking sensors only have to track specific satellites, and communications bandwidth is usually sufficient to produce dense observation passes every time the satellite is visible to the Earth based sensor or ground link. Even if the tracking sensors are not fully dedicated to a specific satellite, the number of observations available for orbit determination is usually not a limiting factor.

One of the more meaningful aspects of orbit determination in a mission support role is that the owner/operators often have the luxury of analysis time. In addition to dedicated tracking sensors, dedicated computers are also usually available for orbit determination and mission support. If it takes a few hours to process 40,000 observations using a high precision dynamic model to produce an orbit accurate enough to meet mission requirements, then a few hours of computer time is made available.

Analysis time includes not only the dedicated computer time needed to accurately process large numbers of observations with high fidelity dynamic models, but time to predict, review, and assess the orbit determination procedures and products as well. Reference 10 and 11 discusses how satellites can incorporate continuous GPS tracking with a high precision orbit determination utility to meet their orbit determination accuracy requirements. Reference 12 discusses how the orbit determination operational procedure for the Ocean Topography Experiment (TOPEX) was pared down to meet specific turn around time requirements. In each case, a great deal of time has been dedicated to studying the orbit determination procedure and techniques. This is how most of the advancements in orbit determination techniques are made.

### **1.2.2 Space Surveillance**

Unlike mission support orbit determination operations, the goal of space surveillance is simple: keep track of every detectable Earth orbiting object with accuracy sufficient to continue the time history of each object. In other words, the goal of space surveillance is to keep track of everything and never lose anything orbiting the Earth. To do so, a space surveillance system must do the following for every detectable Earth orbiting object:

- gather observations
- perform orbit determination
- predict the orbit with sufficient accuracy to gather further observations

The above is a simplification of space surveillance and operational space surveillance systems often face stricter requirements involving collision avoidance, maneuver detection, reentry prediction, etc. [78]. In March 1998, there were 8,644 objects tracked and maintained by the US Space Command [81]. Thus, observations must be gathered for all 8,644 objects, orbit determination must be performed for each object, and a level of accuracy must be maintained such that the objects are easily identified

during the next tracking interval. To serve this role, a space surveillance system faces certain constraints:

- limitations on the type and amount of observations
- the dynamic modeling is simplified and not mission specific
- the analysis time must be focused

The unifying factor for the constraints placed on a space surveillance system is that time and resources are severely limited; all aspects of the orbit determination must be performed quickly and efficiently in order to meet the requirements for each of the thousands of tracked objects. The trade-off for this speed and efficiency is reduced accuracy and analysis time that might be available in a mission support role.

Since all detectable objects must be tracked, space surveillance systems cannot rely on cooperative tracking. Tracking sensors must be able to gather observations of nonoperational satellites, space debris, and other forms of noncooperative spacecraft; therefore, GPS and radio transponder systems are not applicable in space surveillance. Radar and optical observations are better suited for the space surveillance role since nothing of the satellite is required for these tracking systems. Observation types will be discussed in further detail in a later section.

In addition to the limited types of observations, the amount of available observations for the orbit determination process also faces constraints. Tracking stations (such as radar) are expensive to build, operate, and maintain and space surveillance systems face budget issues just as everything else. Therefore, there are limitations on the number of tracking stations available to gather observations and the amount of tracking time devoted to each object.

There are communications and processing issues to consider. If each sensor gathered the maximum number of observations possible for each object and then transmitted them to a main processing station, that could result in hundreds of thousands of observations being sent to the processing center on a daily basis. Assuming the communications architecture could support such

activity, the orbit determination system would require additional time to process all of the observations. Using a limited amount of observations to balance speed and accuracy is a factor in meeting requirements for a space surveillance system.

In order to shorten processing time for each satellite, the dynamic models used in space surveillance orbit determination are often simplified. Typically an analytical (or general perturbation) approach is taken in modeling the satellite motion. Perturbations and solution techniques will be discussed in greater detail in a later section. In space surveillance, there is no tailoring of the dynamics or detailed models to fit the specifications of the individual satellites. Dynamic models that are not mission specific not only require less computationally, but are required since details of each individual satellite or orbiting object are usually unknown. Again, this is a trade-off between efficiency and accuracy.

Although much analysis is done over space surveillance operations as a whole, analysis of the orbit determination of individual satellites is often unscrutinized. Only if a problem occurs or special circumstances (or requirements) dictate it, do analysts take the time to study individual satellites. Typically, all satellites or satellites in the various orbit regimes are treated the same way and analysis is restricted to general studies. References 14, 15, and 16 are examples of analysis performed on generic orbits representing the various orbit regimes. In no case should studies aimed at space surveillance improvements look to improve the orbit determination strategy for a particular satellite.

### **1.3 Sensors and Observation Types**

There are many ways to track a satellite. Like the various orbit regimes, the variety of sensor types can be categorized into broad classes:

- Optical Sensors
- Radar
- Radio Transponders



- Satellite Laser Ranging
- Global Positioning System

Each class of tracking system has its own advantages and disadvantages and is best suited for either a mission support or space surveillance role. Some of the characteristics and examples of the sensor types are discussed below.

### **1.3.1 Optical Sensors**

The basis for optical satellite tracking systems is as follows. First, a digital picture of the satellite is taken by the sensor using a CCD (Charged Coupled Device) camera. Then, computers analyze the digital image and compare the location of the satellite image to the star background. Using knowledge of the locations of the stars through a star catalog, topocentric angular observations can be produced. These angular observations usually take the form of right ascension and declination.

Optical sensors are primarily used in a space surveillance role for geosynchronous and other high altitude tracking since most radars do not have enough power or sensitivity to pick up signal returns from deep space objects. The primary advantage of using an optical system is the ability to track distant objects (provided the object is illuminated sufficiently to register in the CCD camera) although it is possible to track low Earth orbiters as well. A major disadvantage inherent in Earth based optical tracking systems is that clear skies and nice weather are required for operation, and, of course, optical tracking systems using visible wave lengths can only be used at night..

Examples of optical tracking systems include:

- GEODSS
- MSX
- Raven

Even though all three of these systems are classified as optical systems, they are significantly different in implementation and results. Keep in mind that these are just three examples and many other optical tracking systems exist and are used operationally throughout the world.

#### **1.3.1.1 GEODSS**

GEODSS stands for Ground-based Electro-Optical Deep Space Surveillance and consists of three ground stations at Socorro, New Mexico, Maui, Hawaii, and Diego Garcia, British Indian Ocean Territories [17]. The system was developed by MIT's Lincoln Laboratory as the successor to the Baker-Nunn camera for space surveillance use and is used operationally by the US Space Command to gather observations on deep space objects [17].

Accuracy assessments on GEODSS observations reveals noise standard deviations between 10 and 12 arcseconds [13]. Ten arcseconds maps into approximately 1.7 kilometers at geosynchronous altitude.

#### **1.3.1.2 MSX**

MSX stands for Midcourse Space eXperiment and is a test bed for many space based applications. Included in the package is a Space-Based Visible (SBV) sensor for use in space surveillance [18]. MSX was launched in March, 1996 into a circular 880 km altitude orbit. The space surveillance studies are being led by MIT's Lincoln Lab.

The utility of a space-based sensor is the ability to observe the entire geosynchronous belt with only one sensor. Studies have shown that this is possible within 50 hours of continuous sensor observation [18]. Additionally, space-based sensors do not face the weather limitations of Earth-based optical sensors. The drawbacks of a space-based sensor are the price, mission duration, and inaccessibility of the sensor. The SBV accuracy assessments reveal four arcseconds of noise (one standard deviation) in the angular observations of the geosynchronous regime [79]. This maps into approximately 670 m worth of error.

### **1.3.1.3 Raven**

Raven is a new, low cost, portable, optical sensor being developed by the Air Force Research Lab Directed Energy Directorate in Maui. What separates Raven from more traditional optical sensors such as GEODSS is the intense image processing and improved star catalogs used in data reduction. This results in an order of magnitude improvement in accuracy over the GEODSS sites. Raven prototypes exist at Maui and the AFRL Astrodynamics Group in Albuquerque, New Mexico.

The advantages of a sensor like Raven is the low cost (Raven cost approximately \$100,000 to deliver), the portability, and significantly improved accuracy. Drawbacks of the Raven system include the amount of processing involved in producing the astrometric data. Because of the low cost but high accuracy pay-off, the Raven is suited for both space surveillance and possible mission support roles.

The theoretical accuracy of the Raven system is 0.333 arcseconds of noise (one standard deviation) in the angular observations; however, testing of the prototype has shown the noise levels could be closer to one arcsecond [19]. Hopefully, the reduction techniques will be refined such that the Raven system will fulfill its promise of accuracy. One arcsecond at geosynchronous altitude maps into approximately 170 meters of error; 0.333 arcseconds at geosynchronous altitude maps into approximately 57 meters of error.

### **1.3.2 Radar**

RADAR stands for RAdio Detection And Ranging and works in the following manner. First a pulse of radio signal is emitted by the sensor at a given time. This signal travels toward the satellite, is reflected off of the satellite, and returns back to the radar station at a final time. Range is deduced based on the round-trip travel time divided by twice the speed of light. The speed of light is the signal propagation speed and a factor of two is included to reduce the round trip distance to the one way range. Angular observations, usually azimuth and elevation, and range-rate can also be deduced from radar signals.

Typically range is the only observation used for moderate and high accuracy orbit determination. Range-rate is not always computed and the angular observations are generally too

noisy (on the order of 0.02 degrees) to be valuable. The noise level for radar ranges varies not only from sensor to sensor but as a function of time for each sensor. The order of magnitude figure used to describe the noise levels in radar systems is often 50 meters. Reference 13 provides some bias and noise characteristics for a variety of radar (and other) space surveillance sensors.

Radar sensors are best suited for space surveillance. They are all-weather systems and can provide observations of noncooperative objects; however, radars are expensive to build, operate, and maintain. There are also few radars capable of ranging geosynchronous satellites. The Millstone Hill radar belonging to MIT/Lincoln Lab is an example of one of the best deep space radars [20].

A prime of example of a (mostly) radar tracking system is the Space Surveillance Network (SSN) used by the US Space Command in its space surveillance effort. The SSN was originally built for ballistic missile warning, but its mission has expanded to include space surveillance [13]. Reference 13 also provides station names, locations, and characteristics of some SSN radars.

### **1.3.3 Radio Transponders**

There are two basic types of radio transponder systems:

- one-way
- two-way

One-way radio transponder systems involve a radio beacon on the ground or on the satellite, and a receiver on the satellite or on the ground. The radio beacon sends out a time coded signal which is received by the receiver at a later time. The time of travel is then computed and reduced to one way range by dividing by the speed of light (the speed of signal propagation). One-way range systems require the use of precision clocks on board the spacecraft to ensure accurate measurements.

Two-way radio transponders are a lot like radar systems. First, a signal is generated by a radio beacon (usually ground-based). The signal is received by the satellite (or ground-based receiver if the original beacon is satellite based) and then re-transmitted back to the ground station. At the ground

station, the time of flight is converted into range. A major difference between two-way radio transponder and radar systems is the transponder delay inherent in the signal. A transponder delay is the amount of time it takes for the satellite to re-transmit the signal after receiving it. This effect can be accounted for either in the reduction of the range data or in the orbit determination process.

Range-rate can also be deduced from radio transponder systems.

The advantages of radio transponder tracking systems is that they are cheaper than radar, are all-weather, and can implement dual frequency signals to reduce atmospheric effects. Of course, radio transponder systems cannot be used in a space surveillance role since action is required from the tracked satellites. Radio transponders are, however, popular choices for mission support systems-particularly for operations involving multiple satellites.

Radio transponder systems are also fairly accurate. The noise level inherent in the transponder ranges is generally on the order of 10 meters. A drawback of radio transponder systems, however, is that significant sensor range biases are often present, and the sensors can be difficult to calibrate due to bias drifts and lack of realistic reference targets for calibration.

Examples of radio transponder systems include TDRSS, DORIS, TRANET, the AFSCN, and BRTS. BRTS stands for the Bilateral Ranging Transponder System and is the system used by NASA to track TDRSS [21]. TDRSS can also employ four-way tracking schemes where a signal travels from a ground station to TDRSS, to a satellite, back to TDRSS, and then back to a ground station [38].

### **1.3.4 SLR**

SLR stands for Satellite Laser Ranging and works fundamentally like radar systems. First a pulsed signal is emitted from a laser at the station at a given time. This signal travels toward the satellite, is reflected off of the satellite, and returns back to the SLR station at a final time. Range is deduced based on the round-trip travel time divided by twice the speed of light. The speed of light is the signal propagation speed and a factor of two is included to reduce the round trip distance to the one way range. Usually, the return signal of several pulses is combined into one data or "normal" point [22].

Range is the only observation produced with SLR. If properly handled, the noise level for SLR observations is on the order of a few centimeters [23]. Thus, SLR observations are very useful for high accuracy orbit determination. Reference 24 is an example of SLR use in high accuracy orbit determination operations.

SLR sensors are best suited for mission support roles since retro-reflectors are required on the satellites to reflect the laser signal back to the station. However, SLR systems are very expensive to build, operate, and maintain and are thus not attractive to private users. Instead, SLR systems are used to support scientific missions where precise orbit determination is required. The NASA supported SLR Network is a prime example. The SLR Network consists of over 40 stations (six of which are managed by NASA) around the world which routinely track 17 satellites for scientific purposes [25].

Aside from the high cost, another major draw-back of SLR systems is that, like optical systems, nice weather is required for operation. And as previously mentioned, only satellites with retro-reflectors are tracked by the SLR network. The high accuracy pay-off, however, has been sufficient to keep SLR systems in use. References 65-67 provide additional information on the data holding locations, data formats, and station locations of SLR systems.

### **1.3.5 GPS**

The Global Positioning System (GPS) is a joint US Navy and Air Force effort to provide 24 hour all-weather global navigation, timing and positioning services. The system is based on a constellation of 24 satellites plus on-orbit spares in semisynchronous (approximately 12 hour period) orbits broadcasting signals towards the Earth. Aside from meeting its navigation, timing, and positioning requirements, GPS has revolutionized the orbit determination field as well as a number of different applications. A brief overview of the GPS system and how it applies to orbit determination is provided here; however, Reference 26 provides far greater details of the overall system and is the source of information used in this section.

The GPS constellation consists of six orbital planes with four satellites occupying each plane. The planes are all inclined 55 degrees to the equator and have orbits that are near circular with an approximate semimajor axis of 26,560 km.

Each satellite broadcast two signals toward the Earth; these are carried on the L1 and L2 frequencies. The signals carry information in two ways:

- C/A (Course Acquisition) code
- P (Precision) or encrypted Y code

The C/A code is a single frequency (L1) public domain code available for all users while the P code is carried on both frequencies and is encrypted to the Y code for military use. This encryption is known as AS or anti-spoofing since the signal cannot be jammed without knowledge of the Y code. It should be noted that efforts are underway to develop a frequency carrier for civilian use [27].

Dual frequency allows for the linear combination of the signals to nullify atmospheric effects on the signal. This is a major issue for geosynchronous based users since the signals will encounter significant atmospheric affects as they cross the limb of the Earth (the visibility of the GPS constellation to a geosynchronous satellite is discussed in Appendix A).

The observable aspects of GPS are very similar to radio transponder systems; using the time of flight between signal transmission and receipt, a range is calculated. The primary GPS observable is called the pseudorange. The pseudorange is the range calculated on the time of flight of the signal from the GPS satellite to the receiver. This includes clock errors (differences between the GPS satellite and receiver clocks) as well as Selective Availability (SA) effects. SA is another military counter-measure to degrade the inherent accuracy available in GPS by altering the satellite clocks and ephemeris data. SA typically maps up to 90 meters worth of error into the pseudorange.

Another GPS observable available for use is the signal carrier phase. The carrier phase is the difference between the received phase and the receiver internal oscillator. This observable is difficult to

track due to "cycle slips" (where the receiver loses count of the number of received cycles) but very accurate if handled properly.

The GPS signals also include broadcast ephemerides of the GPS satellites which are usually good to 10 meters or better. The locations of the GPS satellites are required to make use of the pseudorange and carrier phase data. If the broadcast ephemerides are not sufficiently accurate, the International GPS Service (IGS) produces precise (20 cm level within two weeks of date) GPS ephemerides available for public use.

To get around the use of SA and AS, the scientific community has developed ways to difference out the atmospheric and degradation effects. This is known as Differential GPS (DGPS). DGPS observables are a product of differencing signals from a GPS satellite to known ground station locations to cancel out the signal errors associated with that satellite. Signals from two satellites to a single receiver can also be differenced to cancel out the receiver errors. Double differenced observations can eliminate both satellite and receiver clock errors. This differencing of signals can reduce the amount of error in the GPS observables from the tens of meters to the centimeter level.

Even without using differential GPS, the orbit determination process can smooth out or even estimate a lot of the observation errors. Since GPS receivers are required on board the tracked satellites, GPS is not suited for space surveillance. GPS is, however, one of the best methods for mission support tracking. GPS is relatively inexpensive, the observations are continuous, and the observing geometry from the GPS constellation to most satellite orbits is continuous.

References 9-12 and 29-30 are examples of high precision orbit determination applications using GPS. GPS is also well suited for medium and low accuracy orbit determination applications as well. Reference 31 is an example of medium accuracy orbit determination applications using GPS and Reference 32 is an example of a low accuracy orbit determination application using GPS.



## 1.4 Orbital Theory

The basis for most analytical studies of satellites, whether it be a Moon orbiting around a planet, a planet orbiting around the Sun, or an artificial satellite in orbit about the Earth, is the two-body problem. The two-body problem addresses the relative dynamics of two point masses attracted to each other by gravity. The gravitation potential is composed of the inverse square law observed by Kepler and proven by Newton for a point mass and no other forces are considered. But the Earth is not a point mass; it is not perfectly spherical and of uniform density. Nor is Earth's central gravity the only force acting upon a satellite in an Earth orbit.

The nonspherical gravitational effects of the Earth are broken up into two classes: zonal and tesseral harmonics. Zonal harmonics are purely latitude dependent while the tesseral terms are a function of both longitude and latitude. Other forces include lunar and solar gravity, solar radiation pressure, atmospheric drag, Earth radiation pressure, tidal effects, thermal effects, thrust, momentum dumps, outgassing, etc.

These factors are labeled perturbing forces or perturbations, because while they are often nonnegligible, they are much smaller than the point mass central body gravitational attraction of the two body problem. Because of the nature of the perturbing forces, most changes are small and can occur within the period of an orbit or over many days and many orbits.

Each conservative perturbation (geopotential and third body gravitational effects) is characterized by a disturbing function, or expression that mathematically describes how the perturbation alters the satellite orbit from the two-body problem. From the disturbing function, analytic expressions for the rates of change of the orbital elements can be derived using Lagrange's Variation of Parameters equations. Nonconservative perturbations (drag, solar-radiation pressure, thermal and thrusting) are characterized by disturbing accelerations, and their effects on the orbital elements can be derived using Gauss' form of the variational equations.

The variational equations describe how the satellite orbital elements change as a function of time. These take the form of nonlinear differential equations. These equations must be integrated to give the satellite state as a function of time; thus, the satellite state can be determined at a different time

given a set of initial conditions. The way these equations are set up and integrated defines the satellite theory or solution method.

In this section, the various perturbations acting on the geosynchronous orbit regime will be described. In addition, a brief overview of the classes of satellite theories will be given with special attention to how the choice of satellite theory affects the orbit determination process.

### 1.4.1 Perturbations

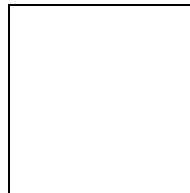
The main perturbing forces acting on a satellite in the geosynchronous regime are:

- central nonspherical gravity
- third body (Lunar-Solar) gravity
- solar radiation pressure
- other

"Other" includes small forces due to thermal venting, Earth tidal and radiation effects, attitude control momentum dumps, and thruster outgassing. Each major perturbation will be described in brief detail below.

#### 1.4.1.1 Central Nonspherical Gravity

The disturbing function,  $R$ , for the nonspherical central gravity perturbation can be shown to be [33]:



(1)

Here,  $R_E$  is the mean radius of the Earth,  $r$  is the distance to the satellite from the center of the Earth,  $\mu$  is the gravitational parameter ( $Gm$ ),  $\phi$  is the satellite latitude, and  $\lambda$  is the satellite longitude. The spherical harmonic coefficients are given by  $C$  and  $S$ . These coefficients are determined empirically and are defined by the particular gravity field (JGM2, GEM10B, WGS72, etc.) in use.

The spherical harmonic terms describe the variation of the shape of the Earth. They are identified by their degree,  $n$ , and order,  $m$ , and can be categorized into three classes:

- zonal harmonics ( $m=0$ )
- tesseral harmonics ( )
- sectorial harmonics ( $n=m$ )

The degree governs how a spherical harmonic varies with latitude, the order is associated with the variation in longitude. It is helpful to think of the order as the number of bumps encountered when traveling around the world on a line of constant latitude. And the difference between the degree and the order ( $n-m$ ) is the number of bumps encountered when traveling from one pole to the other on a line of constant longitude [34]. Figure 1.2 demonstrates this property for some eighth order tesseral harmonics.

The zonal harmonics have the most dominant effect of the spherical harmonics and are characterized by order zero ( $m=0$ ). Substituting  $m=0$  into equation (1) shows the zonal harmonics are independent of longitude. All zonal harmonics contribute long and short periodic effects to the orbital elements and the even zonal harmonics also contribute secular effects to the orbit orientation (right ascension of the ascending node, argument of perigee, and mean anomaly). The magnitude of the zonal harmonic perturbations decreases with altitude but increase with eccentricity (due to the lower perigee altitude).

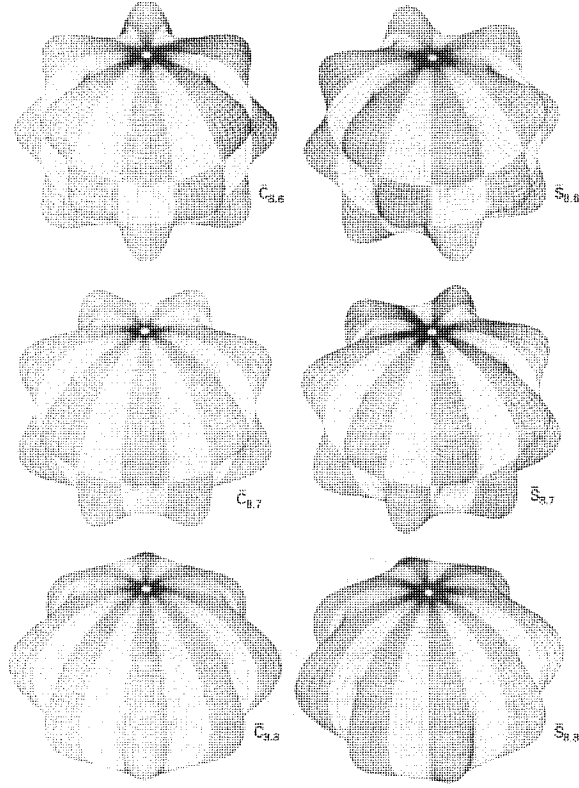


Figure 1.2: The Shapes Produced by Tesseral Harmonics of Degree 8, Order 6, 7, and 8

[Figure from Reference 34]

The tesseral harmonics are characterized by nonzero degree and order ( ).

Sectorial harmonics have equal degree and order ( $n=m$ ) and can be considered a subset of the tesseral harmonics [33]. Tesseral harmonics are the longitude and latitude dependent contributions to the central body gravity perturbations. For most satellites, the main contribution of the tesseral harmonics are short periodic effects known as M-dailies and tesseral linear combinations. M-dailies are tesseral short periodics which repeat  $m$  times per day. At a given latitude, the tesseral  $m$ -dailies disturb a satellite's motion due to gravitational changes caused by the rotation of the Earth's irregular longitudinal mass distribution [33]. Tesseral linear combination short periodics are due to the

combination of frequencies caused by the mean motion of the satellite, the rotation and precession of the orbital plane, and the rotation of the Earth [13, 33].

In addition to the short periodic effects caused by the tesseral harmonics, long period effects can also occur due to tesseral resonance. Tesseral resonance occurs when the satellite's orbital period is commensurate with the rotation of the Earth (i. e. a repeat ground track) and the satellite encounters the same tesseral gravitation forces again and again. Over time, these effects build up to produce very long period oscillations in the orbital elements.

For geosynchronous satellites, the altitude is high enough that only the nonspherical gravitational effects through degree and order four are noticeable. Since geosynchronous satellites rotate with the Earth, however, they do experience a form of deep tesseral resonance. This resonance is responsible for the existence of the longitudinal stable points in the geosynchronous ring and requires 'east-west' station-keeping maneuvers for geosynchronous satellites wishing to remain at a given longitude.

#### 1.4.1.2 Third Body Gravity

The attractive force of gravity between two bodies is given as [36]:

$$F = G \frac{m_1 m_2}{r^2}$$

(2)

where  $G$  is the universal gravitation constant,  $m_1$  and  $m_2$  are the masses of the bodies, and  $r$  is the distance between the bodies. Looking at this equation, it can be seen that as the masses of the attracting bodies increase, the gravitational force increases. Although the Sun and Moon are a considerable distance away (when compared to the radial position of an artificial Earth satellite), their masses are large enough to produce a third body gravitational attraction. Other bodies in the solar system also produce gravitational accelerations on Earth satellites, but only the Sun and the Moon have noticeable effects for most cases (including orbit determination for geosynchronous orbits).

The effects of the perturbations increase with satellite altitude. Secular effects from solar/lunar perturbations can be found in the orbit orientation (right ascension of the ascending node, argument of perigee, and mean anomaly). There are long period effects in the eccentricity, right ascension of the ascending node, argument of perigee, and inclination, and there are short period effects in all of the orbital elements. However, the long period effects are the most interesting; the third-body gravitational effects tend to cause large (15 degree) oscillations in the orbit inclination over a period of approximately 54 years [35].

#### **1.4.1.3 Solar Radiation Pressure**

Solar radiation pressure is the perturbation caused by charged particles emitted from the Sun colliding with a spacecraft. These particles are either reflected specularly, reflected diffusely, or absorbed by the satellite. How these particles affect the satellite depend on the orientation of the satellite with respect to the Sun and on the material properties of the satellite components. In cases where great accuracy is required, attempts are made to model these characteristics; Reference 7 is an example. In other cases, a simple macro-model is used. A macro-model assumes the spacecraft is made up of uniform material but does account for the general shape of the satellite and major component orientation toward the Sun. In the simplest of models, a spherical or "cannon ball" satellite model is used. With a spherical model, the acceleration due to the solar radiation pressure is assumed to be along the Sun-spacecraft direction as all charged particles are reflected off of the sphere.

In most orbit determination cases, a spherical satellite model is sufficient. Even if complex modeling techniques are used, many parameters have to be estimated to account for the unknowns in the model. With a spherical or macro-model, additional parameters can be estimated to account for the solar radiation pressure mismodeling as well.

Solar radiation pressure effects increase with altitude and also depend on the amount of time the satellite is eclipsed by the Earth's shadow. For geosynchronous satellites, the effects are quite large due to the altitude but the shadowing effects are minimal since geosynchronous satellites only have

brief eclipse periods during certain times of the year. The periodic effects caused by solar radiation pressure also depend on the satellites effective area to mass ratio.

#### **1.4.1.4 Other Perturbations Acting on a Geosynchronous Satellite**

Other perturbations acting on geosynchronous satellites include:

- thermal venting
- Earth tidal and radiation effects
- attitude control momentum dumps
- thruster outgassing

These effects are relatively small in the orbit determination process but should be accounted for if high accuracy is required. Generic models exist for Earth tidal and radiation pressure effects but are not generally employed with geosynchronous satellites since their effects are small. For thermal venting, momentum dumps, and outgassing, generic models do not exist and individual models usually include many unknowns which have to be estimated. Instead of including models for these "other" perturbations and estimating their values, it may be more convenient to estimate generic empirical accelerations to account for the unmodeled effects.

The Y-bias of GPS satellites is an example of this type of perturbation. The Y-bias is an empirical acceleration observed in the orbit determination of GPS spacecraft. This acceleration has been attributed to the thermal venting of the GPS satellites out of a particular side of the satellites [8]. It is likely that geosynchronous satellites have similar perturbations due to their long sun-lit periods.

#### **1.4.2 Solution Methods**

A spacecraft's trajectory is propagated by integrating the orbital equations of motion. There are several ways of doing this. The general approach is to reformulate the equations of motion in terms of a new set of orbital elements, solve the transformed set of equations for the orbital elements at a desired time, and then transform the elements back into the desired element set [38].

There are three general ways to approach this problem:



- special perturbation methods
- general perturbation methods
- semianalytic methods

Each method has its own advantages and disadvantages and each method has found a role in orbit determination. References 14 and 15 compare some of the more popular solution methods in terms of accuracy and computation time for orbit determination.

#### **1.4.2.1 Special Perturbation Methods**

The special perturbation method integrates the orbital equations of motion numerically. Doing so allows for the perturbing accelerations on the satellite to be modeled as accurately as possible, assuming a rigorous treatment of coordinate transformations, and results in a very high precision trajectory generator; the Cowell method is a prime example. The Cowell method numerically integrates the equations of motion in terms of the accelerating vector in Cartesian coordinates [38]. While high in accuracy, the special perturbation approach is very costly in terms of computation time. The step sizes used in the numerical integration must be sufficiently small to capture the high frequency periodic effects. Thus, the number of operations and computation time is directly proportional to the length of integration [39]. This is not a limitation in mission support but it is the reason why special perturbation methods have not been generally used in space surveillance (although some cases do require the use of special perturbation methods).

#### **1.4.2.2 General Perturbation Methods**

In the general perturbation approach, the equations of motion are reformulated in such a way, that they can be integrated analytically. This method is computationally efficient but usually only marginally accurate since reformulating the equations such that an analytic solution is possible requires some approximations [38]. Most of the general perturbation approaches are based on Brouwer or Kozai theory.

Since general perturbation theories are analytical, the computation time is nearly independent of the length of integration [39]. This computational efficiency made general perturbation theories natural choices for space surveillance orbit determination roles. Despite advances in computing power, general perturbation theories are still in wide use today for many low accuracy orbit determination and prediction applications.

Reference 39 gives an overview of the Naval Space Command's PPT2 and PPT3 general perturbation theories. It also discusses some aspects of the Air Force Space Command's SGP4 general perturbation theory. Reference 80 provides more information on the Air Force's general perturbation theories.

#### **1.4.2.3 Semianalytic Methods**

Semianalytic methods combine the positive attributes of both the general and special perturbation approaches. In the semianalytic approach, the short periodic contributions to the equations of motion are removed which results in a set of mean element equations of motion [18]. These mean element equations are composed of only secular and long periodic terms and can be efficiently integrated numerically by using large step sizes. With some semianalytic satellite theories, the short periodic terms can be integrated analytically and added to the mean elements at the desired output time. The final result is an orbit propagator that is both accurate and efficient.

Examples of semianalytic approaches include the SemiAnalytic Liu Theory (SALT), the Draper Semianalytic Satellite Theory (DSST), and a Russian semianalytic satellite theory [40, 41, 42].

The Draper Semianalytic Satellite Theory is generally regarded to be the world-class of the semianalytic approaches. The DSST formulation incorporates recursive computations of the geopotential and lunar/solar point mass effects into the spacecraft equations of motion along with atmospheric drag and solar radiation pressure (SRP) models [43]. This gives the user a great deal of flexibility in choosing the force models used in the computations. This also results in being able to choose the model configuration to optimize the speed and accuracy of the program for a given orbit

type at run time. And since DSST is based on nonsingular equinoctial orbital elements, it can be used for nearly all orbit classes.

Many studies have been done to determine the accuracy and efficiency of DSST for both long term ephemeris generation and orbit determination. Comparing DSST mean element ephemeris generation results to actual data observations of a Molniya (highly eccentric) class satellite showed excellent agreement [44] and the results of an orbit determination study showed the DSST accuracy to be close to numerical integration methods (Cowell special perturbation theory) [45]. Reference 16 shows how DSST options can be configured to produce run times comparable to general perturbation methods with an order of magnitude accuracy improvement for a variety of orbit regimes.

The primary advantages to using a semianalytic satellite theory such as DSST are the ability to configure the force modeling options to emphasis computational efficiency or accuracy at run time and the ability to produce meaningful mean elements.

## 1.5 Methods of Orbit Determination

The last factor in the orbit determination process, after the observations, dynamics models, and solution method, is the estimation technique. There are two major classes of estimation techniques used in orbit determination:

- batch least squares
- filters

While the formulation and philosophies of the estimation techniques are different, with all things being equal, the results are quite similar. The differences, however, are worth noting. This section provides an overview of the batch least squares and filter estimation techniques as well as discusses how they relate to the orbit determination solution parameters and error assessments. References 46 and 13 provide additional information about orbit determination estimation techniques.

### 1.5.1 Batch Least Squares Estimation

Batch least squares estimation involves the propagation of a reference trajectory over the length of the data arc from an a priori (or best guess) satellite state. The differences between the real observations and calculated observations based on models and the reference trajectory are called residuals. The goal of batch least squares estimation is to solve for the initial satellite state which minimizes the sum of the square of the residuals. In essence, the batch of residuals are minimized in a least squares sense.

This is an iterative process in which the reference trajectory gets updated after every iteration when a new estimate for the initial conditions is estimated from the previous iteration. The primary advantages of a batch least squares estimation include:

- the solution is not too sensitive to the initial conditions and covariance
- the solution is representative of the entire data arc
- the ability to handle noisy and sparse data

Disadvantages of batch least squares estimation include:

- the solution covariance is only valid at the solution time
- does not easily allow for changing dynamic models
- the iteration process does not provide real time results
- the computation requirements are greater than that of filters

These disadvantages, however, are not significant to preclude the use of a batch least squares estimator in orbit determination studies particularly since other strategies exist for solution and covariance propagation and modeling options to account for dynamic models. The primary advantage of a batch estimator is that estimated parameters (like solar radiation pressure reflectivity coefficients)

are representative of the entire data arc, assuming only one parameter is estimated over the data arc, and may be more accurate in the orbit prediction process.

### 1.5.2 Filters

Filtering refers to sequential estimation algorithms where the estimate of the satellite state is updated with every observation. Here, the *a priori* satellite state and covariance are propagated to the first observation time. Then a correction to the state is estimated based on the current observation residual and covariance. For an extended sequential filter, the correction is applied to the satellite state before propagating to the next observation time. Regular sequential processors continue to refine the correction with each observation and then apply the correction to the initial conditions much the way a batch processor does. In this discussion, the extended sequential processor will be the subject when filters are referenced.

The most famous filter implementation is the Kalman filter although many similar algorithms were established about the same time (1960). Many variations on this theme have been established since that time, some of which are discussed in Reference 46.

Since the satellite state is updated with every observation, the reference trajectory quickly tends to a converged value and iterations are generally not required. This is very useful in applications where real time trajectory updates are required. However, this does not produce the best trajectory over the entire data arc. To get the best solution over the entire data arc, a smoother must be used. A smoother is essentially an iterative process for filters. A smoother takes the satellite state and covariance at the final data point and begins to process backwards through the data such that the initial data points have the benefit of the improved reference trajectory and covariance provided by the rest of the data arc.

The primary advantages of filters include:

- they can include process noise factors in the dynamics models
- they produce current estimates and covariance at each data point

- they can be used for real time applications
- they are more computationally efficient than batch processors

Disadvantages of filters include:

- they are not well suited for noisy or sparse data
- final state parameters might not be best values for predictions
- *a priori* estimates are required for the satellite state and process noise covariance
- quality data may cause a filter to diverge

Again, these disadvantages are not significant and can be corrected by various strategies. A smoother will help filters handle sparse and noisy data as well as help establish better state parameters for predictions. *A priori* estimates can be estimated and process noise parameters (if used) can be determined experimentally. Process noise and limited memory strategies can be used to avoid filter divergence.

The real value of filters lie in the ability to use process noise in the covariance calculations to account for dynamic mismodeling and the production of meaningful covariance over the data arc and prediction span.

### 1.5.3 Solve-for and Consider Parameters

The goal of orbit determination is to estimate a satellite state and any other desired parameters that influence the motion of the satellite. These are called solve-for parameters. The solve-for parameters almost always include the six element satellite state whether it be in the form of position and velocity vectors or an orbital element set. In addition it is also acceptable to solve for parameters in the dynamics that are not known particularly well or cannot be modeled. For geosynchronous orbits this usually includes a solar radiation pressure reflectivity coefficients. Some applications may choose to solve for the gravitational constants of the Earth, Sun or Moon.

The physical meaning of estimating a reflectivity coefficient is to gauge the reflectivity of a satellites materials. However, it is essentially a scale factor used to correct for any errors in the solar radiation pressure modeling (such as the area to mass ratio).

There are also other forms of solve-for parameters meant to account for any shortcomings in the dynamic models. Empirical accelerations can be included in the list of solve-for's to account for any thermal or "other" perturbation effects.

When using a filter, dynamic compensation can also be accomplished through the use of process noise. Process noise is a method of adding small amounts of random noise to the covariance matrix. This essentially de-weights the dynamics in favor of the real world observations which contain error but bounded error. Thus, any error in the dynamic models that may cause a divergence from the real world satellite orbit can be minimized. This is also known as the reduced dynamic technique and example applications can be found in References 9-12 and 28-30. Process noise is a very valuable tool when processing high accuracy data sources such as SLR and GPS. The effectiveness of process noise is, however, lost on poor quality data and limited when used with poor dynamic models.

One must take care when using empirical accelerations and process noise parameters. The solution with the smallest residuals is not always the best orbit. It is still best to trust orbit determination to the best dynamic modeling possible or practical and minimize the use of empirical accelerations or process noise.

If uncertain parameters in the dynamic model are not estimated, the uncertainty of those parameters can still be included in the covariance matrix calculations. This is done through the inclusion of consider parameters. Consider parameters are those parameters whose uncertainties are included in covariance calculations but whose values are not estimated in the orbit determination process. By not including these parameters in the solve-for vector, the confidence of the other solve-for components is not degraded; the number of solve-for parameters should be kept to a minimum to decrease the covariance of the solutions.

The value of consider parameters is that the modeling uncertainties can be included in the solution uncertainties represented by the covariance matrix. An accurate covariance matrix can be

propagated with the predicted orbit to produce meaningful error ellipsoids for the predicted trajectory. This is useful in a variety of space surveillance and mission support applications.

Reference 46 discusses the use of consider parameters in greater detail.

## **1.6 Orbit Determination for Geosynchronous Satellites**

In this section, the orbit determination of geosynchronous satellites is discussed. The challenges, current practices, research areas relevant to this study, and rewards of geosynchronous orbit determination are presented. The role improved angular observations, such as those produced by the Raven optical system, can play in improving the accuracy of geosynchronous orbit determination will also be discussed to provide the motivation for this research.

### **1.6.1 Challenges of Geosynchronous Orbit Determination**

For accurate orbit determination, one would like to have accurate observations and realistic force modeling. For geosynchronous orbits, neither is easy.

As mentioned in Section 1.3, obtaining quality range data for geosynchronous satellites is possible through the use of some radars, radio transponders, SLR, and GPS tracking systems. Range-only orbit determination is an acceptable practice for many medium to high accuracy orbit determination applications since angular observations are generally of poor quality; however, range-only orbit determination does have its limitations, particularly for geosynchronous orbits. Since the geosynchronous satellites do not move a great deal with respect to the Earth, the range-rates of geosynchronous satellites are quite small with respect to the ground stations. This means that small errors in the range measurements result in large uncertainties in the satellite position.

To counter this, multiple tracking stations can be used to try to improve the geometry of the problem; however, the altitude of geosynchronous satellites in comparison to the radius of the Earth is quite large. Thus, even with multiple tracking stations, the geometry of the problem is still poor for resolving range-only orbit determination. This may not be the case for GPS tracking of



geosynchronous satellites. The use of GPS for geosynchronous orbit determination is discussed in the next section.

Traditionally, angular observations have been of little help. A ten arcsecond error (typical for angular observations) maps into approximately 1.7 km or error at geosynchronous altitude. Errors this large fail to improve the ambiguity found in processing range data accurate to the tens of meter level.

There are also modeling issues with geosynchronous orbit determination. For most low Earth orbit applications, solar radiation and thermal effects are small perturbations which can be accounted for by simple models or ignored all together. Ignoring thermal (and other smaller perturbing) effects and using a simple spherical satellite model used for solar radiation pressure calculations can be used for meter level orbit determination over 5 days for low Earth orbiters such as TOPEX [45]. However, at geosynchronous altitudes, these effects are much larger in comparison to the other perturbing effects such as nonspherical Earth and third body gravity. Even for GPS satellites, detailed solar radiation and thermal models are required for high precision orbit determination [8]. With TOPEX and GPS satellites, much analysis time was devoted to producing the detailed models used in their precision orbit determination approaches. With the limited resources and tracking data available to most owner/operators, efforts to produce such models may be impossible. For space surveillance applications, satellite specific models are generally not available.

## **1.6.2 Current Practices and Relevant Research**

When discussing the current geosynchronous orbit determination practices, it is useful to break the discussion up into optical orbit determination which is typically used for space surveillance and radio transponder based orbit determination which is generally used in mission support. The use of GPS in geosynchronous orbit determination can also be treated separately.

### **1.6.2.1 Optical Orbit Determination**

As stated earlier, accuracy requirements for space surveillance orbit determination are based primarily on the ability to predict the orbit for later tracking. With traditional optical sensors, the

desired accuracy for satellite prediction is generally on the order of arc minutes [47]. For a Raven optical sensor, the desired prediction accuracy is around 15 arcminutes. Reference 47 points out that element sets given in the NORAD satellite catalog for Meteosats 2, 3, and 4 degrade to about 12 arcminutes of error over a 32 day prediction. The NORAD element sets were most likely produced with the SGP4 general perturbation theory using angular data from the GEODSS optical sites

Reference 5 discusses the Russian approach of using a semianalytic satellite theory (with a simple solar radiation pressure model) for geosynchronous space surveillance. The tracking data is supplied by the Russian Space Surveillance System optical tracking sensors (12 sensors spread across the former Soviet Union) and is accurate to "several angular seconds" (Reference 47 gives an accuracy assessment for one of the sensors as 1.8-1.9 arcseconds standard deviation). For 69 objects, the prediction error was on the order of 1 arcminute over 60 days.

#### **1.6.2.2 Transponder Based Practices**

For mission support orbit determination, accuracy requirements are based on the mission needs and can often be far more stringent than those for space surveillance. Element sets produced by the Meteosats 2, 3, and 4's owner/operator (ESOC) maintained 1 arcminute accuracy requirement over a 32 day prediction interval in comparison to the 12 arcminute prediction errors inherent in the NORAD space surveillance predictions [47] (Reference 47 gives no mention to fit statistics). ESOC uses a radio transponder system to track its satellites as do most geosynchronous satellite owner/operators. Reference 68 describes the Canadian Telesat's flight dynamics system which uses a real-time filter and a radio transponder observation system for mission support.

NASA's Goddard Space Flight Center uses the Bilateral Ranging Transponder System to track the Tracking Data Relay Satellite System (TDRSS). Orbit determination is performed by batch least squares estimation using the Operational Version of the Goddard Trajectory Determination System (Ops GTDS) [21,48]. TDRSS requirements dictate orbit determination accuracy should be maintained within 100 meters but evaluation of overlapping orbit determination solutions suggest the errors are

typically more on the order of 30 meters [19, 49]. Reference 54 mentions more stringent (25 meter) requirements for TDRSS to support future missions.

Studies have been performed at Goddard by the Flight Dynamics Division which has shown the capability to solve for improved accuracy (below 10 meters) TDRSS orbits by using GPS-based TOPEX precise orbit ephemerides (POE's) [50]. TOPEX carries a TDRSS receiver as well as a GPS receiver for orbit determination purposes. GPS based orbit solutions for TOPEX are accurate to the 15 centimeter level. Using the TOPEX POE's as truth data, the TDRSS observations of TOPEX can be used to back out solutions for the TDRSS orbits.

#### **1.6.2.3 GPS Studies**

The TOPEX/TDRSS technique described above is similar to the high accuracy orbit determination studies performed with GPS. As stated earlier, the advent of GPS has pushed orbit determination accuracy to a new level for low Earth orbiters, but the constellation geometry does not allow for the high visibility of geosynchronous satellites required to produce such precise orbits. There is limited observability of geosynchronous satellites to the GPS constellation, however, and studies have been performed to see how GPS technology can be exploited by geosynchronous users. Appendix A discusses the observability of the geosynchronous orbit regime from the GPS constellation. With the exception of the limited visibility, it is anticipated that the extra viewing geometry provided by GPS observations will make the GPS data type a valuable resource.

References 51, 52, and 70 are autonomous navigation and station-keeping studies performed by the Aerospace Corporation. Since the studies dealt with on-board orbit determination strategies for navigational purposes, their accuracy's were limited by simplified dynamic models. Still, reference 51 shows orbit determination accuracy over a 24 hour arc (using a filtering strategy) to be between 40 and 100 meters using a Y-code receiver or assuming AS and SA are turned off. If the GPS receiver on board the satellite were to carry a rubidium clock, the error could be reduced to the 20 meter level. Furthermore, if GPS satellites broadcast signals upwards (always from the Earth) as well as downwards, the errors would drop to approximately 15 to 20 meters. These results are valuable and can likely be

improved upon using a ground based orbit determination approach containing high fidelity dynamic models.

Similar results were described by a study performed by the French National Space Agency (CNES) [53]. Reference 53 not only considers the use of a GPS receiver on board the geosynchronous satellite, but also studies the use of three pseudolite ground stations in an effort to improve accuracy. The CNES study predicts an error standard deviation of approximately 55 meters for the receiver on board case and down to 23 meters for a case using Ku and C band pseudo-lites. Both values are for a three day arc of data and assume use of the public domain C/A code pseudorange.

Reference 72 summarizes all of the GPS techniques applied to geosynchronous orbit determination at the Jet Propulsion Laboratory (JPL). JPL has also studied the use of a GPS receiver on board a geosynchronous satellite (without accounting for atmospheric effects). The studies show a predicted accuracy of 50 to 80 meters over a 24 hour arc of data when SA is on using a dual frequency receiver. The accuracy improves to 5 to 10 meters when a Y-Code receiver is used or AS and SA are turned off.

The most intriguing use of the GPS constellation to geosynchronous orbit determination is presented by JPL in References 54, 55, and 72. In these studies, a radio transponder on board of a geosynchronous spacecraft (such as TDRSS) is used like a GPS broadcast signal. The signal from the geosynchronous satellite is received on the ground with GPS signals by a GPS receiver at a known location. Then by using GPS techniques, the position of the geosynchronous satellites is estimated as if it were a GPS satellite. This technique works for GPS satellites to produce orbit accuracy's on the 20 cm level. In the published experiments, the overlap accuracy level has been pushed to below 20 meters for a TDRSS satellite; however, this technique faces limitations with the TDRSS satellites since TDRSS transponder signals are broadcast at a very narrow beam width. A wider beam would allow for a better viewing geometry from the ground stations and improved accuracy. Experiments with the INMARSAT satellite showed overlap RMS differences to be on the 10 meter level or less. It is theorized that this technique should be able to produce 2 meter level orbits.

### **1.6.3 The Value of Improved Accuracy**

The value of improved accuracy geosynchronous orbit determination includes the ability to:

- space satellites closer together in the geosynchronous orbit ring
- improve predictions of inactive satellites or other space debris
- produce high fidelity reference orbits for orbit determination studies

The geosynchronous orbit regime is a limited resource in high demand for satellite based applications. Because of this, longitudinal positions in the geosynchronous orbit ring or "slots" are assigned to users through international agencies [56]. Improved accuracy geosynchronous orbit determination may allow for the width of the slots to be reduced thus allowing more satellites into the orbit ring. Or it may allow slot owners to place multiple satellites into a single slot (which could lead to an expansion of the space real estate market).

The production of high fidelity reference orbits for geosynchronous satellites has many applications in astrodynamics. Like the precise orbit ephemerides produced for LAGEOS, TOPEX, and the GPS constellation, precise orbits for geosynchronous satellites could be used in a variety of orbit determination studies including sensor calibration, force model assessments, and estimation technique evaluations. In this study, GPS satellite precise orbit ephemerides have proven to be a valuable resource.

In more of a space surveillance role, improved geosynchronous orbit determination would allow for better prediction of inactive satellites or other forms of space debris. The use of mean element propagators such as those included in the Draper Semianalytic Satellite Theory would be particularly useful for long term predictions of the motion of these inactive objects. Accurate long term predictions of inactive objects may also decrease the tracking requirements for those objects.

### **1.6.4 A Role for Improved Angular Observations**

Satellite owner/operators face a variety of constraints during their mission design and budgetary process. Reference 71 discusses the need to improve orbit determination accuracy and reduce cost and communications bandwidth for high altitude Air Force satellites currently using transponder based (AFSCN) practices. Low cost, high accuracy optical sensors such as the Raven appear perfectly suited for such applications.

Space surveillance systems require tracking of noncooperative targets and the population of high altitude objects is continuously increasing. The results of a Russian space surveillance study demonstrate the potential of improved angular observations combined with an efficient yet accurate satellite theory [47]. A low cost, high accuracy optical sensors such as the Raven could help provide other space surveillance programs with similar capabilities.

The purpose of this study is to show how improved angular observations can aid the orbit determination process for geosynchronous satellites. Range-only orbit determination has traditionally been the best method of geosynchronous orbit determination due to the quality of range observations and poor quality of angular observations, but range-only orbit determination for geosynchronous satellites has limitations due to the geometry of the problem.

With the advent of improved optical sensors such as Raven, it is possible to introduce these improved accuracy angular observations into the orbit determination process as a supplement to high quality range data such as those produced by radar, radio transponder, SLR, and GPS systems. These quality angular observations help resolve the geometric ambiguity of range-only orbit determination.

In addition to supplementing high quality range data, these improved angular observations can be used as the only data source for space surveillance and mission support roles.

## 1.7 Thesis Overview

Section 1.6 was meant to define the purpose of this research and outline the benefits of its pursuit. Sections 1.1 through 1.5 were meant to provide background material in hopes of providing motivation for the choices made in this study.

The second chapter of this study outlines the approach to this study. Included in the methodology is an outline of the various orbit determination scenarios to be studied, the choice of software tools, force model assessment for geosynchronous orbit determination, description of the real data available for this study, description of the data simulation procedure used in the analysis, and validation of the data simulation procedure.

The third chapter presents the results of the mission support and space surveillance studies incorporating improved angular observations in the geosynchronous orbit determination process. The mission support studies examine the limitations of range-only geosynchronous orbit determination, the use of range and angles together, and angles-only orbit determination. The space surveillance studies examine the improvement in accuracy when using improved angular observations in place of traditional accuracy angular observations.

The fourth chapter contains the conclusions of the analysis and outlines future work relevant to this research.

Finally, the relevant appendices are included following the list of cited references.

## **Chapter 2: Approach**



## 2.1 Orbit Determination Scenarios

The orbit determination studies presented in this analysis can be broken up based on their application to either:

- mission support
- space surveillance

For each role, the observation sources (type, number, and location of sites), amount of observations used, and the extent of the dynamic modeling varies. In each scenario, studies are performed to reflect realistic conditions for the basic space surveillance and/or mission support roles.

### 2.1.1 Mission Support Scenario

The mission support orbit determination scenario reflects existing geosynchronous satellite missions using radio transponder data wishing to upgrade or supplement their orbit determination capability or future missions interested in simple, low cost strategies. The primary focus of this analysis is on a geosynchronous satellite with a longitude of approximately 240° longitude (over the California coast) and an inclination of approximately 9°.

The following data situations are investigated

- range-only
- range and angles
- limited range and angles

In the range-only case, an effort is made to understand the limits of range-only geosynchronous orbit determination given an extensive tracking system. The range and angles scenarios include improved angular observations with the extensive range tracking system. Studies are performed to determine how the improved angular observations impact the orbit determination accuracy and how much angular data

is needed. The limited range and angles scenarios investigate the value of the improved angular observations when an extensive range tracking system is not available. The number of range tracking stations is reduced to represent a more cost efficient method of tracking; there are also satellites such as TDRSS where ranging is limited due to the communications requirements of the satellite.

Among other cases, the limited range and angles case considers single site orbit determination and angles-only orbit determination. Single site range-only orbit determination for geosynchronous spacecraft is not possible when the tracking station and the spacecraft are at the same longitude; even when the tracking station and spacecraft are at different longitudes, the results are poor. In the angles-only case, range data may not be available due to a failed radio transponder or GPS receiver on board the spacecraft. Angles-only orbit determination could also serve to verify the orbit location of autonomous satellites where all orbit determination and navigation functions are performed on board the satellite with limited or no ground interaction.

All mission support scenarios are based on real world mission support data acquisitions and solution approaches for a geosynchronous satellite. Additional information on the real data is presented in Section 2.4.

The value of using the improved angular observations as a supplement to range data is measured by comparing the range-only fits to fits incorporating the angular observations.

### **2.1.2 Space Surveillance Scenarios**

The space surveillance scenarios include both angles-only and range and angles orbit determination. In any case, the sites collect very few observations to allow for tracking of a large number of satellites. An example application could be a geosynchronous and near-geosynchronous debris tracking and prediction campaign. Here, hundreds of objects would need to be tracked and orbit determination and prediction performed. Because of these requirements and associated computational burden, the use of general perturbation and semianalytic satellites theories (in addition to special perturbation theory) are investigated. The semianalytic theory could be particularly valuable if accurate mean elements can be derived to support long term predictions.

For the space surveillance scenario, a set of optical sites distributed longitudinally along with a single deep space radar is considered. In the angles-only case, range data may not be available due to the limited availability of deep space radars.

The number of observations used in the space surveillance studies was derived from an assumption of an approximate number of satellites that needed to be tracked. The assumed tracking schedule allowed for a 20 day fit span with tracking every other night (10 nights total) and a 40 day prediction (60 day fit and predict span). Four images are taken of each object per night resulting in eight observation pairs. With 10 nights of tracking, this results in 80 observation pairs or 160 total right ascension and declination observations over the 20 day fit span. Assuming it takes 10 minutes to take four images, then 100 minutes are devoted to each object per 60 days. If the sensor can track for eight hours per night, then approximately 288 objects could be tracked per optical sensor. Of course, this number is optimistic when poor weather and calibration time is accounted for.

The orbit determination studies are performed for one satellite, GOES-10. It is believed that studies on other objects would produce similar results; GOES-10 was chosen due to the availability of real observation data which is discussed in Section 2.4.

To measure the value of the improved angular observations, studies are performed using poorer quality angular observations (such as those produced by GEODSS) and comparing the results to those produce by the improved angular observations.

## **2.2 Analysis Tools**

The orbit determination studies performed as a part of this research involve real data reduction and data simulation capability for a variety of data types. Three software tools were available for use:

- GIPSY/OASIS II
- Ops GTDS
- Draper GTDS

Each tool has its strong points but none are capable of supporting the entire study without modification. The individual analysis tools are described below.

### **2.2.1 GIPSY/OASIS II**

GIPSY/OASIS 2 is a JPL product being used by the Colorado Center for Astrodynamics Research (CCAR) for their GPS orbit determination studies. The heart of the estimation algorithm is a square root information filter/smoothen with extensive force modeling including reduced dynamic modeling (a form of process noise). GIPSY/OASIS stands for GPS Inferred Positioning SYstem / Orbit Analysis and SIMulation Software and the software is also referred to as GOA2. GOA2 is the most accurate of the three tools mentioned; however, GOA2 was designed to process GPS observations only. Some range capability has been added to model SLR data but no optical angular observation models exist. In addition, it is desired to have some general perturbation and mean element modeling available to examine some space surveillance issues of this research; these capabilities do not exist in GOA2.

Since GOA2 lacked angular observation models and general perturbation theories, the software was primarily used in some force model assessment cases. It should be noted, however, that Gipsy was the analysis tool used by JPL in their studies of GPS applications to geosynchronous orbit determination [54, 55, 72].

The version of GOA2 used in these studies is maintained on a SUN workstation in CCAR at the University of Colorado's Department of Aerospace Engineering Sciences.

### 2.2.2 Ops GTDS

Ops GTDS is the Operational Version of the Goddard Trajectory Determination System. Ops GTDS is the main orbit determination tool used by NASA's Goddard Space Flight Center Flight Dynamics Division for daily operations; TDRSS orbits are routinely determined using Ops GTDS.

The estimation algorithm in Ops GTDS is batch weighted least squares. No filtering capabilities exist but generalized (or empirical) accelerations are available in the batch estimator to account for unmodeled dynamics. Ops GTDS has angular, radio transponder, radar, and SLR observation models available for orbit determination and data simulation; however, no GPS capabilities exist in Ops GTDS. Like GOA2, sufficient general perturbation and mean element theories are not available for space surveillance studies.

Since Ops GTDS includes all of the necessary observation models and allows for empirical accelerations to account for unmodeled dynamics, it was used primarily for the mission support studies. Some force model assessment cases were also performed using Ops GTDS.

All Ops GTDS runs were performed on an SGI workstation supported by the AFRL Astrodynamics team.

### 2.2.3 Draper GTDS

Draper GTDS (or DGTDS) is the Draper Research and Development Version of the Goddard Trajectory Determination System. The original version of GTDS, as the name suggests, was developed at the NASA/Goddard Space Flight Center between 1970 and 1976 [33]. A research and development version, R&D GTDS, was developed to evaluate promising methods of operational, nonroutine, and highly precise orbit determination [38].

Draper Laboratory received a copy of R&D GTDS to run on its IBM mainframe computer in 1979. Since 1979, GTDS has been expanded and modified at Draper in several areas including high precision mean element propagation (Draper Semianalytic Satellite Theory), precision determination of mean elements via weighted least squares, and Kalman Filter sequential estimation techniques using

mean elements [6]. DGTDS also has been ported to a variety of platforms including VAX, VAX station, Sun workstations, SGI workstations, PC's (486, Pentium), and (in some form) Macintosh.

Both Draper GTDS and Ops GTDS are distant offspring from the original version of GTDS. Goddard's Flight Dynamics Division still maintains R&D GTDS although a separate version called Analysis GTDS is now used as a test bed before modifications are incorporated into Ops GTDS. The Goddard version of R&D GTDS was also modified extensively over the years. Many of these modifications have found their way into Ops GTDS (which in some aspects is better than DGTDS) such that there are substantial differences between Ops and Draper GTDS.

Like Ops GTDS, DGTDS has all of the required observation models except for GPS. Unlike Ops GTDS, DGTDS has maintained and expanded some filter functionality including process noise capability. However, the lack of a smoother limits the applicability of the filter for this research. There are some GPS capabilities in DGTDS meant to be used for simulation and covariance analysis but these are limited in scope. As part of this research, a more modern GPS data processing structure was implemented into DGTDS but was not fully completed and the GPS analysis was not pursued.

Advantages of using DGTDS include the general perturbation and mean element theories available for space surveillance studies. Since the force modeling lacks empirical accelerations, however, it was not used in the mission support studies (more information on the force model requirements are given in Section 2.3).

The version of DGTDS used in this analysis was operated from a 486 desktop PC.

## 2.3 Force Model Assessment

As stated in Section 1.4, the primary perturbations acting on a geosynchronous object are:

- central nonspherical gravity
- third body (Lunar-Solar) gravity
- solar radiation pressure
- other

where "other" includes momentum dumps, thermal, tidal, and Earth radiation effects.

In this analysis, central nonspherical gravity is modeled through degree and order four using the Joint Gravity Model 2 (JGM2). Reference 16 shows there is no significant drop in accuracy when truncating the gravity field from degree and order 21 to degree and order 4 for a geosynchronous satellite over short arcs. These results were verified using DGTDS over a nine day fit span.

Point mass models are used to calculate the effects of the Sun and Moon's gravitational accelerations (the position of the Sun and Moon are provided by JPL ephemerides). At geosynchronous altitude the effects of nonspherical gravity from the Sun and the Moon are negligible as are gravitational effects from other planets. The effects of the other planets were gauged using the Gipsy software.

A spherical satellite model with a constant reflectivity coefficient scale factor is used for modeling solar radiation pressure effects. It was anticipated that satellite macro-modeling would be required for accurate geosynchronous orbit determination. However, tests conducted using Ops GTDS and Precise Orbit Ephemerides (POE's) of GPS satellites showed for a satellite with large solar arrays perpendicular to the Sun, a spherical satellite model with a scale factor is almost as accurate as using a macro-model for the satellite. Appendix B talks about GPS POE's and where they are publicly available.

For the mission support scenarios, a constant along-track acceleration is used to account for unmodeled dynamics. This was necessary due to daily momentum dumps performed by the satellite the studies were modeled after. Without the inclusion of the empirical acceleration, the real data fits would have been poor. For the space surveillance studies, the along-track acceleration was not included.

The other "other" perturbation effects are not included in the dynamic modeling since their effects are either small (such as tidal effects) or not well known (such as thermal effects). Empirical accelerations can be used to account for these unmodeled effects. The empirical accelerations also serve to model solar radiation pressure effects not included in the spherical satellite modeling.

In the mission support studies, a Cowell special perturbations theory is used in the satellite propagation with the force models described above.

For the space surveillance cases, three satellite theories are used in the space surveillance cases: Cowell special perturbation theory, Draper Semianalytic Satellite Theory (DSST), and a version of the SGP4 general perturbation theory. The Cowell propagator included the force models described above (4x4 geopotential, Lunar/Solar point mass effects, and solar radiation pressure with aspherical satellite and cylindrical shadow model).

The DSST propagator was configured using the Fonte-Sabol optimal input deck [16]. The DSST Fonte-Sabol optimal input deck has the force model options configured to balance speed and accuracy and include a 4x4 geopotential in the AOG (averaged orbit generator),  $J_2^2$  effects in the AOG and SPG (short periodic generator), zonal short periodics, Lunar/Solar point mass effects in the AOG, numerical third body short periodics (includes weak time dependence), and solar radiation pressure with a spherical satellite and cylindrical shadow model in the AOG and the SPG. Default settings were used with all of the included SPG models.

SGP4 is a common name which is often associated with a class of general perturbation propagators used by the Air Force Space Command. The propagator used in this work is more correctly identified as DP4 and it includes  $J_2$ ,  $J_4$ , and  $J_2^2$  secular effects,  $J_2$  and  $J_3$  long period effects, truncated  $J_2$  short periodics to zeroth order in eccentricity,  $n=2,3$  and  $m=2$  tesseral harmonic resonance corrections, and first order double averaged Solar/Lunar point mass long period effects [15, 69]. No third-body short periodic or solar radiation pressure effects are modeled in the SGP4 theory. In this work, the DP4 propagator is used and referred to by the more common SGP4 label. Reference 80 describes the family of theories often referred to as SGP4 in greater detail.

It should be noted that the SGP4 model used in this analysis is the version incorporated into DGTDS by Darrell Herriges in 1987 as part of his Masters thesis work at MIT [69]. This version of SGP4 is not the official version of the SGP4 code used by US Space Command and has not been verified and validated by US Space Command. No conclusions about the performance of the US Space Command space surveillance operations, in any way, should be inferred from this analysis.

## 2.4 Available Real Data



An effort was made to gather real observation data to support these studies. The real world observation data serves two purposes:

- provide real world results to base simulation studies on
- support conclusions made using simulated data

The next two subsections describe the real data used in the mission support and space surveillance scenarios.

### **2.4.1 Mission Support Data**

As stated earlier, the primary focus of this analysis is on a geosynchronous satellite with a longitude of approximately 240° longitude (over the California coast) and an inclination of approximately 9°. Two observation sources were available for this satellite:

- radio transponder data
- Raven data

The observation stations, distributions, number of observations, and accuracy assessments of these data source are described in the following subsections.

#### **2.4.1.1 Radio Transponder Data**

The satellite is supported by a system of eight ground station radio transponders at five distinct geographic locations which produce high accuracy range observations for use in orbit determination. Table 2.1 describes the stations and the amount of data obtained from each station over the time period of January 18-27, 1998. The satellite owner/operator supplied radio transponder data from January 15 through February 10, 1998, but only the data between January 18 and January 27 was

used in this analysis since Raven tracking began on January 18 and the satellite maneuvered on January 27.

Each pass of tracking collected 30 sets of observations; this resulted in a total of 810 observation sets from the 27 passes over the nine day period of study. The length of each pass never exceeded 30 minutes and was sometimes as short as 7 minutes. Figure 2.1 plots the temporal distribution of the observations.

Table 2.1: Radio Transponder Ground Stations

Station Number	Location	Number of Passes
1	Hawaii	4
2	Hawaii	3
3	Vandenberg AFB, CA	3
4	Vandenberg AFB, CA	5
5	Colorado Springs, CO	3
6	New Hampshire	3
7	New Hampshire	2
8	Thule, Greenland	4

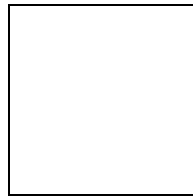


Figure 2.1: Radio Transponder Observation Distribution

Each observation set consisted of a range, azimuth, and elevation observation. The quality of the angular observations was very poor (worse than 20 arcseconds of noise, one standard deviation) so only the range observations were used. The range data was similar in quality to the BRTS data cited in Reference 54.

#### 2.4.1.2 Raven Data

An extensive Raven tracking campaign was performed as a part of this research by the AFRL Astrodynamics group in Albuquerque, New Mexico. An effort was made to track the geosynchronous satellite from January 19 through February 1, 1998. With the exception of January 21, data was collected every night from the Albuquerque Raven site. Table 2.2 describes the Raven data collected from January 19 through January 27.

Table 2.2: Mission Support Raven Data Summary

Date	Start Time (UTC)	End Time (UTC)	Number of Images
Jan. 19	6:31	10:47	61
Jan. 20	3:46	9:20	175
Jan. 21	N/A	N/A	0
Jan. 22	4:27	9:25	40
Jan. 23	4:31	10:25	172
Jan. 24	9:03	10:18	47
Jan. 25	7:19	11:31	103
Jan. 26	2:54	10:07	170
Jan. 27	4:42	10:38	147

The Raven optical sensor produces topocentric right ascension (RA) and declination (Dec) observations. From each image, 2 observation pairs are produced so that roughly 3660 observations were available for this research. Problems were encountered early in the tracking campaign that limited tracking, but towards the end of the tracking campaign, over 200 images were being captured per night and the tracking span lasted roughly eight hours.

Based on the success of the Raven tracking campaign and previous experiences with the telescopes in Maui and Albuquerque, the simulation studies in the mission support analysis assume that the sensors can operate six out of nine days on average. While the tracking campaign collected data from Albuquerque 13 out of 14 days, such luck with the weather cannot always be expected. The data collection time roughly translates to less than two minutes per image.

### 2.4.1.3 Raven Data Accuracy Assessment

As a check of the Raven data accuracy, a comparison was made between the Raven angular observations and a reference orbit produced by fitting to the radio transponder data described in Section 2.4.1.1. Later in this analysis, it will be shown that the range based orbit is likely accurate to the 30 meter level. Figure 2.2 shows the differences between the Raven observations and the range based reference orbit for January 19 and 22. The differences are plotted versus true anomaly of the satellite.

Figure 2.2 clearly indicates a systematic error in the declination observations. The magnitude of the periodic error is greater than 6 arcseconds which maps into 1 kilometer at geosynchronous altitude. This is too large of an error to be present in the reference orbit. To make sure the error was in the Raven observations, the range based reference orbit was verified by comparing it to the orbit determination solution produced by the satellite owner/operators.

This error trend had not been observed in any previous Raven studies. An effort was made to revisit several of the Raven data comparisons to reference orbits for GPS, TDRSS, and GOES-10 satellites. The error trend was not apparent for those cases.



Figure 2.2: Raven Observations Compared to Range Based Reference Orbit

Prior to the geosynchronous satellite tracking campaign, several nights were spent tracking GPS satellites for the purpose of calibration. Most of the GPS passes were short, less than one hour, and identifying a 12 or 24 hour periodic error trend would not be easy since the errors due to the

systematic error would be masked by the noise in the data. There was one pass that lasted close to two hours. Figure 2.3 shows the difference between Raven observations of GPS PRN31 and the IGS Precise Orbit Ephemeride on January 13, 1998. More information on the IGS precise orbits is provided in Appendix B.

A significant difference between Figure 2.2 and Figure 2.3 is that the biases have been removed from Figure 2.2. The systematic error trend is again obvious in the declination residuals. For the GPS satellite, the amplitude appears to be six times larger. This would seem to indicate an inclination dependence considering the inclination of the geosynchronous satellite is  $9^\circ$  and the inclination the GPS satellite is  $55^\circ$ . An inclination dependence would also explain why the trends were not observed in the TDRSS or GOES-10 data sets since they are at near  $0^\circ$  inclinations. The previous GPS arcs were too short to identify the trends; examining half of the data in Figure 2.3, it is difficult to identify a systematic error.



Figure 2.3: Raven Observations Compared to GPS Reference Orbit

At the completion of this research, the source of the error was still not confirmed. It is believed to be a problem in the handling of precession and nutation in the image processing. A bonus of these problems, however, was an impromptu education in the concepts of astrometry.

Without rectifying the image processing problems with the Raven data, the observations were useless. The real data analysis accuracy assessment does indicate the quality of the data, however. Looking at a very short arc of the geosynchronous satellite data reveals the noise level uncorrupted by

the systematic errors. Figure 2.4 plots the Raven observation differences with the range based reference orbit with biases removed. The figure reveals noise levels (one standard deviation) on the order of 1.25 arcseconds for right ascension and 0.7 arcseconds for declination.



Figure 2.4: Short Arc Raven Observations

The accuracy in these observations is a measured improvement over previous studies [75]. The improvement can be attributed to a new right ascension gear and a darker telescope location. Further improvements are expected in the fall of 1998 with the incorporation of more accurate star catalogs and better streak end point detection in the CCD image processing. The Raven image processing used in this analysis used the Hubble Guide Star Catalog (GSC) and References 76 and 77 discuss the advent of more accurate catalogs.

When first proposed, the theoretical accuracy of the Raven was believed to be 0.333 arcseconds, this study assumes angular observation accuracies of 1.0 arcsecond for right ascension and 0.5 arcseconds for declination (noise level, one standard deviation). This is a reasonable assumption given the current performance and the anticipated improvements.

#### 2.4.2 Space Surveillance Data

GOES-10 is the latest in a series of Geostationary Operational Environmental Satellites used by the National Oceanic and Atmospheric Administration (NOAA) for meteorological purposes. The GOES-10 satellite was launched on April 25, 1997 and placed into geosynchronous orbit at 105° west

longitude [73]. The initial launch and early orbit phasing support was performed by the Goddard Space Flight Center Flight Dynamics Division. The AFRL Astrodynamics group participated in a study of a close approach between the GOES-10 satellite and the uncontrolled Telstar-401 satellite in August, 1997 [74]. From the tracking that proceeded the close approach, three data sources were available for GOES-10:

- radio transponder data
- radar data
- Raven data

The observation stations, distributions, number of observations, and accuracy assessments of these data source are described in the following subsections.

#### **2.4.2.1 Radio Transponder Data**

After GOES-10 performed a small maneuver on August 18, 1997, it was tracked by the GSFC GOES-10 team for a day to produce a post-maneuver satellite state. A radio transponder space to ground link system (SGLS) was used to calculate range and Doppler observations of the satellite from four ground stations (two of which are co-located). From these observations, an osculating element set was produced using Ops GTDS. The GSFC GOES-10 team provided the element set which is used to propagate a reference orbit in this analysis.

#### **2.4.2.2 Radar Data**

As part of the close approach study, a request was made to US Space Command for observations of GOES-10. US Space Command provided several days of observations from the Millstone Hill deep space radar located in Massachusetts. The radar observations consisted of range (r), range-rate (rr), azimuth (az), and elevation (el). Only the observations collected after 0 hr, August 19

UTC time were used to avoid corrupting the solutions with pre-maneuver observations. The observations ran through August 21 for a total of three days of radar data.

Figure 2.5 gives the temporal distribution of the radar observations (as well as the Raven observations). In the figure, the MLH represents the Millstone Hill radar range observation nondimensionalized differences from the radio transponder based reference orbit.

Figure 2.5 shows the radar observations were collected in brief passes. Each of the eight two minute passes collected four observations sets. This provided a total of 32 observation sets or 128 total observations over the three days. The range and range-rate data were of excellent quality but the angular observations from the radar were poor.

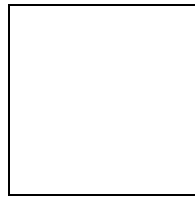


Figure 2.5: GOES-10 Observation Distribution

(MLH R- Millstone Hill Range, RME RA- Maui Right Ascensions, VTA RA- Abq. Right Ascensions)

#### 2.4.2.3 Raven Data

One night of tracking occurred from each of the Raven sites as both Maui and Albuquerque tracked GOES-10 for several hours on August 21, 1997. Figure 2.5 shows the temporal distribution of the angular observations along with the Millstone Hill radar data. In the figure, RME represents the Maui Raven station and VTA represents the Albuquerque Raven station.

The Raven sites collect topocentric right ascension and declination observations. The observations from the Albuquerque site were similar in accuracy to the results presented in Reference 75 while the quality of the Maui observations was slightly lower due to a variety of circumstances (low elevation, clouds, location of a full Moon). Table 2.3 list the number of observations and the noise standard deviation from both sensors.



The table shows there were 48 total (24 RA and 24 Dec) angular observations from the Albuquerque site and 58 total (29 RA and 29 Dec) from Maui. In the table, the statistics are broken into "open" and "close" sets of observations. This refers to the observations pairs taken from the beginning of the satellite streak in the Raven CCD image when the CCD shutter opens and the end of the satellite streak when the CCD shutter closes. Some timing problems have been observed in the Raven system and treating the "open" and "close" data as separate stations allows for better estimation of these errors. Calibration work is planned to identify the source of the timing errors and possibly offer solutions. Reference 75 explains the "open" and "close" concept in more detail.

Table 2.3: Space Surveillance Raven Data Summary

	RA (arcsec)		DEC (arcsec)	
	Number of Observations	Noise Standard Deviation	Number of Observations	Noise Standard Deviation
VTA open	12	3.12	12	1.56
VTA close	12	1.73	12	1.30
RME open	15	5.71	15	1.86
RME close	14	4.01	14	0.805

The quality of the data, in comparison to that presented in the Mission Support Data subsection, indicates that this data was obtained before some improvements (darker location, new right ascension gear) were made to the Raven system. The large systematic error in the observations does not appear since GOES-10 is at near zero inclination. Some systematic error is surely present in the data but it is masked by the noise in the data.

## 2.5 Analysis Methodology

Section 2.4 documented the collection of real observation data for use in this research. Analysis of the Raven data, however, revealed systematic errors in the improved angular observations which make most of the data unusable; therefore, data simulations were used to investigate the impact

these observations would have on the geosynchronous orbit determination problem once the errors are removed. This section gives an overview of the data simulation procedure and a validation of that procedure. To ensure the integrity of the data simulations, comparisons were made between real and simulated range-only cases. If the simulated data fits are similar to the real data cases, it would build confidence in the results of the simulated cases. Then conclusions could be drawn about the utility of the improved angular observations from the simulations.

### **2.5.1 Data Simulation Approach**

The first step in a data simulation procedure is to develop a "truth" orbit or reference trajectory. The truth orbit is the ephemeris from which the simulated observations are constructed. For the mission support cases, the truth model was established by fitting to the radio transponder range data over a nine day fit span from January 18 to January 27. The best estimate of the satellite state, solar radiation pressure reflectivity constant, empirical along-track acceleration, and range station biases derived from the fit were used as the truth orbit. For the space surveillance cases, the NASA/GSFC radio transponder based element set and reflectivity constant were used as the truth orbit. In both cases, the reference trajectory is integrated over the period of interest using the GTDS Ephemeris Generation program.

Next, the truth orbit is used to construct simulated observations with the GTDS Data Simulation program. The ground stations and tracking schedules were constructed to reflect realistic tracking conditions. For the mission support cases, the tasking was scheduled to reflect the real world data collection. The estimated radio transponder range biases were added to the simulated observations as was random noise at the level observed in the real observations. For the space surveillance cases, the tasking was based on an assumed number of objects that needed to be tracked. No biases were included in the space surveillance studies.

Fits are then made to the simulated observations using the GTDS Differential Correction program. In all cases, the satellite state and solar radiation pressure reflectivity coefficient (when applicable) were estimated. For the mission support cases, a constant along-track acceleration was also

estimated. The force models used in the truth trajectory and estimated trajectory can be slightly different to account for errors in the dynamics. For the mission support cases, however, the force models used in the truth and estimation process were the same; it is believed the uncertainty in the along-track acceleration and solar radiation pressure reflectivity coefficient provided enough error in the dynamics. The space surveillance cases did use slightly different models in the truth and estimation process but it had negligible impact on the results.

Assessments of accuracy can be made by comparing the trajectory derived from the simulated observations to the truth trajectory from which the simulated observations were created; the best estimate of the orbit based on the simulated observations is compared to the truth orbit using the GTDS Ephemeris Comparison program. The compare program provides the errors of the estimated orbit in terms of orbital elements, Cartesian components, or radial, cross-track, and along-track components.

### **2.5.2 Validation of the Data Simulation Approach**

To validate the data simulation procedure and establish confidence in the results of the data simulations used in this analysis, real and simulated data cases are compared for the geosynchronous satellite described in the mission support scenario. Since the angular observations were corrupted, only the radio transponder range data is used here. The available data, stations, and observation distributions are described in Section 2.4.

First, fits were made to the nine days of radio transponder range observations described previously in Table 2.1 and Figure 2.1. Table 2.4 describes the force modeling used in the Ops GTDS Differential Correction program's weighted least squares batch estimator. The estimated parameters included the satellite position and velocity, a single reflectivity constant for solar radiation pressure, and a constant along-track acceleration over the entire fit span. The along-track acceleration was required to account for daily momentum dumps performed by the satellite. This configuration was used in all of the Mission Support analysis.

Two real data cases were investigated. The first orbit solution, Case 1, estimated range biases from all radio transponder ground stations. The second solution, Case 2, did not estimate the range

biases but used the reported bias values provided by the satellite operator from each sensor. The two orbit solutions were then compared over the 9 day fit span at 20 minute intervals.

Table 2.4: Mission Support Orbit Generator Models

Integrator	Cowell Special Perturbations
Step Size	400 s
Geopotential	4x4 JGM2
Third Body	Solar, Lunar point masses (JPL DE 118,200)
Solar Radiation Pressure	Spherical Body, Single Reflectivity Coefficient, Cr
Empirical Acceleration	Constant Along-Track

The comparisons, Case 1 minus Case 2, showed periodic differences in the radial direction (24 meter amplitude, 48 meters from peak to peak) and cross-track direction (293 meter amplitude), and an along-track drift (from -63 meters to -373 meters) with periodics (on the order of 40 meters). These are sizable differences that can be attributed to the difference in range station bias values. Table 2.5 shows the difference between the reported range station bias values used in Case 2 and the estimated values obtained from Case 1.

Table 2.5: Real Data Range Bias Differences

Station Number	Estimated - Reported (m)
1	-11.26
2	-16.70
3	0.75
4	-0.10
5	7.34
6	13.75
7	37.06
8	42.53

Part of the bias differences in Table 2.5 can be attributed to atmospheric effects. The data processing did not include atmospheric effects, and the differences have some elevation angle dependence. However, there does appear to be differences between the reported values and the

estimated values aside from atmospheric effects. Consider Stations 6 and 7, these stations are collocated so the atmospheric effects should be similar for both. Yet the bias differences are on the order of 20 meters. For Stations 1 and 2, the difference is over 5 meters. Either the calibration for these stations is poor or the bias solutions are poor. It should be pointed out that maintaining calibration of these radio transponder sensors is nontrivial considering the bias drift in the sensors and the coupling with the satellite radio transponder delays.

Next, a data simulation was set up to replicate the real range data scenario. The stations and tracking patterns (passes and density) were represented as closely as possible to reflect the real world conditions. Noise was added to the simulated data based on the observation standard deviation reported from the real data cases. Biases were added to all stations based on the real data Case 1 range bias solutions. The Case 1 real data solution was used as the "truth" orbit from which the simulated observations were constructed.

Fits were then performed to the simulated data: one case, SimCase 1, in which all range station biases were estimated and another case, SimCase 2, in which the reported bias values (different from the truth biases by the values listed in Table 2.5) were used. The *a priori* bias values for both cases were the reported bias values (unless otherwise noted, the rest of the data simulations used the "truth" values as *a priori* guesses to speed convergence). The SimCase solutions were then compared to the "truth" orbit used to construct the simulated observations.

Comparing SimCase 2 to the truth orbit showed periodic differences in the radial direction (24 meter amplitude, 48 m from peak to peak) and cross-track direction (299 meter amplitude), and an along-track drift (from -62 meters to -361 meters) with small periodics (on the order of 40 meters). This confirms the notion that range errors, in the form of biases for this case, lead to large position errors in geosynchronous orbit determination.

Table 2.6 lists the orbit differences between the truth orbit and real data solution, Case 2, and simulated data solution, SimCase 2. The table shows that the data simulations are representative of the real world conditions. Figure 2.6 summarizes this data simulation verification/validation procedure.

Table 2.6: Real Data and Simulated Data Comparisons

Difference (m) from SimCase 1, "truth"	Real Data Case 2	Sim Data SimCase2
Radial Periodics	24	24
Cross-Track Periodics	293	299
Along-Track Min,Max	-63,-373	-62,-361

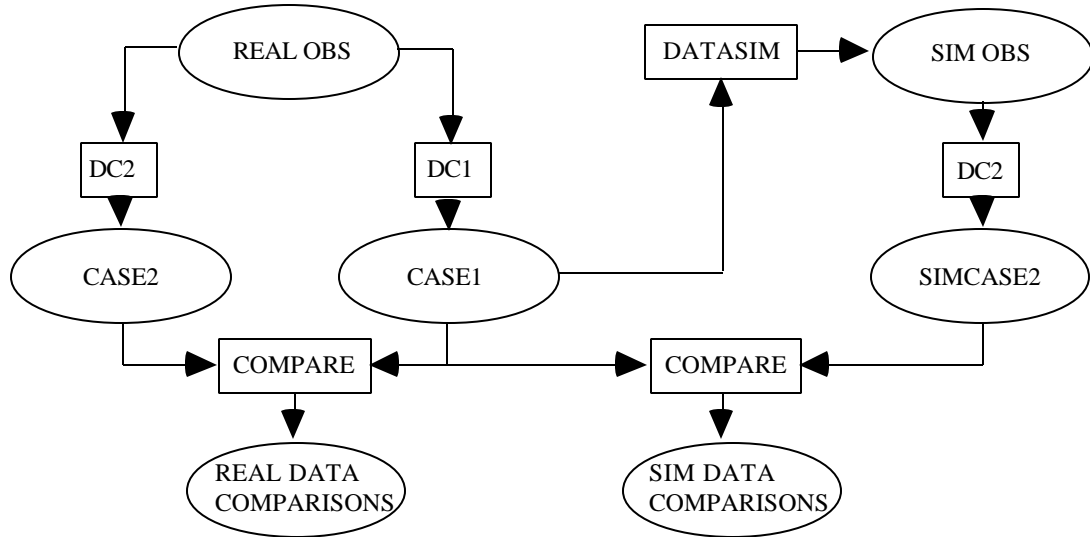


Figure 2.6: Data Simulation Validation Procedure

It is interesting to note that orbital accuracy from real data studies is usually inferred from solution overlaps; if the same bias errors are present in the overlapping real data solutions (i.e. if the reported bias values are used in both fits), the along-track biases will effectively cancel in the overlap comparison leaving the analyst unaware of the large errors!

Comparing SimCase 1 to the truth orbit showed periodic differences in the radial direction (0.6 meter amplitude, 1.2 m from peak to peak) and cross-track direction (1.3 meter amplitude), and an along-track drift (from -31 meters to -35 meters) with small periodics (on the order of 1 meter). Table 2.7 shows the difference between the SimCase 1 range station bias solutions and the truth values used in the simulated observations.

Table 2.7 shows bias solution errors below 3.5 meters. These results appear to be consistent with the real data cases and show that the biases can be estimated given the amount of data available for this satellite. However, the amount of error remaining in the range stations bias solutions does lead to an along-track bias of 30 meters.

Table 2.7: Simulated Data Range Bias Differences

Station Number	Estimated - Truth (m)
1	3.26
2	3.42
3	0.06
4	0.05
5	-1.33
6	-2.79
7	-3.21
8	-1.01



## **Chapter 3: Results**

### 3.1 Mission Support Analysis and Results

The Mission Support Analysis and Results section is broken up into four subsections: range-only, extensive range and angles, limited range and angles, and extensions to other data types.

The Range-Only section investigates the limitations of range-only orbit determination for a geosynchronous satellite with an extensive range tracking network. Studies investigate how the solution accuracy changes with the length of fit span, different inclinations, and leaving a station bias unestimated.

The Extensive Range and Angles section investigates how improved angular observations impact the geosynchronous orbit determination problem given an extensive range tracking system. Studies investigate how the number of optical stations, the density of the angular observations, the number of nights of optical tracking, different inclinations, and the length of the fit span affect the solution accuracy.

The Limited Range and Angles section looks at how the improved angular observations affect the geosynchronous orbit determination problem given a more limited range tracking system. First, the range-only problem is revisited to see how the solution is affected by fewer range stations. Next, improved angular observations are added to the limited range scenario. Then studies are performed to investigate the use of single site range and angles orbit determination and angles-only orbit determination.

The Extension to Other Data Types section is a discussion on the potential of improved angular observations to supplement other data types such as SLR and GPS data.

#### 3.1.1 Range-Only

In the range-only studies, an effort is made to understand the limitations of the range-only geosynchronous orbit determination solution given an extensive tracking system.

Table 2.5 shows that there are large differences between the reported bias values and the estimated bias values for all of the range stations. In SimCase 1, it was shown that the biases could be estimated to the 3.5 meter level (recall Table 2.7).

Assuming the real data Case 1 bias solutions for Stations 6 and 7 are accurate to 3.5 meters and that the differences between the bias solutions and the reported values are on the order of 10-20 meters, one must then conclude that the range station calibration bias values can not be much more accurate than 10-20 meters. The calibration must be on the several meter level (better for some stations, worse for others). The SimCase 1 results showed that bias errors on the 3 meter level lead to a 30 meter along-track error in the orbit solution. It would appear that the reported bias values have errors larger than 3 meters and using them results in considerably larger orbital errors (recall SimCase 2).

Figure 3.1 shows orbital errors for the best range-only orbit solution where all biases were estimated. This solution corresponds to SimCase 1 discussed in the data simulation validation, Section 2.5.2.

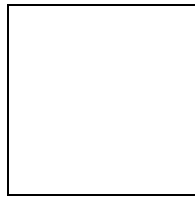


Figure 3.1: Best Range-Only Orbit Solution Errors

To improve the orbit determination accuracy for a geosynchronous orbit, the range station biases must be better determined. The following subsections investigate how the bias solution errors and resulting orbital errors change with the length of fit span and different inclinations. Studies also investigate the affect of not estimating a bias for a single range station.

#### 3.1.1.1 Variable Fit Span

Studies were performed to see if the bias solutions could be improved by changing the amount of data used in the fits. If the fit span is shortened to below 9 days, the bias solutions worsen; there is not enough data to estimate the biases effectively. If the fit span is lengthened to 13 days, the bias solutions do not improve; this can be partly attributed to the uncertainty in the dynamic models over longer periods of time. Table 3.1 shows the real data bias solution standard deviations for the 9 and 13 day fit spans. The 9 day case corresponds to Case 1. The standard deviations for the 9 day fit are fairly

consistent with the errors in the simulated data bias solutions, SimCase 1 (Table 2.7). The differences in the bias solutions are on the same order of magnitude as the standard deviations. When estimating station biases, there will always be some uncertainty in the solutions.

Table 3.1: Real Range Data Bias Solution Standard Deviations

Station	9 Day Fit (m)	13 Day Fit (m)
1	7.89	8.42
2	7.91	8.51
3	0.18	0.14
4	0.16	0.14
5	2.87	3.09
6	7.23	7.76
7	7.22	7.75
8	2.26	2.41

### 3.1.1.2 Observability at Lower Inclinations

Next, the effect of lowering the geosynchronous orbit's inclination on the bias solutions was investigated. Range-only simulation studies were performed for satellites at approximately  $9^\circ$  (as in SimCase 1),  $4^\circ$ , and  $0^\circ$  inclinations. The other initial orbital elements (semimajor axis, eccentricity, etc.) were kept the same for the three cases. The results show that observability of the range station biases is lost as the inclination is lowered. With less observability, the bias solutions get worse. As the bias solutions get worse, the orbit solutions get worse. Table 3.2 shows the bias solution errors for the three different inclination cases. Table 3.3 shows the orbital errors. The  $9^\circ$  inclination case differs slightly from SimCase 1 since slightly different bias values and initial conditions were used. For the  $0^\circ$  inclination case, Station 8 was not visible, and all of the Station 6 observations were edited out in the differential correction process.

Table 3.2: Bias Errors for Range-Only Inclination Cases

Station Number	$i=9^\circ$ (m)	$i=4^\circ$ (m)	$i=0^\circ$ (m)
1	2.91	7.78	529.82
2	3.06	7.92	530.33
3	0.07	0.13	6.41
4	0.05	0.09	6.52
5	-1.09	-2.86	428.00
6	-2.47	-6.92	N/A
7	-2.88	-7.33	-482.86
8	-0.93	-2.31	N/A

Table 3.3: Orbit Errors for Range-Only Inclination Cases

Difference (m) from truth	$i=9^\circ$	$i=4^\circ$	$i=0^\circ$
Radial Periodics	0.6	0.6	1.8
Cross-Track Periodics	1.7	1.9	127
Along-Track Min,Max	-27,-31	-78,-81	-5444, -5457

Some additional discussion on the loss of the range station bias observability appears to be in order. For a geostationary satellite (a geosynchronous satellite with zero inclination and eccentricity), the range-rate to any ground station, assuming two-body dynamics, is zero. Thus, any geostationary satellite will have the same zero range-rate to any ground station regardless of the position of the geostationary satellite or the ground station. With zero range-rate, the range history for any geostationary satellite will be constant. By allowing a free bias term in the range observation model, the satellite position is unconstrained to be anywhere in the geostationary ring; in essence, the longitude is unobservable.

Of course, perturbations will disrupt any true geostationary orbit but the range-rate is still small enough to make estimating all range station biases for a near geostationary case difficult with range-only data.

### 3.1.1.3 A Station Bias Not Estimated

Clearly, one can not solve for all biases at lower inclination orbits with only range data. The next step would be to solve for all station biases except one. Simulation studies indicated that it is unwise to choose a station that was at the same longitude as the satellite when deciding which bias not to estimate. Doing so results in larger errors. For these studies, it was decided to leave the bias in Station 5 unestimated.

Fits to the simulated observations for the original  $9^\circ$  inclination orbit were generated for cases having 0, 1, 5, and 10 meter errors in the Station 5 bias. The rest of the station biases were estimated. Table 3.4 shows the relationship between the error in the Station 5 bias and the resulting along-track orbit error; the trend appears linear as shown in Figure 3.2. Additional studies to determine this relationship mathematically and to generalize for other stations and satellites were not undertaken; however, the studies observed that if the station with the unestimated bias is at the same longitude of as the geosynchronous satellite, the slope of the linear trend was several times larger. For instance, not estimating range biases for Stations 3 and 4 results in close to 100 meters of along-track error despite errors of only 0.75 meters and -0.10 meters in the station biases. Reference 82 outlines analytic methods which would likely provide insight into how station locations influence orbit solutions.

Recall Table 2.5 to see that the difference between the estimated station bias and the reported value was 7.34 meters which would result in an long track error of over 200 meters. If the calibrated value of the range bias were 1 meter, the along-track bias would still be on the order of 30 meters.

Table 3.4: Single Station Bias and Resulting Along-Track Errors

Station 5 Bias Error (m)	Along-Track Bias (m)
0	0
1	29.5

5	144
10	285

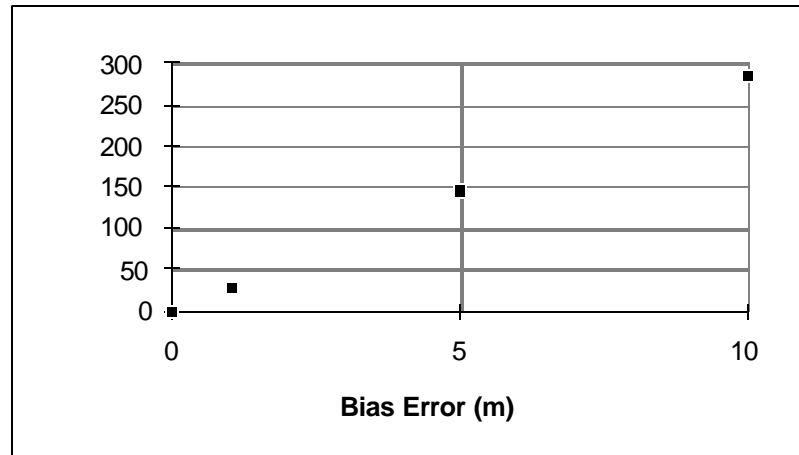


Figure 3.2: Along-Track Error as a Function of a Single Station Unestimated Bias Error

#### 3.1.1.4 Summary

From the range-only studies, it was observed that the reported bias values of the range stations are accurate to the several meter level at best. All range biases can only be estimated for inclined orbits, and that still leaves up to several meters of uncertainty in the solutions. Not choosing to solve for one or more biases is limited by the error in the unestimated biases which can lead to fairly large orbital errors. Under all circumstances it was found that small errors in the range observations lead to significant along-track errors in the orbit solutions. Thus, the range-only solutions are limited by the accuracy of the range sensor calibration or the ability to solve for the sensor biases. If the biases are very well known, the range-only solution has proven to be quite accurate; however, for the 9° inclination case presented, the calibration is poor and estimating biases has proven to deliver orbits only to the 30 meter level and possibly much worse for lower inclination cases.

Figure 3.1 shows orbital errors for the best range-only orbit solution where all biases were estimated.

### 3.1.2 Extensive Range and Angles

After recognizing the limitations of range-only geosynchronous orbit determination, improved angular observations were introduced to the simulations studies.

In all of the simulation cases involving angular data, 1" of noise (one standard deviation) was added to the right ascension observations, and 0.5" of noise was added to the declination observations. This is a reasonable assumption based on current Raven data processing and the improvements expected in the near future from new star catalogs and refined end point detection. No biases were added to the angular observations. This assumption is based on the ability of optical sensors to calibrate themselves using objects with well known positions such as reference stars or GPS satellites.

The primary range and angles scenario included the same range stations and observations as the primary range-only case (reflecting the real world tracking for this satellite) and two optical sensors. The optical sensors were located in Albuquerque, New Mexico, and Maui, Hawaii, also the location of two Raven telescopes. Some studies included a third optical site at Vandenberg AFB, California, collocated with Range Station 3.

It was assumed that the optical sensors could track six out of the nine nights of the fit span. This is a reasonable assumption based on the history of the Raven sites. Actually, the Raven telescope in Albuquerque was able to track the satellite eight out of the nine nights during this particular fit span. Unfortunately, the observations were not available for this study due to the image processing problems discussed in Section 2.4.1.3. Each sensor tracked for eight hours each night in the simulation studies. For most of the simulated cases, the tracking was distributed such that the Maui station tracked on the nights of January 18-23 and the Albuquerque station tracked on January 20 and January 22-26. The simulations also assume the optical sensors could record observations at a rate of one observation pair (right ascension and declination) per minute. This roughly reflects the data collection ability of the current Raven sensors.

Like the real and simulated data cases described in the data simulation validation, the estimated parameters in the differential correction process included position, velocity, reflectivity



coefficient, along-track acceleration, and all range biases. In all cases the differential correction process weighted the observations according to the amount of noise added in the data simulation.

The primary range and angles case described above (2 optical sensors, 6 nights tracking from each, 8 hours per night, 1 obs pair per minute) reflects a scenario in which two telescopes are dedicated to tracking the geosynchronous satellite. Other cases are variations of this scenario in which parameters were varied, such as the number of optical tracking stations, nights of optical tracking, and density of the angular observations. Studies also investigate the effect of lower inclinations and shorter fit spans on the range and angles geosynchronous orbit determination problem.

The primary data simulation case produced 2886 observation pairs from each optical station for a total of 11544 angular observations, compared to 827 range observations from the eight simulated radio transponders.

Fitting to the range and angles data produced outstanding results. Table 3.5 contains the bias estimation errors, Table 3.6 provides the orbital errors for the range and angles case in comparison to the best range-only case, and Figure 3.3 plots the orbital errors for the range and angles case over time.

Figure 3.3 shows the along-track bias due to the uncertainty in the bias solutions is gone. The bias solutions themselves are an order of magnitude better than in the range-only case. It appears that the range and angles solution has difficulty in capturing the along-track acceleration. This results in a small drift in radial error and a parabolic run-off in the along-track direction. Closer study of the range-only cases shows a similar along-track run off masked by the scale of the along-track errors.

Table 3.5: Range and Angles Range Bias Errors

Station Number	Estimated - Truth (m)
1	0.21
2	-0.11
3	0.03
4	-0.04
5	-0.27
6	0.31
7	0.05

8	0.22
---	------

Table 3.6: Range and Range and Angles Orbit Errors

Difference (m) from Truth	Range-Only	Range and Angles
Radial Periodics	0.6	0.2
Cross-Track Periodics	1.7	1.9
Along-Track Min,Max	-27,-31	0, 2.5

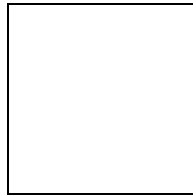


Figure 3.3: Primary Range and Angles Orbit Solution Errors

The range and angles orbit solution is more accurate than the range-only case. The range and angles case did, however, include two more viewing stations (only one was geographically distinct) and an additional 11544 observations obtained from long, dense passes. To demonstrate the angular observations do, in fact, bring additional, useful information to the orbit determination process, a range-only case replicating the primary range and angles tracking scenario was created. Here, the optical sensors in Albuquerque and Maui were designated as radio transponders collecting range. The tracking schedule was kept identical to the range and angles case. A bias was added to the new range stations since biases are a real world characteristic of these sensors and, as demonstrated above, calibration can be poor. The new biases were included as estimated parameters in the differential correction.

The fit to the 10 station range case showed improvement over the 8 station range-only case but bias uncertainties and along-track errors remained. The orbit solution had 0.4 meter (0.8 meter peak to peak) radial periodics, 5.2 meter cross-track periodics, and an along-track bias of approximately 20 meters. Clearly, the angular observations provide a different type of information that is very valuable to the geosynchronous orbit determination problem.

It should be noted that the 10 station range case contained fewer observations than the range and angles case since the Albuquerque and Maui stations produced one range observation every minute of tracking instead of two angular observations. This does not impact the conclusions, however, since the angular observation density can be decreased to one observation pair every two minutes and a similar level of accuracy is maintained (to be discussed more later in this section).

Once it was determined that the improved angular observations could help improve geosynchronous orbit determination accuracy, studies were performed to investigate how much angular data is required to make significant improvements.

### 3.1.2.1 Number of Optical Sensors

The first parameter considered was the number of optical stations. Several scenarios were studied where the number of observations (total nights tracking and observation density) were kept equal while the number of viewing stations was varied between one and three. Table 3.7 shows the orbit errors for the three most telling cases (12 total nights tracking, 1 obs pair/minute). Here the distribution was kept identical across the three cases. For the one station case, the Maui station coordinates were changed to coincide with the Albuquerque station; for the three station case, two nights of tracking from Albuquerque and Maui were transferred to a station at Vandenberg AFB.

Table 3.7: Number of Optical Stations and Orbital Errors

Optical Stations	1	2	3
Radial Periodics (m)	0.2	0.1	0.2
Cross-Track Periodics (m)	1.9	1.5	1.4
Along-Track Min,Max (m)	0,2.5	0,3.1	0,3.6

Table 3.7 shows little variation from one to three stations. Figure 3.4 shows the along-track bias as a function of the number of optical sensors for several different tracking scenarios. Keep in mind that the observation distribution varies between some of the cases and this affects the results. There is also some variance from case to case that may be on the order of several meters. In general, it appears that the number and location of the viewing stations has little impact on the orbit accuracy with all other things (observation distribution and number) being equal.

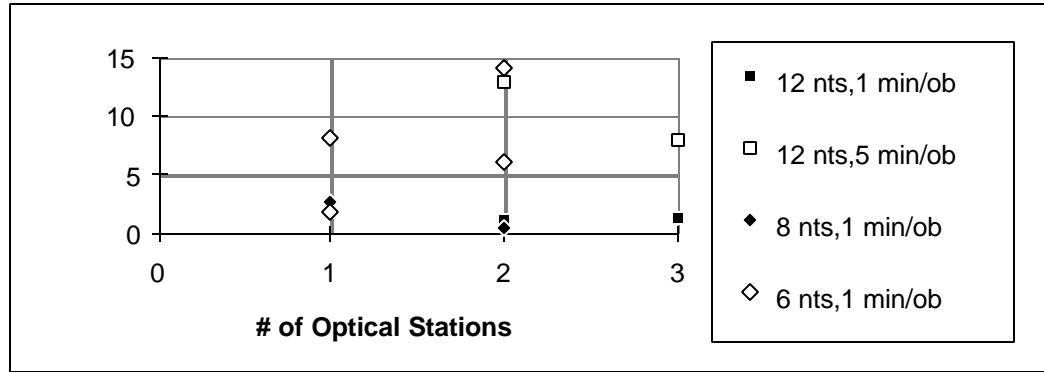


Figure 3.4: Along-Track Accuracy as a Function of Optical Station Number

### 3.1.2.2 Optical Observation Density

After varying the number of optical viewing stations, several simulation cases were performed varying the density of the angular observations. In addition to the primary case density of one observation pair per 1 minute, data simulations generated cases where the angular observations were collected at the rate of one observation pair per 2, 5, 10, 20, and 40 minutes. Three scenarios were considered: two optical stations tracking for six nights each (12 nights total), two optical stations tracking for four nights each, and three optical stations tracking for six nights each. Table 3.8 shows the along-track bias for all of the cases, and Figure 3.5 plots the information. In both the table and the figure, the along-track bias is taken as the mean of the absolute minimum and maximum along-track errors.

Table 3.8: Along-Track Error as a Function of Optical Density

Density (min/obs)	3 sta, 18 nts (m)	2 sta, 12 nts (m)	2 sta, 8 nts (m)
1	1.4	1.2	0.6
2	1.4	2.5	3.4
5	7.5	8.0	3.0
10	13.7	7.4	6.9
15	2.3	5.0	18.5
20	12.9	17.4	16.6
40	15.8	21.2	N/A

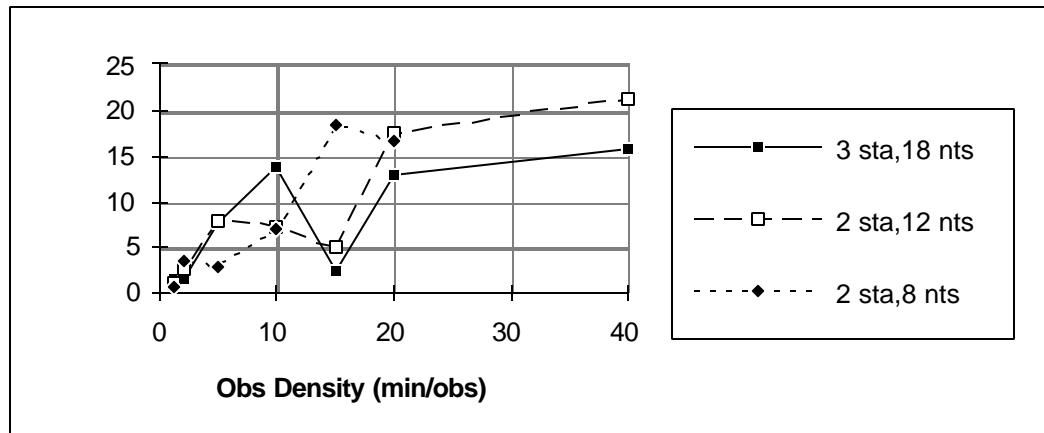


Figure 3.5: Along-Track Accuracy as a Function of Optical Data Density

Both Table 3.8 and Figure 3.5 show a fair amount of uncertainty in the solutions for the 5 to 15 minute per observation density results. The figure does indicate a general trend for the along-track error as a function of observation density, however. It appears that for all of the cases examined, along-track biases are present in the solutions with optical observation densities less than two minutes per observation pair. It also appears that the error/density relationship is a function of the number of nights of tracking; the 18 nights tracking case fairs better than the 12 and 8 nights tracking cases. This dependence could be linked to the total number of observations or the distribution of the observations.

### 3.1.2.3 Nights Tracking Optically

Some links of orbit accuracy to the number of nights of optical tracking have already been observed. The next data simulation cases were performed to investigate the dependence of orbit accuracy on the number of nights of optical tracking. The variable number of nights scenarios included several different data distributions; even with an equal number of observations, different data distributions produce varying orbit accuracies. In practice, weather conditions dictate the number of nights tracking and observation distribution from the optical sensors; one should not expect to have more than six out of nine nights of clear tracking for the optical sensors on average. These studies try to understand, in a general sense, how the orbit accuracy degrades with fewer nights tracking.

Simulations were conducted ranging from one to three optical stations, over 6, 8, 10, 12, and 18 nights with an observation density of one observation pair per minute. Figure 3.6 shows the along-track errors as a function of the number of nights of optical tracking. Each data point in the figure represents the along-track error for a data simulation scenario. Again, the along-track bias is taken as the mean of the absolute minimum and absolute maximum along-track errors. The figure shows that along-track errors become prevalent below eight nights of optical tracking. If it is assumed one station can track six out of nine nights, then one must conclude that two optical sensors are required to eliminate the along-track errors. Further studies modeled one and two optical stations with an observation density of ten minutes per observation pair for 6, 8, 10, and 12 days with similar conclusions.

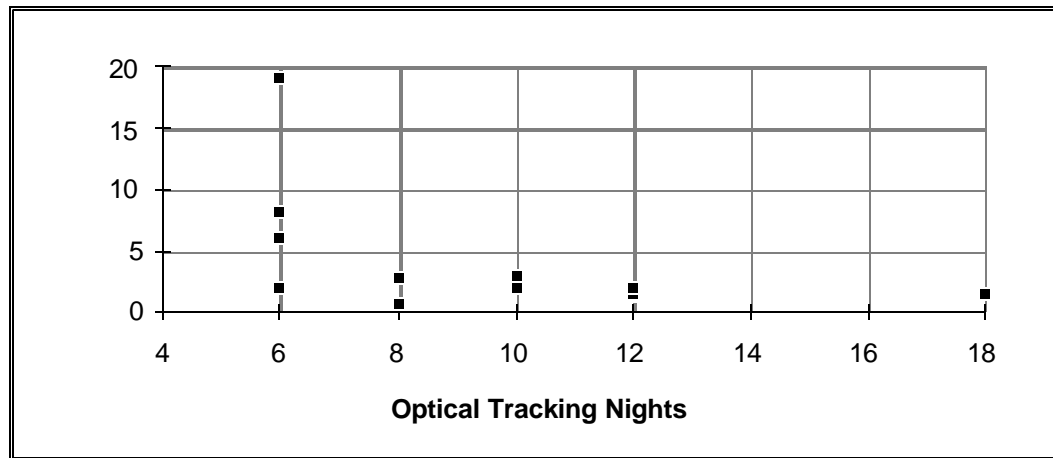


Figure 3.6: Along-Track Errors as a Function of Nights of Optical Tracking

#### 3.1.2.4 Lower Inclinations

For the range-only case, it was observed that it becomes more and more difficult to estimate the range station biases as the geosynchronous orbit inclination decreases. For the  $9^\circ$  inclination case, the biases could be effectively estimated to a greater accuracy level than the apparent accuracy of the reported bias values. For the  $0^\circ$  inclination case, the bias solutions were terrible, limiting the range-only case to the accuracy of the reported bias values.

For the  $9^\circ$  inclination case, it was shown that supplementing the range observations with improved angular observations allows for the estimation of all bias values far more effectively and reduces all resulting orbital errors to the meter level. With the lower inclination cases, similar results were produced. Table 3.9 contains the orbital errors for  $0^\circ$ ,  $4^\circ$ , and  $9^\circ$  inclination cases using the primary range and angles tracking scenario (two optical stations, 12 nights tracking, one observation pair per minute). Compare the values in Table 3.9 to the range-only values in Table 3.3.

Table 3.9: Orbit Errors for Range and Angles Inclination Cases

Difference (m) from truth	$i=9^\circ$	$i=4^\circ$	$i=0^\circ$
Radial Periodics	0.2	0.1	0.3
Cross-Track Periodics	1.5	1.6	2.3
Along-Track Min,Max	0, 2.9	0, 2.7	0, 2.1

### 3.1.2.5 Shorter Fit Spans

The additional volume of angular observations allows the fit span to be reduced and still accurately solve for all range station biases. For the range-only case, at least nine days of tracking were needed to estimate the biases effectively, and the orbit still contained 30 meters of error. For the primary range and angles case, reducing the fit span from nine to five days did not reduce accuracy at all. When reducing the fit span to further, the differential correction estimation algorithm did not converge.

To counter the convergence problems over the short fit spans, additional angular observations were added and the range station biases were not estimated. A data simulation was constructed with the same range station tracking as in the primary range-only and range and angles scenarios and optical tracking from the Albuquerque and Maui sites on both January 18 and 19. Each optical sensor tracked for eight hours per night collecting one observation pair per minute.



A one day fit was attempted but did not converge despite having extra angular data and not estimating biases.

A two day fit was made to the simulated observations and then compared to the truth orbit. Figure 3.7 shows the orbital errors. In the figure, it can be seen that the fit span errors are quite small despite not estimating biases, and the errors only build in the prediction. The option to reduce the fit span could be valuable for satellites where the dynamics are difficult to model over longer fit spans or for post-maneuver orbit determination.

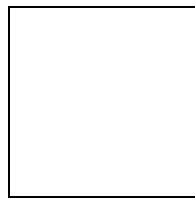


Figure 3.7: Two Day Fit Orbital Errors

#### 3.1.2.6 Summary

In the extensive range and angles cases, it is shown that improved angular observations help resolve the range bias ambiguity present in the range-only cases. With the angular observations, all range biases can be effectively estimated; this includes low inclination cases.

The studies show that eight nights of optical tracking is desirable over the nine day fit span. This implies that two optical stations are needed to produce high accuracy orbits. However, the desired density (2 minutes per observation pair), allows the tracking sites to track two satellites. Thus, two satellites could conceivably share two optical sensors with better results than each satellite monopolizing single optical sensors.

In addition to helping estimate range biases over longer fit spans, the additional angular data allows for accurate orbital solutions over short fit spans, two days was demonstrated, which is valuable for post-maneuver orbit solutions and cases where the long term dynamics are not well modeled.

### 3.1.3 Limited Range and Angles

Up to this point, all of the data simulations modeled an extensive range tracking network: eight stations at five distinct geographic locations spanning from Hawaii to Thule, Greenland, to New Hampshire. In this subsection, scenarios are investigated where the range tracking network is far more limited. Efforts are made to determine if the optical observations allow the number of radio transponder range stations to be reduced or even eliminated (angles-only orbit determination). The  $9^\circ$  inclination case was used for all studies.

### 3.1.3.1 Range-Only

The first studies investigate how reducing the number of tracking stations affects orbit accuracy for the range-only case. The primary range-only case consisted of eight range stations at five distinct locations. A data simulation case was constructed to reduce the number of stations to five; the three pairs of collocated stations were combined into one station. Another simulation reduced the number of stations to three: Station 2 in New Hampshire, Station 3 in Vandenberg AFB, CA, and Station 5 in Colorado Springs, CO. The remaining station tracking passes were distributed among the three stations. In all range-only cases, the total number of observations were kept roughly equal (approximately 827). Biases were modeled and estimated for all stations.

Table 3.10 shows the orbital errors for the eight, five and three station range-only cases. As the number of range stations is reduced, the orbital errors increase. It is particularly interesting to note that the amplitude of the cross-track periodics increases as the number of stations and viewing geometry decreases. Figure 3.8 plots the orbital errors over the nine day fit span for the three station case.

Single site range-only orbit determination is not possible for geosynchronous satellites when the satellite is at the same longitude as the tracking station, and it is very difficult and undesirable when the station is at a different longitude. Reference 82 provides analytic methods which would likely provide more insight into the degradation of the orbit solution with fewer stations.

Table 3.10: Limited Range-Only Orbital Errors

Difference (m) from truth	8 Stations	5 Stations	3 Stations
Radial Periodics	0.6	0.6	0.4
Cross-Track Periodics	1.7	9	15
Along-Track Min,Max	-27,-31	-31,-33	-97,-100

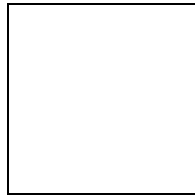


Figure 3.8: Three Station Range-Only Orbital Errors

### 3.1.3.2 Range and Angles

The next simulation studies included improved angular observations to supplement the limited range observations. The first scenario, Case 3a, consisted of adding six nights of optical tracking from Maui with a one observation pair per minute density to the three range station case described above. The orbital errors showed that the angular observations from only six nights of tracking was sufficient to estimate the three range station biases accurately. It appears that with fewer range biases to estimate, fewer angular observations are needed to resolve the range ambiguity. Figure 3.9 plots the orbital errors for the three range station plus single optical station fit.

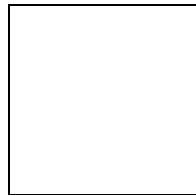


Figure 3.9: Three Range Station Plus Single Optical Station Orbital Errors

Two additional cases were considered where the tracking was limited to the three range stations. This time, the range data was limited to the number of observations collected by the three stations during the eight range station scenario; in essence, the range data from the other five stations is ignored. In addition to the three range stations, one case (Case 3b) included two optical sites (Albuquerque and Maui) and one (Case 3c) included a single optical sensor (Maui). Table 3.11 contains the orbital errors for all three range station plus angles cases. The table shows that accurate orbits are possible when combining a single optical sensor with fewer range stations.

Table 3.11: Three Range Station Plus Angles Orbit Errors

Difference (m) from truth	Case 3a	Case 3b	Case 3c
Radial Periodics	0.2	0.4	0.7
Cross-Track Periodics	1.9	1.1	5.5

Along-Track Min,Max	1.2,2.5	0.5.1	0.6.0
------------------------	---------	-------	-------

### 3.1.3.3 Single Site Range and Angles

With the success of the three range station plus angles cases, single site range and angles orbit determination for the geosynchronous satellites was investigated. The scenario included a single radio transponder, Station 1, and optical sensor both located in Hawaii. Three simulations were performed varying the amount of range data available; all three cases included six nights of optical tracking spanning eight hours per night and collecting an observation pair every minute. The first case, Case 4a, collected only the four passes (approximately 120 observations) present in the eight range station scenario. The second case, Case 4b, combined the Station 1 and 2 passes to collect seven passes (approximately 210 observations). The third case, Case 4c, lengthened the seven passes to collect a total 775 range observations (still less than the eight station case). In all cases, a bias was added to the range data and estimated in the differential corrections.

Table 3.12 contains the orbital errors for the three single site cases. Figure 3.10 plots the orbital errors for Case 4c. From the figure and the table, it can be seen that very accurate orbits can be produced from the single site range and angles scenario. Additional range data helps reduce the radial drift and along-track run off present in some of the range and angles cases. In Table 3.12 Cases 4a and 4b clearly contain some along-track run off.

Table 3.12: Single Site Range and Angles Orbit Errors

Difference (m) from truth	Case 4a	Case 4b	Case 4c
Radial Periodics	4.8	1.0	0.5
Cross-Track Periodics	5.8	9.2	1.3
Along-Track Min,Max	0,36.2	0,9.0	0,-4.6

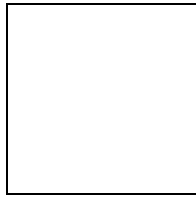


Figure 3.10: Single Site Range and Angles Orbit Determination Errors

#### 3.1.3.4 Angles-Only

The next scenario was designed to determine the potential of angles-only geosynchronous orbit determination. Two cases were investigated. The first reflected the primary tracking scenario of optical sites in Albuquerque and Maui, each tracking six nights spanning the entire nine day fit span and collecting an observation pair every minute. The second case only utilized the optical sensor in Albuquerque (single site angles-only geosynchronous orbit determination). To strengthen the single site result, a seventh day of tracking was added on January 18. Table 3.13 contains the orbital errors for the angles-only cases. Figure 3.11 plots the orbital errors for the two sensor solution.

Table 3.13: Angles-Only Orbit Errors

Difference (m) from truth	2 Optical Sensors	1 Optical Sensor
Radial Periodics	3.2	12.1
Cross-Track Periodics	0.8	6.7
Along-Track Min,Max	0,14.5	0,56

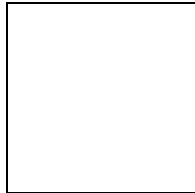


Figure 3.11: Two Station Angles-Only Orbit Determination Errors

For angles-only geosynchronous orbit determination to be successful, fairly long fit spans and a wide data distribution are required. Without range data, the angular observations have a difficult time solving for the radial component of the satellite position in much the same way range-only solutions

have difficulty solving for the along-track component. This radial uncertainty leads to large along-track run off and very poor predictions. Through longer fit spans and data distributions, the period of the satellite helps define its altitude. However, the observation distribution from optical sensors is weather dependent which makes angles-only orbit determination unreliable. It is interesting to note that the studies show the two optical sensor case can theoretically provide better fit accuracy than the eight station range-only case.

### **3.1.3.5 Summary**

In the limited range and angles studies, the results showed that as the number of range stations decreases, the number of angular observations required to accurately solve for all range station biases and bring the orbit determination solution accuracy to the meter level also decreases. For a three station range-only case, orbit errors were on the order of 100 meters; when a single optical site is added, however, the solution accuracy is again brought to the meter level. This indicates that the improved angular observations allow for a reduction in the number range stations required to produce accurate geosynchronous orbits.

An extension of this concept is single site range and angles geosynchronous orbit determination. Here, a single station containing both a radio transponder or other ranging system is combined with an optical sensor providing improved angular observations. The angular observations resolve the along-track and cross-track components of the satellite location and replace the need for multiple range stations to provide viewing geometry and bias estimation; The range observations accurately resolve the altitude of the satellite. The results are very accurate orbits from a compact, cost effective tracking system.

Studies investigated the use of angles-only geosynchronous orbit determination. Two optical stations tracking the geosynchronous satellite without any range support produced orbits on the 10 meter level, but the data requirements made the angles-only option unattractive since weather may not allow for the necessary data collection.

### 3.1.4 Extension to Other Data Types

In this section, the results of the radio transponder range and angles studies are extended to cover the SLR and GPS data types. No further simulations or analysis are undertaken; instead, an understanding of the effect of improved angular observations is combined with knowledge of the other data types to discuss the role these data types could play in geosynchronous orbit determination.

#### 3.1.4.1 SLR

The range-only studies demonstrated that the accuracy of range-only geosynchronous orbit determination is limited by the knowledge of the range station biases or the ability to estimate those biases. Additionally, several stations are needed to resolve the along-track and cross-track components of the satellites position. If several stations are available, however, and the biases of the range observations are well determined, range-only geosynchronous orbit determination can produce accurate results.

Unlike most radio transponder and radar ranging systems, SLR systems are usually very well calibrated. Since SLR systems are used for precise orbit applications, much more care is given to the proper calibration and understanding of the sensor characteristics than for many other data sources. From an accuracy standpoint, SLR systems should be capable of delivering high accuracy geosynchronous orbits.

The limitations of SLR systems in general make this scenario unlikely. Due to the cost of SLR systems, the number of observing stations may not be available to ensure the viewing geometry is suitable for precise orbits or the cost of supporting the necessary number of stations could be high. Additionally, it is unclear how many existing SLR stations are capable of ranging geosynchronous satellites.

By supplementing a small number (one or two) SLR stations with improved angular observations, precise orbits for geosynchronous objects may be produced with far less cost. Combining these data sources does raise a concern about proper data weighting and the ability of the



angular observations to impact the orbit solution in the presence of the very accurate SLR data however.

#### **3.1.4.2 GPS**

The use of GPS data in geosynchronous orbit determination has intrigued many organizations as cited in Section 1.6. If a GPS receiver were placed on board a geosynchronous satellite, the range-rate between the GPS constellation and the geosynchronous satellite should provide for far more accuracy than ground based range-only orbit determination. Selective availability, however, corrupts the GPS observables enough to significantly degrade the orbit solutions.

If selective availability is not a factor, either from being turned off, differential GPS, wide area augmentation system, or the use of a military Y-code receiver, other studies have shown that accurate orbits can be produced using a GPS receiver on board a geosynchronous satellite. The JPL studies show that orbits can be produced to the 5 to 10 meter level using this technique [72]. With selective availability on, however, the results degrade to worse than 50 meters.

Assuming some sort of method is in place to counter selective availability effects, it is not likely worth the effort to procure an optical sensor to provide angular observations if the GPS-only accuracy is below 10 meters.

Currently, selective availability is turned on, there is no standard wide area augmentation system in place, differential schemes would require a GPS ground station on the opposite side of the world from the geosynchronous satellite, and military Y-code receivers are hard to come by even in the military. Therefore, an optical sensor may be a sensible approach to reducing the orbit determination accuracies to the 10 meter level or better. Additionally, with the success of the angles-only studies, optical sensors could be employed as back-ups and provide validation to GPS based and autonomous orbit determination practices.

## 3.2 Space Surveillance Analysis and Results

The Space Surveillance Analysis and Results section is broken up into three subsections: angles-only, range and angles, and real data results. The Angles-Only section investigates the space surveillance scenario using only angular observations in the geosynchronous orbit determination process. Studies investigate how the solutions change when improved angular observations are used in place of traditional accuracy angular observations. Additionally, studies investigate how the number of optical stations affect solution accuracy. The Range and Angles section investigates how improved angular observations impact the geosynchronous orbit determination problem given a small amounts of radar range tracking in addition to the angular data. The real data results are based on the GOES-10 results from Reference 74 and serve to support the data simulation results.

GOES-10, at approximately  $105^\circ$  west longitude, is used as an example in the space surveillance studies. The truth orbit was created based upon the NASA/GSFC radio transponder reference orbit provided as part of the GOES-10/Telstar-401 close approach analysis in Reference 74.

In the simulation studies, data simulations were performed to investigate the impact improved angular observations would have on a geosynchronous space surveillance scenario. First, studies are performed using traditional accuracy angular observations with 10 arcseconds of noise (one standard deviation) in right ascension and 12 arcseconds of noise in declination. These numbers are based on the GEODSS performance parameters in Reference 13. Next, the studies are repeated using improved angular observations with 1.0 arcsecond of noise in right ascension and 0.5 arcseconds of noise in declination. No biases were added to the data since the optical sensors should be well calibrated. The impact of the improved angular observations is measured in the improvement of the orbit determination accuracy fitting to the simulated data.

Up to three optical tracking sites were considered: one in Maui, Hawaii, one in Albuquerque, New Mexico, and one in Millstone Hill, Massachusetts. Raven sites exist in Maui and Albuquerque and the Millstone Hill location was contrived based on the deep space radar location. The primary scenario used only the Albuquerque and Maui sites. Additional angles-only studies investigated how the number of optical sites affect the orbit determination accuracy.

As mentioned in Section 2.1.2 , the number of observations used was based on an assumption of the amount of data the Raven telescopes could collect and a requirement to track over 200 objects. All space surveillance studies assume four images are taken of an object every other night, at 3, 6, 9, and 12 hours UTC, over the span of 20 nights (10 nights tracking total). Each image contains two observations pairs resulting in 80 observation pairs containing both right ascension and declination over the 20 day fit span. The fit is then predicted for 40 days beyond the fit span. This results in a fit plus predict span of 60 days and allows for over 200 objects (theoretically 288) to be tracked per optical site. The time of interest from the study spanned from August 19 to October 19, 1997.

As discussed in Section 2.4, three orbital theories were used: Cowell special perturbation theory, Draper Semianalytic Satellite Theory (DSST), and a version of the SGP4/DP4 general perturbation theory. The Cowell propagator is the most accurate, the DSST propagator using the Fonte-Sabol optimized input deck sacrifices some accuracy for speed, and the SGP4 propagator is far less accurate but much faster. By employing the three theories, the effect of the improved angular observations can be weighed against the accuracy of the orbital theory. When using both the Cowell and DSST theories, a single solar radiation pressure reflectivity coefficient is estimated, in addition to the satellite orbital elements, as part of the orbit determination process; the SGP4 theory does not include solar radiation pressure models.

To provide dynamic mismodeling, the truth orbit was propagated, using Cowell special perturbation theory, with an 8x8 GEM-T3 geopotential while the Cowell and DSST fits used a 4x4 JGM2 geopotential; the SGP4 theory uses a WGS-72 geopotential up to degree 4. Table 3.14 describes the dynamic models used in the space surveillance studies. The satellite theories were discussed in greater detail in Section 2.3.

It should be noted that the tracking scheduled used in this analysis was created by the author and does not reflect any operational procedures of the US Air Force or US Space Command. Additionally, the SGP4 model used in this analysis is the version incorporated into DGTDS by Darrell Herriges in 1987 as part of his Masters thesis work at MIT [69]. This version of SGP4 is not the official version of the SGP4 code used by US Space Command and has not been verified and validated by US

Space Command. No conclusions about the performance of the US Space Command space surveillance operations, in any way, should be inferred from this analysis.

Table 3.14: Space Surveillance Dynamic Models

	Cowell Truth	Cowell Fit	DSST	SGP4/DP4
Geopotential	8x8 GEM-T3	4x4 JGM2	4x4 JGM2 AOG Zonal SPG, $J_2^2$ SPG	Simplified Model through $J_4$ with $n=2,3$ and $m=2$ tesseral correction WGS-72
Third-Body	Solar/Lunar Point Masses	Solar/Lunar Point Masses	Solar/Lunar Point Masses in AOG & SPG with numerical weak time dependence	Double Averaged Solar/Lunar Point Masses to First Order
Solar Radiation Pressure	Spherical S/C, Single Cr	Spherical S/C, Estimate Cr	Spherical S/C, AOG & SPG Estimate Cr	None

### 3.2.1 Angles-Only

In the angles-only studies, data simulations were performed to investigate the impact improved angular observations would have on a geosynchronous space surveillance scenario where all tracking is performed using optical sensors. First, studies are performed using traditional accuracy angular observations with 10 arcseconds of noise (one standard deviation) in right ascension and 12 arcseconds of noise in declination. Then, the studies are repeated using improved angular observations with 1 arcsecond of noise in right ascension and 0.5 arcseconds of noise in declination. The impact of the improved angular observations is measured in the improvement of the orbit determination accuracy fitting to the simulated data. The first studies only consider optical sites in Maui and Albuquerque, but studies are performed to investigate how the number of optical stations affects the orbit solution accuracy.

### 3.2.1.1 Traditional Angular Observations

Three fits were made to the traditional accuracy angular observations. The first used Cowell special perturbation theory, the second used DSST, and the third used SGP4. Table 3.15 gives the maximum and RMS (root mean square) errors for the three cases during the fit and predict spans. Figures 3.12 through 3.14 plot the orbital errors from the truth orbits for the Cowell, DSST, and SGP4 cases, respectively.

Table 3.15: Traditional Angles-Only Space Surveillance Orbital Errors

Satellite Theory	Fit		Fit Plus Predict	
	RMS (m)	Maximum (m)	RMS (m)	Maximum (m)
Cowell	678	1412	2598	8358
DSST	676	1420	1674	3974
SGP4	4658	18140	27240	88052

Figure 3.12 shows that the Cowell fit has substantial periodic errors in all three components. During the fit and predict, the radial errors range from 700 meters to 200 meters and then grow to almost 2 kilometers during the prediction. The cross-track periodics have amplitudes close to 400 meters. The majority of the error growth occurs in the along-track direction. Aside from the periodics which grow to 4 kilometers in amplitude by the end of the prediction period, there is a nonlinear error run-off in the along-track direction. The majority of the along-track error growth can be attributed to the dynamic mismodelling caused by the higher order resonance terms.

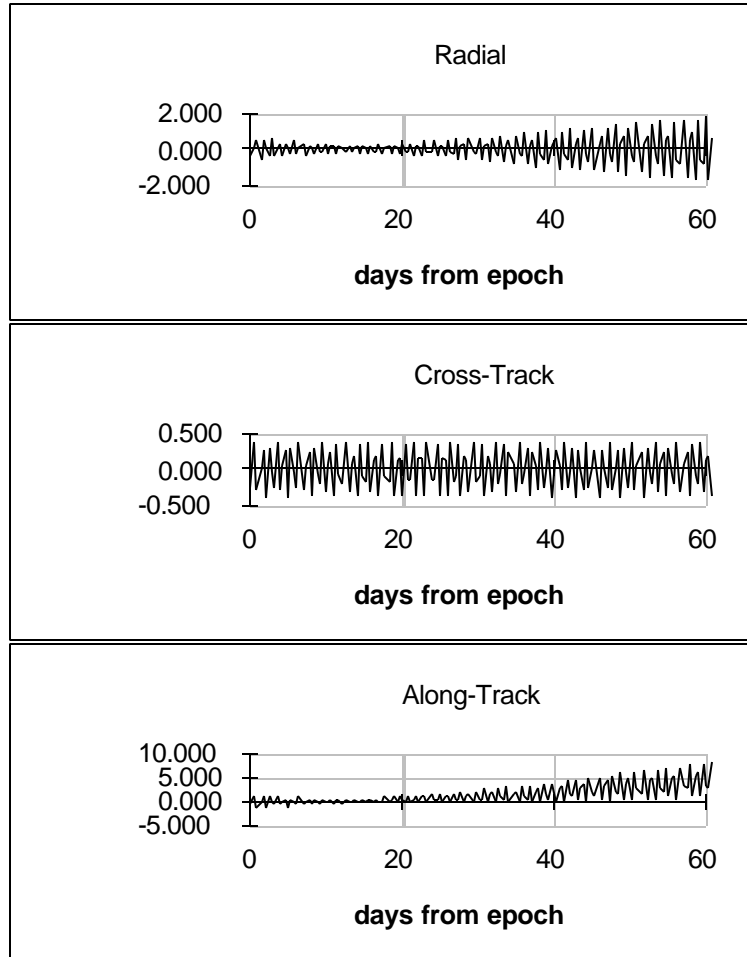


Figure 3.12: Traditional Angles-Only Space Surveillance Cowell Orbital Errors

Figure 3.13 shows that the DSST fit looks a lot like the Cowell fit particularly in the radial and cross-track components. This is not unexpected since the DSST input options used produce an orbit generator that is close in accuracy to the Cowell method. The major difference between the Cowell and DSST fits is the along-track run-off is not nearly as severe in the DSST case. The along-track trend is similar for both cases during the fit span, but the error tends back towards zero for the DSST case rather than run-off like in the Cowell case. No simple explanation was apparent since the DSST theory is only modelling the geopotential up to degree and order 4. These results do not imply that the DSST orbit generator is superior to the Cowell (the truth orbit is Cowell based so the Cowell cases should have a slight modeling advantage) but they illustrate the point that unexpected results often arise in these

types of studies when data is sparse. It is possible that the error growth due to the modelling error and the estimation error have cancelled each other out in this case.

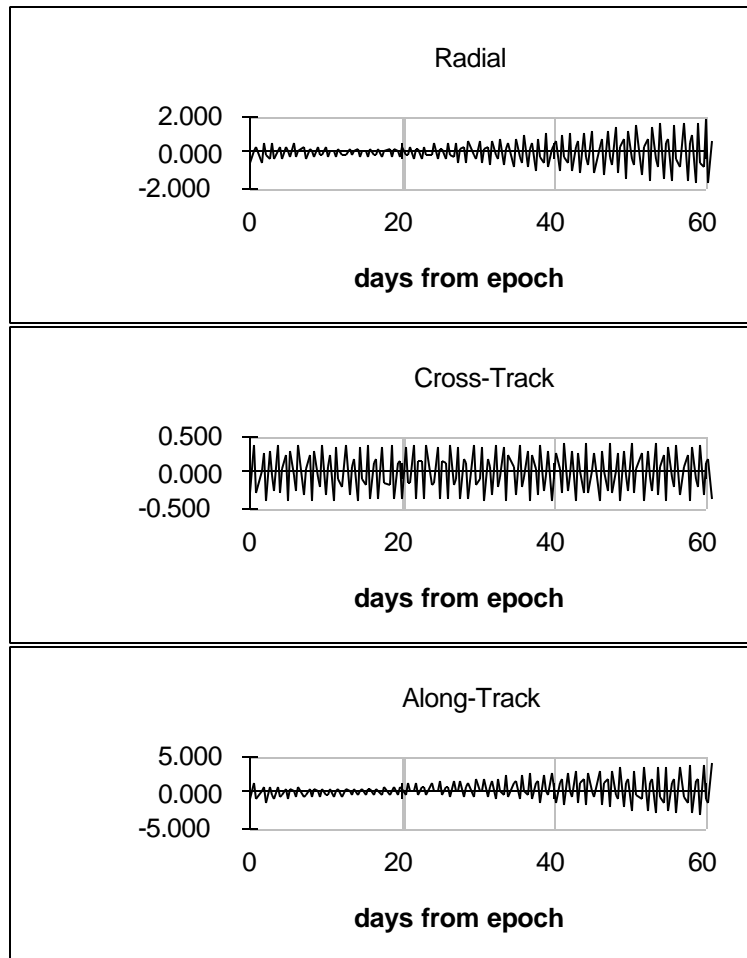


Figure 3.13: Traditional Angles-Only Space Surveillance DSST Orbital Errors

As seen in Figure 3.14, the orbital errors for the SGP4 case are about an order of magnitude larger than the Cowell and DSST cases. The radial periodics range from 4 to 2 to 10 kilometers while the cross-track periodics range from 2 to 1 to near 4 kilometers in amplitude. The along-track periodics are large but are masked by the run-off in that direction which grows to nearly 90 kilometers by the end of the fit span. In the error plots, the effects of dynamic mismodeling can be seen in the cross-track error growth and long periodic changes in the along-track error growth. The magnitudes of these errors are not unexpected due to the limitations of the satellite theory.

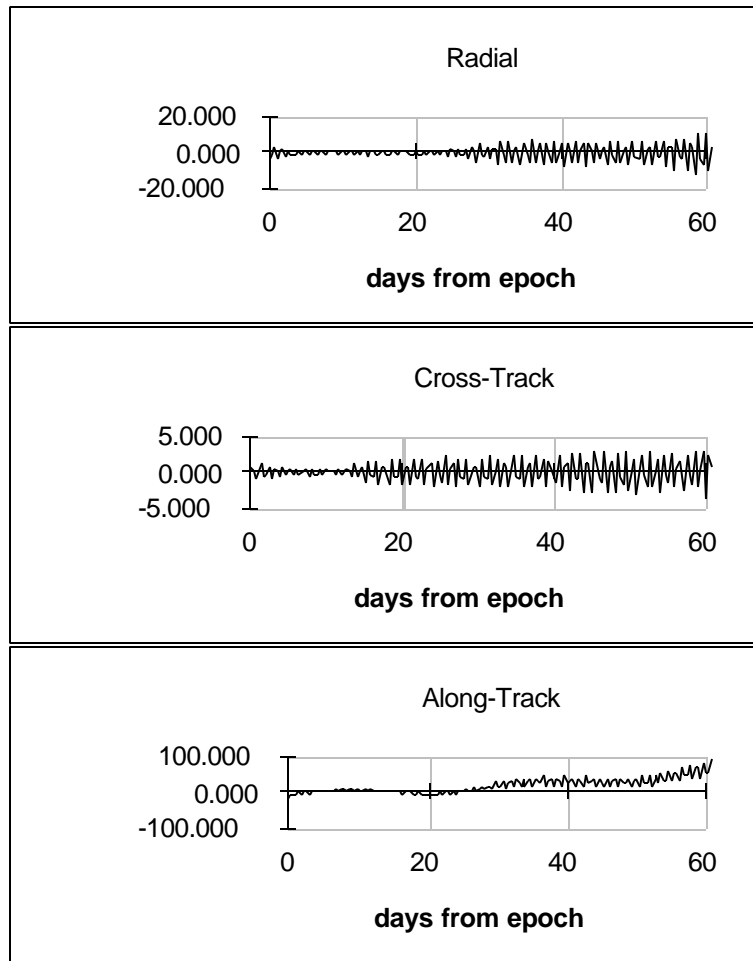


Figure 3.14: Traditional Angles-Only Space Surveillance SGP4 Orbital Errors

### 3.2.1.2 Improved Angular Observations

The next simulation studies used improved angular observations in place of the traditional accuracy observations. As in the traditional accuracy studies, three fits were made to the improved accuracy angular observations using Cowell special perturbation theory, DSST, and SGP4. Table 3.16 gives the maximum and RMS (root mean square) errors for the three cases during the fit and predict spans. Figures 3.15 through 3.17 plot the orbital errors from the truth orbits for the Cowell, DSST, and SGP4 cases, respectively.



Table 3.16: Improved Angles-Only Space Surveillance Orbital Errors

Satellite Theory	Fit		Fit Plus Predict	
	RMS (m)	Maximum (m)	RMS (m)	Maximum (m)
Cowell	91	234	1640	4356
DSST	87	207	660	1972
SGP4	4643	19209	28513	90840

Figure 3.15 shows that the Cowell fit to the improved angular observations has reduced the amplitude of the periodic errors by an order of magnitude in all three components. During the fit and predict, the radial errors range from 70 meters to 25 meters and then grow to 200 meters during the prediction. The cross-track periodics have amplitudes less than 20 meters and the along-track periodics are practically nonexistent in the presence of the along-track run-off. Like the traditional accuracy angles-only case, the along-track run-off is substantial and grows to over 4 kilometers by the end of the predict span. The improved angular observations reduce the periodic errors but appear to have little impact on the along-track error run-off during the prediction. This is not unexpected considering the improved angular observations cannot account for limitations in the dynamic models.

Additional test were conducted using an 8x8 JGM2 gravity model with the Cowell propagator to determine the role of dynamic mismodelling in the along-track error growth. Given the space surveillance tracking scenario, three data simulations were constructed using perfect (zero noise), improved, and traditional accuracy angular observations. Fits were then made to the three cases using a 4x4 and then 8x8 JGM2 geopotential. The results showed that the along-track error was greatly reduced when the 8x8 geopotential model was used. Table 3.17 summarizes these results. It appears that the dynamic mismodelling results in 3.7 km of the along-track error for all three cases.

Table 3.17: Dynamic Modelling and Maximum Along-Track Errors

Observations	4x4 Geopotential	8x8 Geopotential
Perfect	3.78 km	0.10 km
Improved	4.36 km	0.68 km
Traditional	8.33 km	4.65 km

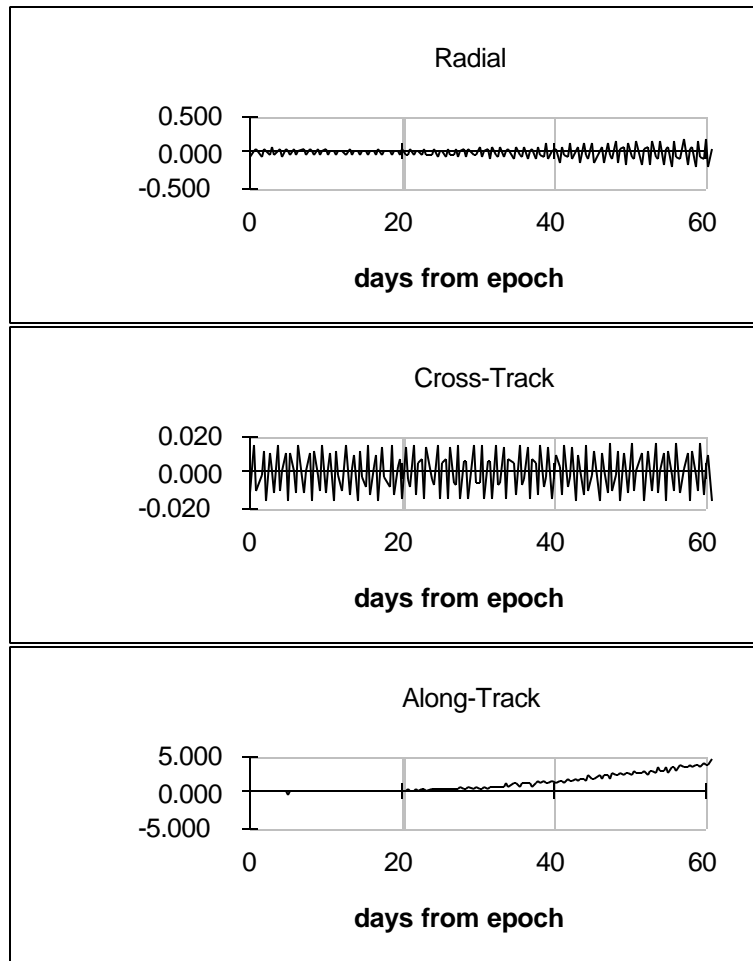


Figure 3.15: Improved Angles-Only Space Surveillance Cowell Orbital Errors

It should be noted that the maximum along-track errors presented in Table 3.17 are a combination of the along-track error run-off and the periodic errors; this is why the traditional angular observation maximum errors are considerably worse than the other two cases. The mean along-track error for the traditional angular observations 8x8 case was around 1 kilometer. Looking at the mean along track error for the three 8x8 cases indicates that the more accurate angular observations do, in fact, reduce the along-track error growth.

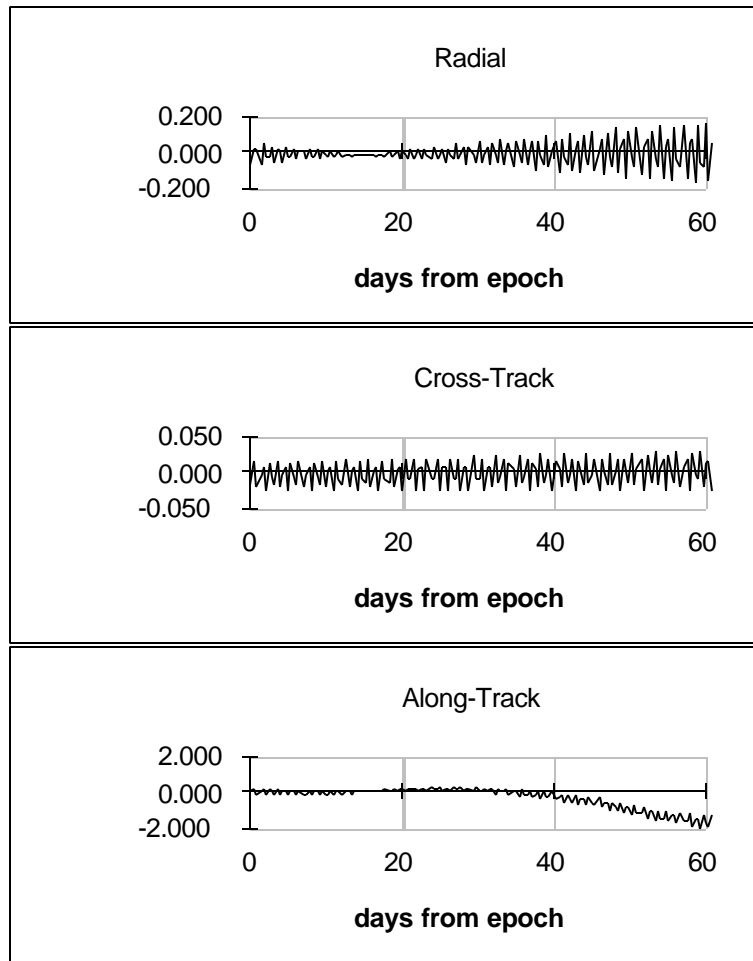


Figure 3.16: Improved Angles-Only Space Surveillance DSST Orbital Errors

Figure 3.16 shows that the DSST fit, once again, looks a lot like the Cowell fit particularly in the radial and cross-track components. The major difference between the Cowell and DSST fits is the along-track run-off back towards zero and begins to run-off in the opposite direction. Like the Cowell case, the improved angular observations greatly reduce the periodic errors in all three components but do not appear to help the along-track run-off in the presence of significant dynamic mismodelling.

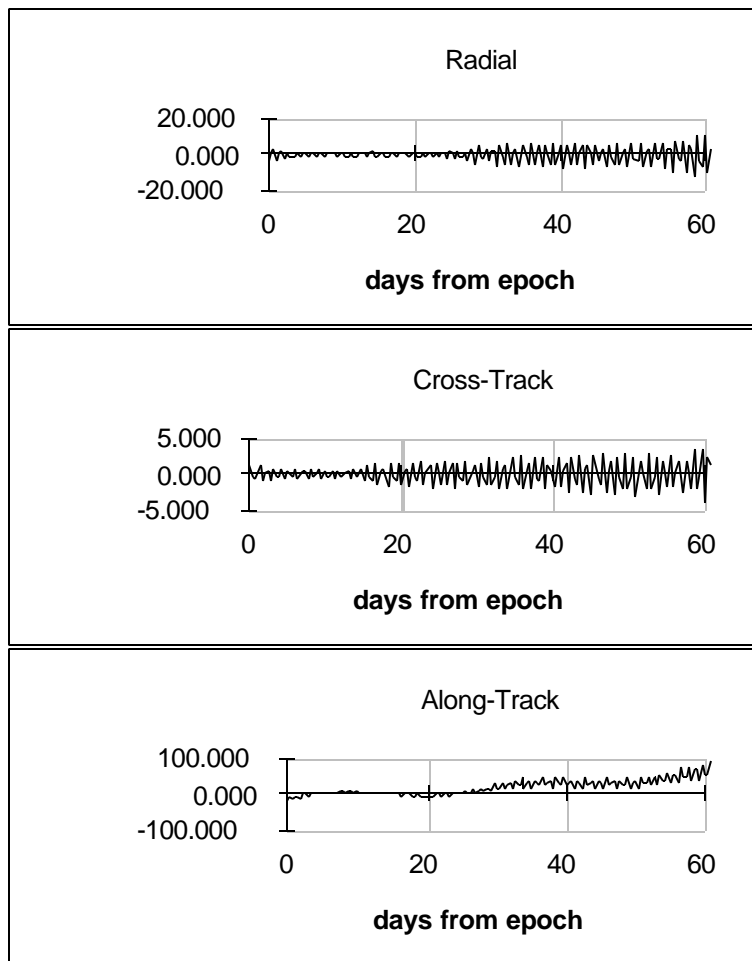


Figure 3.17: Improved Angles-Only Space Surveillance SGP4 Orbital Errors

Figure 3.14 and Figure 3.17 are not identical. As seen in the plots and by the RMS and maximum errors in Tables 3.15 and 3.16, the improved angular observations have little effect when coupled with the low accuracy SGP4 propagator. This is not at all surprising given that the errors in the satellite theory over the 20 day fit span are comparable to the errors in the traditional angular observations. An analogy is entering numbers into a computer; it doesn't matter if you type in 20 or 200 significant digits if the computer can only hold 16 because 16 is all you are going to get out of it.

### 3.2.1.3 Number of Stations

The next set of angles-only simulation studies focused on changing the number of optical stations. Only the Cowell cases were run, but in addition to the two optical station case, one and three optical station cases were investigated. In all cases, the number of observations was kept the same. For the one station case, all images were taken from the Albuquerque optical site. For the two station case, two images were taken from Albuquerque and two images were taken from the Maui station each night of tracking. When three stations were used, two images were taken from Albuquerque and one image was taken from each of the Maui and Millstone Hill sites each night of tracking.

Table 3.18 gives the RMS (root mean square) and maximum orbital errors over the fit and predict span for the three cases using improved angular observations. The table shows that there is only a small improvement when going from one to three optical stations given the same number and data distribution. Cases run with traditional accuracy angular observations provided the same conclusions.

Table 3.18: Number of Stations and Angles-Only Space Surveillance Orbital Errors

Number of Optical Stations	Fit		Fit Plus Predict	
	RMS (m)	Maximum (m)	RMS (m)	Maximum (m)
1	100	264	1684	4520
2	91	234	1640	4356
3	92	244	1652	4390

It was hoped that the three station case might improve the orbital accuracy significantly since three optical stations should be able to get a better altitude fix through triangulation. Perhaps the greatest advantage to more stations would be to provide more observations and a wider data distribution. Perhaps if three sites were tracking simultaneously, the orbit solutions would show more improvement. These additional studies were not pursued. Multiple stations do provide protection against foul weather, however. Weather effects on optical satellite tracking was not taken into account in the space surveillance simulation studies.

#### 3.2.1.4 Summary

From the angles-only results, the value of improved angular observations can be seen in the reduction of periodic errors in the orbit determination solutions when using a high accuracy satellite theory such as Cowell special perturbations or DSST. When coupled with a low accuracy satellite theory such as the DGTDS version of SGP4, the improved angular observations had no impact on the results. Even when using high accuracy theories, however, the improved angular observations do not appear to reduce the along-track error run-off in the orbit prediction in the presence of significant dynamic mismodelling; when an 8x8 geopotential is used, the improved angular observations do help reduce the along-track error growth. If the studies were limited to the fit spans, the improved angular observations could increase the solution accuracy by an order of magnitude. The nature of the space surveillance studies required the consideration of long predictions. By utilizing more optical sensors, perhaps the long predictions could be avoided. The improved angular observations do increase the overall orbit solution accuracy even when taking the prediction into account; the improvement is most significant during the fit and early prediction.

Additional studies showed that the number of optical tracking stations have little impact on the accuracy of the results if the number of observations and data distributions are kept equal. The greatest contribution increasing the number of stations may be able make is increasing the number of available observations, reducing the prediction spans, and providing insurance against foul weather.

### 3.2.2 Range and Angles

The space surveillance range and angles studies mirrored that of the angles-only traditional and improved angular observation studies with the exception that a single pass of radar data was added to the range and angles simulations. All studies considered optical sites in Maui and Albuquerque and a deep space radar located in Millstone Hill. The radar contributed one pass of range data to the simulation studies over the 20 day fit span. The radar pass collected a range value every 30 seconds over 1.5 minutes on August 19, 1997 for a total of four radar range observations. Random noise was added to the range observations based on the observed values from the Millstone Hill deep space radar in Reference 74. Like the optical data, no biases were added to the radar range data since calibrating such a sensor should not be difficult given the ability to track objects with well known positions like GPS satellite. The impact of the improved angular observations is measured in the improvement of the orbit determination accuracy fitting to the simulated data.

#### 3.2.2.1 Traditional Angular Observations

Following the angles-only approach, three fits were made to the range and traditional accuracy angular observations. The first used Cowell special perturbation theory, the second used DSST, and the third used SGP4. Table 3.19 gives the maximum and RMS (root mean square) errors for the three cases during the fit and predict spans. Figures 3.18 and 3.19 plot the orbital errors from the truth orbits for the Cowell and DSST cases, respectively.

Table 3.19: Range and Traditional Angles Space Surveillance Orbital Errors

Satellite Theory	Fit		Fit Plus Predict	
	RMS (m)	Maximum (m)	RMS (m)	Maximum (m)
Cowell	741	1449	1063	2615
DSST	749	1471	2681	7552
SGP4	5069	17768	27806	88994

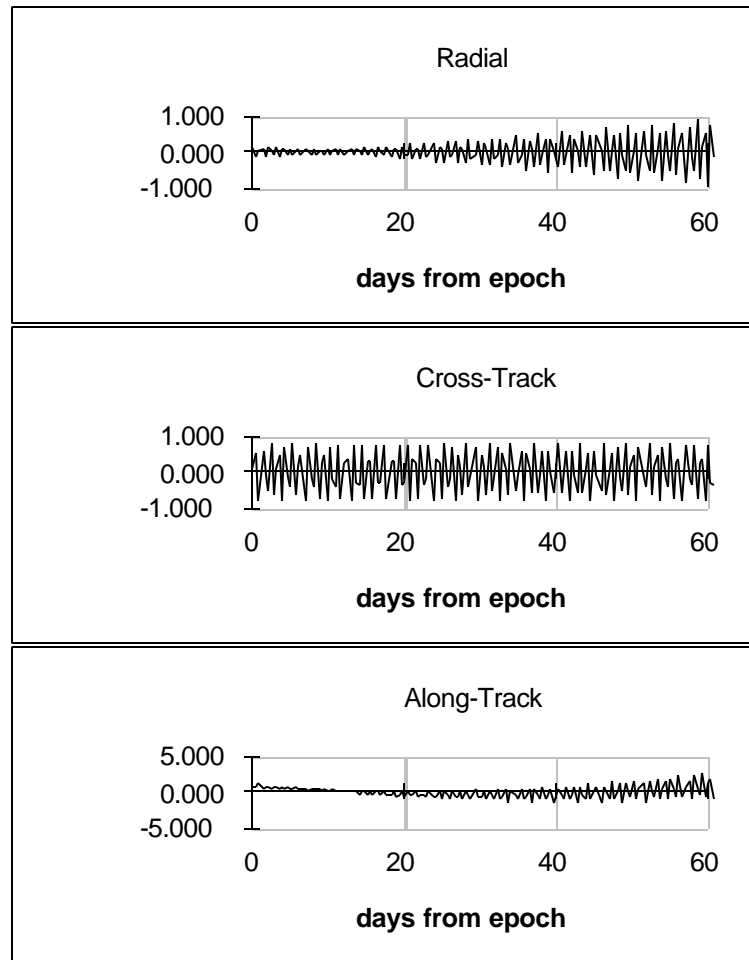


Figure 3.18: Range and Traditional Angles Space Surveillance Cowell Orbital Errors

Like the angles-only case, Figure 3.18 shows that the Cowell fit has substantial periodic errors in all three components. During the fit and predict, the radial errors range from 180 meters to 90 meters and then grow to 800 meters during the prediction. The cross-track periodics have amplitudes of 800 meters which is unexpected since the angles-only cross-track errors were only on the order of 400 meters. The along-track error growth is much better behaved in the range and angles case. Much like the DSST angles-only cases, the along-track error curves back toward zero rather than run-off.



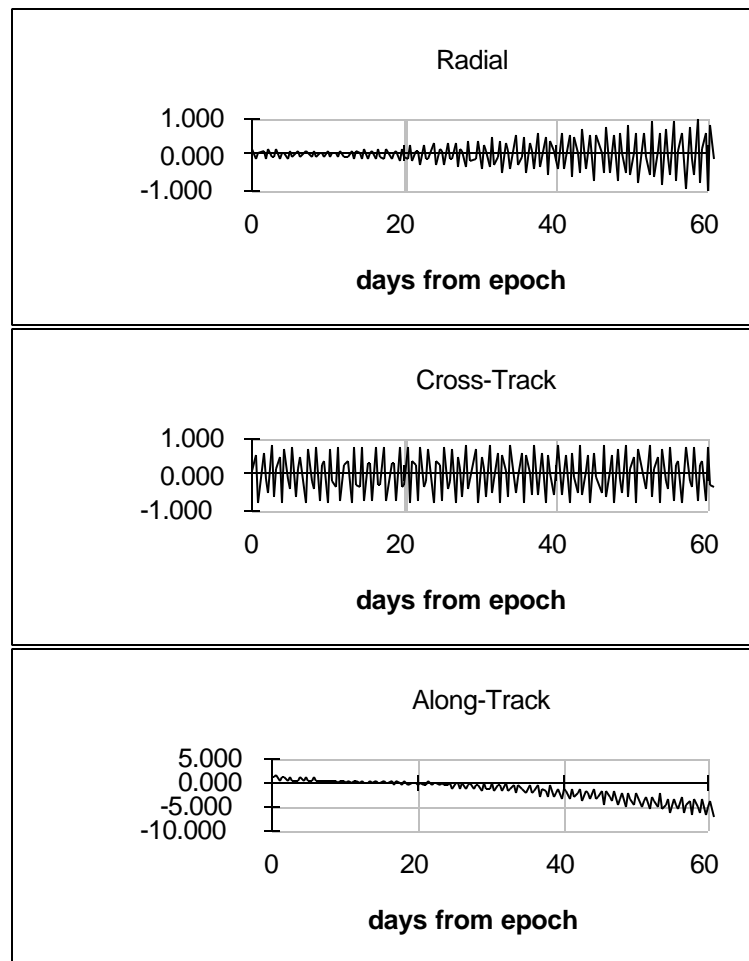


Figure 3.19: Range and Traditional Angles Space Surveillance DSST Orbital Errors

Figure 3.19 shows that the DSST fit again follows the Cowell fit particularly in the radial and cross-track components. In this case the along-track error growth has a substantial run-off unlike in the Cowell case. Again, it is believed this is due to higher order tesseral resonance terms not included in the fit models. For both the Cowell and DSST range and angles cases, the only improvement that can be clearly identified over the angles-only cases is the reduction in the magnitude of the radial and along-track periodics but these are countered by the unexplained increase in the cross-track periodics; the RMS and maximum values of the range and traditional angles cases is comparable to the traditional angles-only cases.

The orbital errors for the SGP4 case are also very similar to the angles-only cases. Again, the magnitudes of these errors are not unexpected due to the limitations of the satellite theory.

### 3.2.2.2 Improved Angular Observations

The next simulation studies used improved angular observations in place of the traditional accuracy observations. As in the previous space surveillance studies, three fits were made to the improved accuracy angular observations using Cowell special perturbation theory, DSST, and SGP4. Table 3.20 gives the maximum and RMS (root mean square) errors for the three cases during the fit and predict spans. Orbital error plots are not given since the error histories are almost identical to the improved angles-only cases shown in Figures 3.15 through 3.17. The only exception is that the along-track run-off for the Cowell and DSST cases are both closer to 3 kilometers by the end of the prediction span as Table 3.18 indicates.

Table 3.20: Range and Improved Angles Space Surveillance Orbital Errors

Satellite Theory	Fit		Fit Plus Predict	
	RMS (m)	Maximum (m)	RMS (m)	Maximum (m)
Cowell	65	146	1429	3584
DSST	94	202	1071	3048
SGP4	5101	22093	29012	91106

The Cowell fit to the improved angular observations has reduced the amplitude of the periodic errors by an order of magnitude over the traditional angular observations in all three components. During the fit and predict, the radial errors range from 2 meters to 500 meters during the prediction. The cross-track periodics have amplitudes of 34 meters and the along-track periodics are practically nonexistent in the presence of the along-track run-off. While the along-track error is very small during the fit, as indicated by the relatively small errors listed in Table 3.20, the along-track run-off grows to 3.5 kilometers by the end of the predict span. The Cowell range and angles cases introduce a new novelty where the case with the improved angular observations actually has a larger along-track run-off than

the traditional angles case. This is unexplained but could be a result of the error growth due to the estimation error and the error growth due to the dynamic mismodelling cancelling each other out..

The DSST fit looked a lot like the Cowell fit in all components with the exception of the direction of the along-track drift illustrated in Figures 3.15 and 3.16. Like the Cowell case, the improved angular observations greatly reduce the periodic errors in all components and the improved angles also reduced the along-track run-off for the DSST case. There is no improvement over the improved angles-only case.

The SGP4 results were almost identical to the traditional angles-only, improved angles-only, and range and traditional angles cases and do not require further discussion.

### 3.2.2.3 A Second Range Pass

Since the single radar range pass had minimal affect on the space surveillance results, an additional pass was added on August 29, 1997. The second pass was similar to the first in that it lasted only 1.5 minutes and produced four range observations. Fits were made to the range and traditional accuracy angular observations and range and improved angular observations using the Cowell and DSST theories. Table 3.21 list the RMS and maximum orbital errors for the DSST cases; the Cowell cases produced very similar results. Figure 3.20 plots the orbital errors for the additional range and traditional angles DSST case and Figure 3.21 plots the orbital errors for the additional range and improved angles DSST case.

Table 3.21: Additional Range and Angles Space Surveillance DSST Orbital Errors

Angular Observations	Fit		Fit Plus Predict	
	RMS (m)	Maximum (m)	RMS (m)	Maximum (m)
Traditional	449	761	1182	2892
Improved	90	193	1113	2961

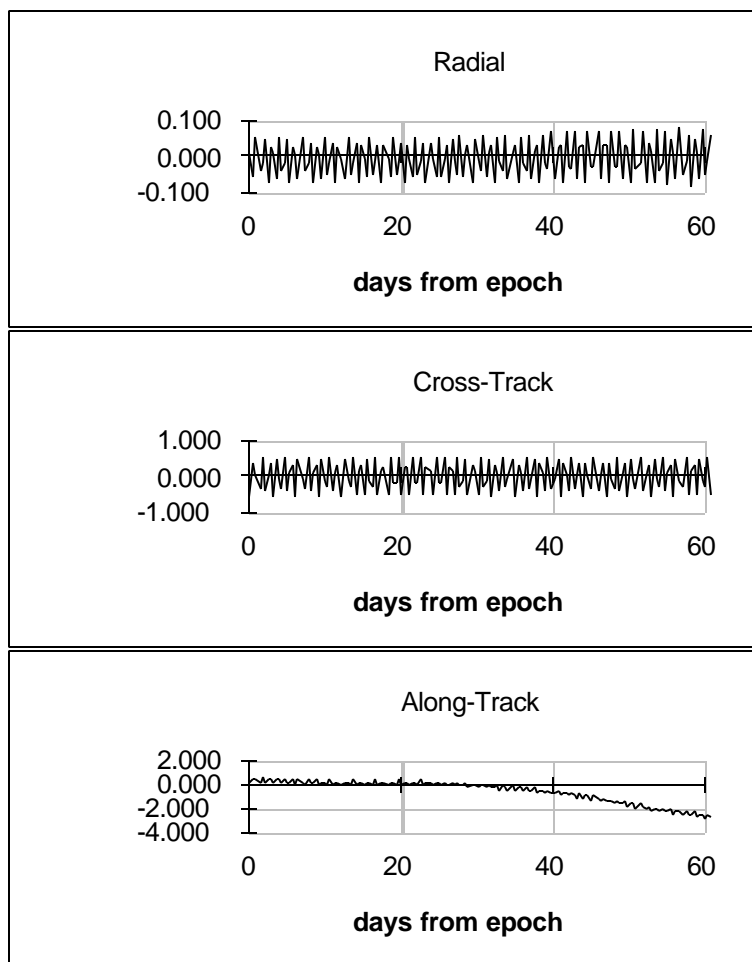


Figure 3.20: Additional Range and Traditional Angles Space Surveillance DSST Orbital Errors

The second range pass provides a great deal of improvement over the traditional angles-only and range and traditional angles cases. The radial periodics are reduced from up to a kilometer to 60 meters. The cross-track periodics are still large and near 600 meters in amplitude, but this is still an improvement over the other traditional angles cases. The along-track run-off also shows a reduction in the periodic errors and is almost indistinguishable from the improved angular observation cases. This is not totally unexpected since the additional range data help provide an accurate fix on the orbital altitude and reduces the radial error which maps into along-track improvements as well.

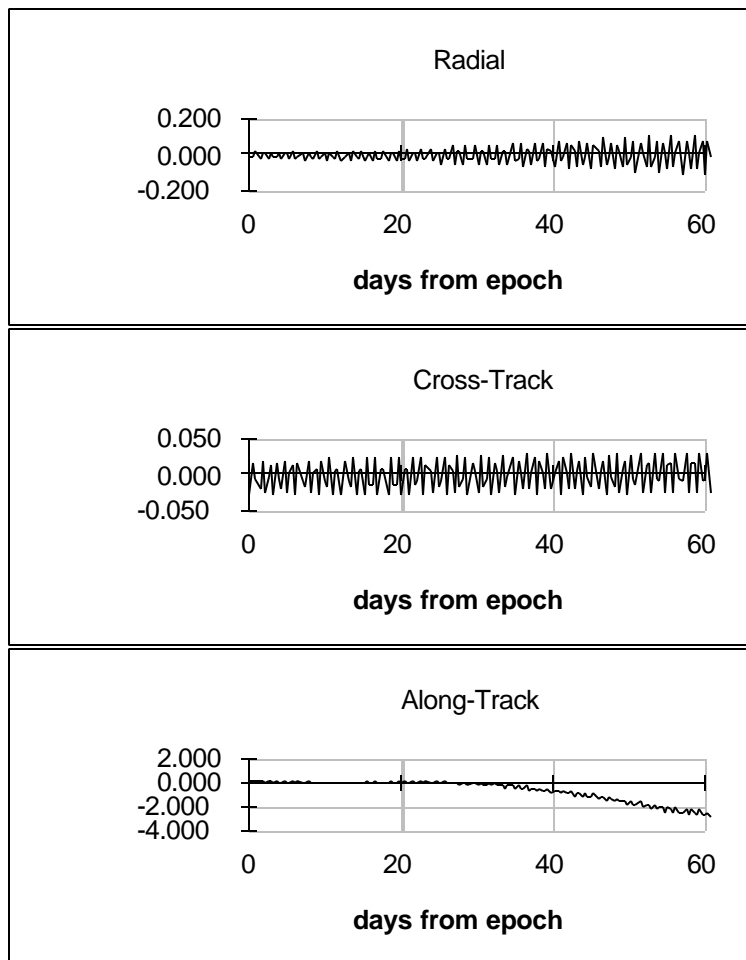


Figure 3.21: Additional Range and Improved Angles Space Surveillance DSST Orbital Errors

Adding the second range pass to the improved angular observations makes little difference. Figure 3.21 shows very similar error trends as the other improved angular cases (recall Figure 3.16). Comparing the additional range and traditional angles case in Figure 3.20 to the additional range and improved angular observations in Figure 3.21 shows the only real improvements are in the radial and cross-track periodics. While this results in a large fit span improvement, these effects are relatively small in comparison to the along-track run-off over the predict span.

#### 3.2.2.4 Summary

The range and angles space surveillance cases supported the conclusions of the angles-only space surveillance studies: the improved angular observations greatly reduce periodic errors in all components of satellite position when the observations are coupled with an accurate satellite theory. This produces near an order of magnitude improvement in the fit span accuracy but along-track run-off errors due to dynamic mismodelling still corrupt the solutions to a great extent. If additional range data is added to the problem, the value of the improved angular observations is reduced since the high accuracy range observations help resolve the periodic errors when using traditional accuracy angular observations. Over the prediction span, the additional range plus traditional angles solution accuracy is as accurate as the additional range plus improved angles solutions. During the fit and early prediction, however, the errors in the improved angles orbits are considerably smaller than the traditional angles based orbits, and the improvement is most evident in the cross-track direction. The reduction of the periodic has significance in the geosynchronous and near-geosynchronous debris tracking and prediction example of a space surveillance application since the solution error ellipsoid used in collision probabilities would be narrowed by the use of the improved angular observations.

#### 3.2.3 Real Data Analysis

While sufficient real data was not available to replicate the data simulation results, results of the real data analysis of the Telstar-401/GOES-10 close approach, the first orbit determination application of the Raven sensor in Albuquerque, do support the data simulation conclusions. Those results, from Reference 74, are presented here.

Section 2.4.2 outlined the real data available for the analysis. Accurate information regarding the noise and bias characteristics of the tracking sensors was not available and there was insufficient data to estimate the bias parameters adequately; therefore, the GSFC GOES-10 reference orbit was used to calibrate the observing sensors. The assumption here was that the errors in the GOES-10 reference orbit were small in comparison to the system biases. The biases found by comparing the observation to

the GSFC reference orbit were applied during the estimation process and the standard deviations of the observation types were used as weights.

To evaluate the performance and value of the improved angular observations in the geosynchronous orbit determination process, the GOES-10 observations were processed in the combinations outlined in Table 3.22. In the table, SSN represents the Millstone Hill radar site, VTA represents the Albuquerque Raven site, and RME represents the Maui Raven site. The VTA and RME only combination (without the SSN data) was not investigated since the satellite altitude could not be resolved with only one day of angles-only data.

Table 3.22: GOES-10 Orbit Determination Data Cases

Case 1	all data (SSN + VTA + RME)
Case 2	SSN data only
Case 3	SSN and VTA data
Case 4	SSN and RME data

For most runs, bias parameters were not estimated, the solar radiation pressure reflectivity coefficient was not estimated (the one corresponding to the GSFC reference orbit, along with the area and mass, was used), and the data weights were determined from the calibration run. Some additional analysis occurred where range bias parameters and/or reflectivity coefficient were estimated, and different data weights were tried; these did not have an impact on the results. In all cases, the Cowell special perturbations theory propagator was used with an 8x8 JGM2 geopotential, Solar/Lunar point mass effects, and a spherical satellite solar radiation pressure model.

At the end of each differential correction, the estimated state was propagated ahead to August 27, 1997 (one day past the predicted close approach). This orbit was then compared to the GSFC GOES-10 reference orbit. Again, the assumption is that the errors contained in the GOES-10 reference orbit are smaller than the errors in the orbit produced by the Raven and SSN data. The results and conclusions of the Raven performance presented are based upon these orbit differences. It is understood that the

GSFC GOES-10 reference orbit contains errors and that the differences presented here are not strict orbit errors.

Table 3.23 contains the orbit differences between the GSFC GOES-10 reference orbit and the four orbit determination cases studied. Figures 3.22 through 3.25 plot the radial, cross-track, and along-track differences over the fit and predict period between the GSFC GOES-10 reference orbit and the orbits we produced for Cases 1-4, respectively.

Table 3.23: Orbit Differences from GSFC GOES-10 Reference Orbit

	Radial (R)	Cross-Track (XT)	Along-Track (AT)	Max. Position Diff.
Case 1 (SSN,VTA,RME)	-22 m bias + 25 m periodic	3 m periodic	-500m to 1200 m (+250 m/day drift)	1229 m
Case 2 (SSN)	-23 m bias + 225 m periodic	2243 m periodic	-500m to 1200 m (+250 m/day drift)	2518 m
Case 3 (SSN,VTA)	-23 m bias + 14 m periodic	201 m periodic	-500m to 1200 m (+250 m/day drift)	1235 m
Case 4 (SSN,RME)	-23 m bias + 20 m periodic	47 m periodic	-500m to 1200 m (+250 m/day drift)	1241 m



Figure 3.22: Case 1 Orbit Differences to GSFC GOES-10 Reference Orbit

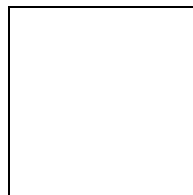






Figure 3.23: Case 2 Orbit Differences to GSFC GOES-10 Reference Orbit



Figure 3.24: Case 3 Orbit Differences to GSFC GOES-10 Reference Orbit



Figure 3.25: Case 4 Orbit Differences to GSFC GOES-10 Reference Orbit

From Table 3.23 and Figures 3.22 to 3.25, common trends can be observed. Most notably, each solution has a radial offset of -22 to -23 meters which results in an along-track drift of roughly 250 meters/day. This radial offset is likely due to three related sources:

- reference orbit error
- range bias error

- estimation error

From the results, it can be determined that the short arc of Raven angular observations has little impact on the radial component of the solution. This is not unexpected since a short arc of angular observations was not sufficient to resolve significant radial errors (on the order of kilometers) without the use of range data.

The areas in which the most significant differences are seen are the periodic differences. Case 1, where data from all three stations was used, shows excellent agreement with the GSFC reference orbit. Case 2 has large differences, most significantly in the cross-track direction. Cases 3 and 4 show a great deal of improvement over Case 2 but do not match the agreement of Case 1.

The improvement in periodic errors are consistent with the space surveillance data simulations. In the presence of high quality range data, a relatively small number of angular observations help reduce the periodic errors in all components but do not affect the along-track run-off. One could argue that the cases with the Raven data have more viewing stations and more observations, but the simulation and real data results still indicate that the improved angular observations do play a major role in reducing the periodic errors.

The mission support simulation analysis determined that improved angular observations help reduce any bias or radial ambiguity in range data and subsequently reduce along-track errors. There are two major differences between the mission support cases and the GOES-10 real data cases: one, the mission support cases assumed more accurate angular observations, and two, the mission support cases showed that a large amount of angular data is required to outweigh the high accuracy range observations. In the GOES-10 real data analysis, only a handful of angular observations were available over a short arc and there was not enough angular information to estimate a range bias effectively.

## **Chapter 4: Conclusions and Future Work**

## 4.1 Conclusions

Many of the conclusions have been presented in the summary subsections of the Results chapter. They are presented again in this chapter to provide a final overview and summary of the findings of this research.

### 4.1.1 Mission Support

The mission support analysis focused on understanding the limitations of range-only geosynchronous orbit determination. Then, simulation studies were performed to investigate the use of improved angular observations with an extensive range tracking network. Next, the extensive range tracking network was reduced and even eliminated to see if optical sites producing improved angular observations could reduce the number of tracking stations required to generate accurate geosynchronous orbit solutions. All simulation studies were based on real data acquisitions for a geosynchronous satellite. The validity of the simulations was tested by comparing real data range-only solutions to simulated results with great success.

From the range-only studies, it was observed that the reported bias values of the range stations are accurate to the several meter level at best. All range biases can only be estimated for inclined orbits, and that still leaves up to several meters of uncertainty in the solutions. Not choosing to solve for one or more biases is limited by the error in the unestimated biases which can lead to fairly large orbital errors. Under all circumstances it was found that small errors in the range observations lead to significant along-track errors in the orbit solutions. Thus, the range-only solutions are limited by the accuracy of the range sensor calibration or the ability to solve for the sensor biases. If the biases are very well known, the range-only solution has proven to be quite accurate; however, for the  $9^\circ$  inclination case presented, the calibration is poor and estimating biases has proven to deliver orbits only to the 30 meter level and possibly much worse for lower inclination cases.

In the extensive range and angles cases, it was shown that improved angular observations help resolve the range bias ambiguity present in the range-only cases. With the angular observations, all range biases can be effectively estimated; this includes low inclination cases.

The studies show that eight nights of optical tracking is desirable over the nine day fit span to support bias estimation for the eight station range tracking network. This implies that two optical stations are needed to produce high accuracy orbits. However, the desired density (2 minutes per observation pair), allows the tracking sites to track two satellites. Thus, two satellites could conceivably share two optical sensors with better results than each satellite monopolizing single optical sensors.

In addition to helping estimate range biases over longer fit spans, the additional angular data allows for accurate orbital solutions over short fit spans, two days was demonstrated, which is valuable for post-maneuver orbit solutions and cases where the long term dynamics are not well modeled.

In the limited range and angles studies, the results showed that as the number of range stations decreases, the number of angular observations required to estimate all range station biases accurately and bring the orbit determination solution accuracy to the meter level also decreases. For a three station range-only case, orbit errors were on the order of 100 meters; when a single optical site is added, however, the solution accuracy is again brought to the meter level. This indicates that the improved angular observations allow for a reduction in the number range stations required to produce accurate geosynchronous orbits.

An extension of this concept is single site range and angles geosynchronous orbit determination. Here, a single station containing both a radio transponder or other ranging system is combined with an optical sensor providing improved angular observations. The angular observations resolve the along-track and cross-track components of the satellite location and replace the need for multiple range stations to provide viewing geometry and bias estimation; The range observations accurately resolve the altitude of the satellite. The results are very accurate orbits from a compact, cost effective tracking system.

Studies investigated the use of angles-only geosynchronous orbit determination. Two optical stations tracking the geosynchronous satellite without any range support produced orbits on the 10 meter level, but the data requirements made the angles-only option unattractive since weather may not

allow for the necessary data collection. Angles-only geosynchronous orbit determination could provide an effective validation or redundancy to GPS-based autonomous orbit determination.

A major assumption in all of the mission support simulation studies was that the angular data contained no biases. It is believed that biases in the optical sensors should be well determined since the sensors can track objects with well known positions, such as reference stars or GPS satellites. It is unclear to what level the biases will be known. The range and angles orbit determination cases will thus be limited by the accuracy of the optical sensor calibration. If the optical sensors are calibrated to the 0.05 arcsecond level, this would result in an approximate 10 meters of error in the orbit solutions.

#### **4.1.2 Space Surveillance**

The space surveillance studies focused on the how improved angular observations increase orbit determination accuracy over solutions obtained with traditional angular observations. GOES-10 was used as an example since real data was available to support the simulation study results. Three orbit propagators, Cowell special perturbations, Draper Semianalytic Satellite Theory (DSST), and an unofficial version of SGP4 present in Draper GTDS, were combined with a tracking schedule designed to track over 200 objects per optical site to form a space surveillance scenario meant to represent a fictitious geosynchronous and near geosynchronous debris tracking campaign. First, an angles-only scenario was investigated with up to three optical sites. Then, studies included one and two passes from a deep space radar to supplement the angular data. It should be noted that the space surveillance studies presented here are of the author's creation and in no way reflect the operational practices or performance of the US Air Force or US Space Command.

From the angles-only results, the value of improved angular observations can be seen in the reduction of periodic errors in the orbit determination solutions when using a high accuracy satellite theory such as Cowell special perturbations or DSST. When coupled with a low accuracy satellite theory such as the DGTDS version of SGP4, the improved angular observations had no impact on the results. Even when using high accuracy theories, however, the improved angular observations do not appear to help reduce the along-track error run-off in the orbit prediction when the run-off is caused by

dynamic modelling errors; when the dynamic modelling error is reduced, the improved angular observations appear to help the along-track run-off as well. If the studies were limited to the fit spans, the improved angular observations could increase the solution accuracy by an order of magnitude. The nature of the space surveillance studies required the consideration of the predictions. By utilizing more optical sensors, perhaps the long predictions could be avoided. The improved angular observations do increase the overall orbit solution accuracy even when taking the prediction into account; the improvement is most significant during the fit and early prediction.

Additional studies showed that the number of optical tracking stations have little impact on the accuracy of the results if the number of observations and data distributions are kept equal. The greatest contribution increasing the number of stations may be able make is increasing the number of available observations, reducing the prediction spans, and providing insurance against foul weather.

The range and angles space surveillance cases supported the conclusions of the angles-only space surveillance studies: the improved angular observations greatly reduce periodic errors in all components of satellite position when the observations are coupled with an accurate satellite theory. This produces near an order of magnitude improvement in the fit span accuracy but along-track run-off errors still corrupt the solutions to a great extent. If additional range data is added to the problem, the increase in accuracy is reduced since the high accuracy range observations help resolve the periodic errors when using traditional accuracy angular observations. Over the prediction span, the additional range plus traditional angles solution accuracy is as accurate as the additional range plus improved angles solutions. During the fit and early prediction, however, the errors in the improved angles orbits are considerably smaller than the traditional angles based orbits, and the improvement is most evident in the cross-track direction. The reduction of the periodic has significance in the geosynchronous and near-geosynchronous debris tracking and prediction example of a space surveillance application since the solution error ellipsoid used in collision probabilities would be narrowed by the use of the improved angular observations.

Real data analysis showed improvement in periodic errors consistent with the space surveillance data simulations. In the presence of high quality range data, a relatively small number of

angular observations help reduce the periodic errors in all components but do not affect the along-track run-off.

## 4.2 Future Work

Future work possibilities include areas of research that would be beneficial to the development and application of optical sensors producing improved angular observations and areas of research that could improve geosynchronous orbit determination. There are four areas of natural continuation for this research:

- further simulation studies
- Raven development
- real data analysis
- GPS studies

The following subsections discuss these future work possibilities.

### 4.2.1 Further Simulation Studies

The results presented here have lead to fairly strong conclusions but many of the cases have shown some uncertainty which serves to cloud the trends. Recall the mission support cases investigating the desired density of the optical observations; conclusions can be drawn from Figure 3.5 but there is uncertainty in the true nature of the error growth with moderate density (5-10 observation pairs per minute) optical observations. Recall the space surveillance cases where either the Cowell results or the DSST results would contain significant along-track run-off while the other would not despite both theories having similar accuracy attributes. Further Monte Carlo style data simulation studies would help reduce the impact of the unexpected results. GTDS is not currently set up for Monte Carlo data simulations.



Additional data simulations could also target the space surveillance studies. The results presented here are not representative of any real world space surveillance systems. To measure the value of the improved angular observations, a realistic scenario should be emulated.

All conclusions presented here are only applicable to geosynchronous orbits. Further studies could target other orbit regimes such as the highly eccentric, high altitude orbits, supersynchronous orbits, and heliocentric orbits. The range-only limitations demonstrated for geosynchronous orbits may not be present for these orbit classes but obtaining range data for these objects may be more difficult, particularly for space surveillance applications.

In addition to strictly numerical studies, analytic approaches could be taken to investigate the value and use of the improved angular observations in geosynchronous orbit determination. Reference 82 outlines a methodology that could be applied in this manner.

#### **4.2.2 Raven Development**

The results presented in this work are valid for any optical sensor; however, the Raven optical sensor has already demonstrated that it can deliver very accurate angular observations. The Raven sensor has not fulfilled its potential and there are several areas that need to be addressed in the development of the system. First and foremost, the image processing problems that produce the systematic errors in the observations, demonstrated in Section 2.4.1.2, must be corrected. That would allow for the calibration and real data analysis to continue.

The calibration effort should be able to identify sources of error in the Raven system. Once identified, steps could be taken to eliminate the sources of error. Two known sources of error include the streak endpoint detection and the star catalog. Improving streak endpoint detection will take a great deal of analysis and, likely, trial and error. New star catalogs are currently being developed that are considerably more accurate than the Hubble Guide Star Catalog currently implemented in the astrometry calculations.

The Raven team in Maui are also discussing different ways of how the Raven tracks. Currently, images are taken while the telescopes tracks sidereally. Thus the stars appear as points in

the images and the satellites appear as streaks. A disadvantage of this approach is that the imperfections in the telescope motion translate into nonlinearities in the satellite streak and stars that are not as focused as they could be. An alternative would be to take images while the telescope is stationary, sometimes called stare mode or ballistic mode; here, the stars would appear to be streaks in the image due to the rotation of the Earth and the satellite may also appear to be a streak depending on its relative motion to the ground station.

### **4.2.3 Real Data Analysis**

As discussed in Section 2.4, many Raven images have been collected but are unusable due to the Raven image processing problems. Once the image processing problems are corrected, a great deal of real data analysis will be possible. First, a calibration campaign will have to be completed using the several nights of GPS data collected. This should define the biases of the Raven sensor and help identify error sources and areas of future improvement.

Once the calibration is completed, analysis can take place using the data collected on the geosynchronous satellite the mission support studies are based on. These studies should validate the conclusions drawn in this analysis.

Further real data analysis could investigate the use of filters to better handle the daily momentum dumps performed by this satellite. Studies of this nature could also advance the techniques of geosynchronous orbit determination in much the same way the TOPEX/Poseidon has advanced the knowledge of low Earth orbit determination.

#### **4.2.4 GPS Studies**

Many references have been given regarding the use of GPS signals in the geosynchronous orbit regime. These studies have been fairly limited in scope, however. Further studies in GPS applications to geosynchronous orbit determination could include differential GPS approaches and scenarios involving pseudolites. Most of the previous studies, aside from the GPS-Like or GPS Enhanced Tracking demonstrated by JPL, have lacked the innovation shown in many of the TOPEX studies.

In addition to GPS-only studies, investigations could be undertaken to determine if the GPS signals could be supplemented with other data sources, such as improved angular observations, to improved results. GPS receiver-on-board studies have shown there is error in the orbit solutions, particularly when SA is present, that the improved angular observations may be able to reduce.

## **Bibliography**

- [1] Sellers, Jerry Jon, *Understanding Space: An Introduction to Astronautics*, McGraw Hill, Inc., New York, NY, 1994.
- [2] Gordon, Gary D., and Morgan, Walter L., *Principles of Communications Satellites*, John Wiley and Sons, Inc., 1993.
- [3] Draim, John E., "Lightsat Constellation Designs", AIAA Satellite Communications Conference, March 1992, AIAA-92-1988-CP.
- [4] Pensa, A.F., Powell, G.E., Rork, E.W., Sridharan, R., "Debris in Geosynchronous Orbits", presented at the AAS/AIAA Space Flight Mechanics Conference, Austin, TX, Feb 12-15 1996. AAS 96-118.
- [5] Yurasov, V., Moscovsky, A., "Geostationary Orbit Determination and Prediction", US - Russian Space Surveillance Workshop, Poznan, Poland, July 4 - 6, 1996. Held in conjunction with IAU Colloquium 165, Dynamics and Astrometry of Natural and Artificial Celestial Bodies.
- [6] Cefola, P., Proulx, R., Metzinger, R., Cohen, M., Carter, D., "The RADARSAT Flight Dynamics System: An Extensible, Portable, Workstation-based Mission Support System", AIAA/AAS Astrodynamics Conference, Scottsdale, Arizona, August 1-3, 1994. AIAA 94-3726.
- [7] Antreasian, Peter G., Rosborough, George W., "Prediction of Radiant Energy Forces on the TOPEX/POSEIDON Spacecraft", *Journal of Spacecraft and Rockets*, Vol. 29, No. 1, pp 81-90, January- February 1992.
- [8] Fliegel, H. F., Gallini, T. E., Swift, E. R., "Global Positioning System Radiation Force Model for Geodetic Applications", *Journal of Geophysical Research*, Vol. 97, No. B1, pp 559-568. Jan. 10, 1992.
- [9] Hyung, Jin Rim, Davis, George W., Schutz, Bob E., "Gravity Tuning Experiments for the Precise Orbit Determination of the EOS Altimeter Satellite (EOS ALT/GLAS) Using the GPS Tracking Data", AAS/AIAA Space Flight Mechanics Meeting, Austin TX, Feb. 13-16, 1996. AAS 96-165.
- [10] Irish, Kelly, et al, "Precision Orbit Determination for GFO and GFO-2", AIAA/AAS Space Flight Mechanics Meeting, Austin TX, Feb. 13-16, 1996. AAS 96-185.

- [11] Davis, George W., Schutz, Bob E., "Precise Orbit Determination for the EOS ALT/GLAS Satellite Orbit", AIAA/AAS Astrodynamics Specialist Conference, San Diego CA, Jul 29-31, 1996. AIAA 96-3607.
- [12] Cangahuala, Laureano, et al, "TOPEX/Poseidon Precision Orbit Determination: 'Quick-Look' Operations with SLR and GPS Data", AAS/AIAA Astrodynamics Specialist Conference, Halifax, Nova Scotia, Canada, August 14-17, 1995. AAS 95-368.
- [13] Vallado, David A., *Fundamentals of Astrodynamics and Applications*, published by McGraw Hill, New York, 1997.
- [14] Barker, William N., Casali, Stephen J., Wallner, Richard N., "The Accuracy of General Perturbations and Semianalytic Satellite Ephemeris Theories", AAS/AIAA Astrodynamics Specialist Conference, Halifax, Nova Scotia, Canada, August 14-17, 1995. AAS 95-432.
- [15] Fonte, Daniel J., et al, "Comparison of Orbit Propagators in the Research and Development Goddard Trajectory Determination System (R&D GTDS) - Part I: Simulated Data", AAS/AIAA Astrodynamics Specialist Conference, Halifax, Nova Scotia, Canada, August 14-17, 1995. AAS 95-431.
- [16] Fonte, D. J., Sabol, C., "Optimal DSST Input Decks for Various Orbit Types", Phillips Lab Technical Report, PL-TR-95-1072. June, 1995. Available through AFRL Astrodynamics Group: AFRL/VSSS/Astrodynamics, Kirtland AFB, NM 87117.
- [17] "Ground-based Electro-Optical Deep Space Surveillance", GEODSS fact sheet available through the world wide web as: <http://www.aoc.com/GEODSS1.html>
- [18] Burnham, W. F., Sridharan, R., "Geosynchronous Surveillance with a Spaced-Based Sensor", AAS/AIAA Space Flight Mechanics Meeting, Austin TX, February 12-15, 1996. AAS 96-214.
- [19] Wallace, Scott, Sabol, Chris, Carter, Scott, "Optical Sensor Calibration Using GPS Reference Orbits", presented at the MIT/Lincoln Lab Space Control Workshop, Lexington, MA, March 1997.
- [20] Millstone Hill Observatory Web Page, <http://www.haystack.edu/cgi-bin/TOC.cgi>

- [21] Oza, D. H., et al, "Assessment of Orbit Determination Solutions for TDRSS Users", available through the world wide web as  
*<http://tipalpha1.gsfc.nasa.gov/tip/html/fdd/9507003/9507003.htm>*
  
- [22] "NASA/CDDIS Dat Holdings SLR Web Page", *<http://cddisa.gsfc.nasa.gov/cddis.html>* through the "Description of CDDIS Data Sets", then "SLR" links.
  
- [23] Springer, Tim, personal discussion on 24 January, 1997. Mr. Springer is a participating member in the Center for Orbit Determination in Europe and the Astronomical Institute of the University of Berne, Sidelerstrasse 5, CH-3012, Bern, Switzerland. e-mail: *[springer@aiub.unibe.ch](mailto:springer@aiub.unibe.ch)*, www: *<http://ubeclu.unibe.ch/aiub/>*.
  
- [24] Scharroo, Remko, "ERS-1 Operational Orbit Determination" available through the world wide web as *<http://dutlru8.lr.tudelft.nl/ers/operorbs/ersorbit.html>*. This document is an excerpt from "Processing of ERS-1 and TOPEX/Poseiden Altimeter Measurements", by E. Wisse, M. C. Naeije, and R. Scharroo as BCRS report 93-11, Netherlands Remote Sensing Board, ISBN 90-5411-092-9, December, 1993.
  
- [25] "NASA/CDDIS SLR and LLR Web Page", *<http://cddisa.gsfc.nasa.gov/cddis.html>* through the "Description of CDDIS Data Sets", "SLR", then "SLR (under 'About the CDDIS SLR archive' section)" links.
  
- [26] Leick, Alfred, *GPS Satellite Surveying*, 2nd Edition, published by John Wiley & Sons, Inc., New York, 1995.
  
- [27] DOT/DOD Press release, "DOT and DOD assure GPS access for Civil Users", DOT Contact: Bill Mosley, (202) 366-5571, DOD Contact: Col. Queenie Byars, (703) 697-5131. February 27, 1997.
  
- [28] Lichten, Stephen M., "Estimation and Filtering for High Precision GPS Positioning Applications", *manuscripta geodaetica* (1990) 15:159-176.
  
- [29] Yunck, Thomas P., Sien-Chong Wu, Jiun-Tsong Wu, and Catherine L. Thornton, "Precise Tracking of Remote Sensing Satellites with the Global Positioning System", *IEEE Transactions on Geoscience and Remote Sensing*, Vol. 28, No. 1, January 1990.

- [30] Wu, S. C., Yunck, T. P., Thornton, C. L., "Reduced-Dynamic Technique for Precise Orbit Determination of Low Earth Satellites", *Journal of Guidance, Control, and Dynamics*, Vol. 14, No. 1, January-February 1991. pp 24-30.
- [31] Cefola, Paul J., Carter, Scott, Proulx, Ron, "Precision Orbit Determination from GPSR Navigation Solutions", AIAA/AAS Astrodynamics Specialist Conference, San Diego CA, Jul 29-31, 1996. AIAA 96-3605.
- [32] Guinn, Joseph R., Munson, Timothy N., Vincent, Mark A., "Autonomous Spacecraft Navigation for Earth Ground Track Repeat Orbits Using GPS", AAS/AIAA Space Flight Mechanics Meeting, Austin TX, February 12-15, 1996. AAS 96-184.
- [33] Fonte, D. J., *Implementing a 50x50 Gravity Field Model in an Orbit Determination System*, M.S. Thesis, Department of Aeronautics and Astronautics, MIT, 1993.
- [34] King-Hele, D. G., *A Tapestry of Orbits*, Cambridge University Press, 1992.
- [35] Chobotov, Vladimir A. (editor), *Orbital Mechanics*, Published by American Institute of Aeronautics and Astronautics, Inc., 307 L'Enfant Promenade SW, Washington, DC 20024-2518. 1991.
- [36] Battin, Richard H., *An Introduction to the Mathematics and Methods of Astrodynamics*, Published by American Institute of Aeronautics and Astronautics, Inc., 307 L'Enfant Promenade SW, Washington, DC 20024-2518. 1987.
- [37] Friesen, Larry Jay, et al, "Analysis of Orbital Perturbations Acting on Objects in Orbits Near Geosynchronous Earth Orbit", *Journal of Geophysical Research*, Vol. 97, No. E3, pp. 3845-3863, March 25, 1992.
- [38] Computer Sciences Corp. and NASA Goddard Space Flight Center (Editors), *GTDS Mathematical Theory Revision 1*, Contract NAS 5-31500, Task 213, July 1989.
- [39] Schumacher, Paul W., Jr., Glover, Robert A., "Analytical Orbit Model for U.S. Naval Space Surveillance: An Overview", AAS/AIAA Astrodynamics Specialist Conference, Halifax, Nova Scotia, Canada, August 14-17, 1995. AAS 95-427.



- [40] Liu, J., France, R., Hujsak, R., "Application of a Semianalytic Orbit Theory Using Observed Data", *Journal of the Astronautical Sciences*, Vol. 31, no. 1, pp. 49-61. Jan-March, 1983.
- [41] Danielson, D. A., Neta, B., Early, L. W., "Semianalytic Satellite Theory (SST): Mathematical Algorithms", Technical Report for Period July 1992 - January 1994. Prepared for the Naval Postgraduate School, Monterey, CA 93943. NPS-MA-94-001.
- [42] Yurasov, V., "Universal Semianalytic Satellite Motion Propagation Method", US - Russian Space Surveillance Workshop, Poznan, Poland, July 4 - 6, 1996. Held in conjunction with IAU Colloquium 165, Dynamics and Astrometry of Natural and Artificial Celestial Bodies.
- [43] McClain, W., "A Recursively Formulated First-Order Semianalytic Artificial Satellite Theory Based on the Generalized Method of Averaging, Volume I.", Contract NAS 5-24300, Task Assignment 880. June 1978. Available through W. McClain, Draper Lab, 555 Technology Square, Cambridge, MA, 02139.
- [44] Fieger, M. E., *An Evaluation of Semianalytical Satellite Theory Against Long Arcs of Real Data for Highly Eccentric Orbits*, M. S. Thesis, Dept. of Aeronautics and Astronautics, MIT, January, 1987.
- [45] Carter, Scott S., *Precision Orbit Determination from GPS Receiver Navigation Solutions*, Master of Science Thesis submitted to the Dept. of Aeronautics and Astronautics, MIT, June, 1996.
- [46] Born, George, Tapley, Byron, Schutz, Bob, *Fundamentals of Orbit Determination*, distributed as class notes for ASEN 5070 & 5080, Introduction to Statistical Orbit Determination I and II, University of Colorado, Boulder, CO.

- [47] Rundenko, Sergei P., et al "Some Results of the Analysis of the Geosynchronous Satellite Observations", Conference on Astrometry and Celestial Mechanics, Poznan, Poland, September 13-17, 1993. Proceedings published as *Dynamics and Astrometry of Natural and Artificial Celestial Bodies* by the Astronomical Observatory of the A. Mickiewicz University, Poznan, Poland, 1994.
  
- [48] Doll, C. E., et al, "Accurate Orbit Determination Strategies for TOPEX/Poseidon using TDRSS", available through the world wide web as:  
<http://tipalpha1.gsfc.nasa.gov/tip/html/fdd/9507002/9502002.htm>
  
- [49] Personal discussion with Lt. Scott Wallace, AFRL/VSSS/Astro, Kirtland AFB, NM. Scott Wallace is no longer with the AFRL Astrodynamics Group.
  
- [50] Personal discussion with C. Ed Doll, NASA/Goddard Space Flight Center, Flight Dynamics Division, Greenbelt MD. Ed Doll has since retired.
  
- [51] Ananda, M. P., Jorgensen, P. S., "Orbit Determination of Geostationary Satellites Using the Global Positioning System", *Proceedings of the Symposium on Space Dynamics for Geosynchronous Satellites*, CNES, Toulouse, France, August 1985.
  
- [52] Chao, C. C., et al, "Autonomous Stationkeeping of Geosynchronous Satellites Using a GPS Receiver", AIAA/AAS Astrodynamics Conference, Hilton Head Island, SC, Aug. 10-12, 1992. AIAA 92-4655.
  
- [53] Ferrage, Jean-Luc Issler, et al, "GPS Techniques for Navigation of Geostationary Satellites", ION-95; Proceedings of the 8th International Technical Meeting of the Satellite Division of the Institute of Navigation, Palm Springs, CA, September 12-15, 1995.
  
- [54] Haines, B. J., et al, "GPS-Like Tracking of Geosynchronous Satellites: Orbit Determination Results for TDRS and INMARSAT", AAS/AIAA Astrodynamics Specialist Conference, Halifax, Nova Scotia, Canada, August 14-17, 1995. AAS 95-372.
  
- [55] Haines, B. J., et al, "A Novel Use of GPS for Determining the Orbit of a Geosynchronous Satellite: The TDRS/GPS Tracking Demonstration", origin unknown, copy available through Chris Sabol, [sabolc@plk.af.mil](mailto:sabolc@plk.af.mil) or [sabol@debris.colorado.edu](mailto:sabol@debris.colorado.edu)

- [56] Larson, Wiley J., Wertz, James R., *Space Mission Analysis and Design*, 2nd Edition, published jointly by Microcosm, Inc, Torrance, CA, and Kluwer Academic Publishers, Boston. 1992.
- [57] Sabol, Chris, "PHillips Lab User Interface Developed for Draper GTDS- Update 1", November 1996. Available through Chris Sabol at [sabol@debris.colorado.edu](mailto:sabol@debris.colorado.edu) or [sabolc@plk.af.mil](mailto:sabolc@plk.af.mil).
- [58] International GPS Service for Geodynamics, "About the IGS", available on the world wide web as <http://igsb.jpl.nasa.gov/about.html>.
- [59] GPS Informations und Beobachtungssystem (GIBS) {The GPS Information and Observation System}, "Ephemerides of the International GPS Geodynamic Service (IGS)", available via the world wide web at [http://gibs.leipzig.ifag.de/cgi-bin/eph\\_igs.cgi?en](http://gibs.leipzig.ifag.de/cgi-bin/eph_igs.cgi?en).
- [60] Spofford, P. R., Remondi, B. W., "The National Geodetic Survey Standard GPS Format SP3", available via anonymous ftp to [igsb.jpl.nasa.gov](ftp://igsb.jpl.nasa.gov) as [/igsb/data/format/sp3\\_docu.txt](ftp://igsb.jpl.nasa.gov/igsb/data/format/sp3_docu.txt)
- [61] International Earth Rotation Service, "Explanatory Supplement to IERS Bulletins A and B", March 1996. Available through the world wide web as <ftp://maia.usno.navy.mil/ser7/iersexp.sup> or <http://gibs.leipzig.ifag.de/MISC/IERS/bulletinb.guide>.
- [62] "GPS Constellation History and Status", available through the world wide web as [http://gibs.leipzig.ifag.de/cgi-bin/gps\\_constell.cgi?en](http://gibs.leipzig.ifag.de/cgi-bin/gps_constell.cgi?en).
- [63] US Naval Observatory, "GPS Constellation Status", available through ftp to [igsb.jpl.nasa.gov](ftp://igsb.jpl.nasa.gov) as [/igsb/general/gps/constell.gps](ftp://igsb.jpl.nasa.gov/igsb/general/gps/constell.gps). Downloaded daily from USNO's Automated Data Service (ADS).
- [64] McCarthy, D. D., "IERS Technical Note 21: IERS Conventions (1996)", July 1996. Available through the world wide web at <http://maia.usno.navy.mil/conventions.html>.
- [65] Crustal Dynamics Data Information System (CDDIS), "TREE.ANON", "TREE.DIS", and "TREE.IGS", text files available via anonymous ftp to [cddis.gsfc.nasa.gov](ftp://cddis.gsfc.nasa.gov). Updated 19 February, 1997.

- [66] Crustal Dynamics Satellite Laser Ranging, "Onsite Normal Point and Engineering Quicklook Format", text file available via anonymous ftp to *cddis.gsfc.nasa.gov* as *formats/cstg.format*. Revised 1996.
  
- [67] University of Texas Center for Space Research, "Center for Space Research Lageos Station Coordinates and Velocities", available through anonymous ftp to *ftp.csr.utexas.edu* as *pub/csr\_eop/annual/csr94l01.ssc*.
  
- [68] Kes, F. C., Lagowski, R. G., Grise, A. J., "Performance of the Telesat Real-Time State Estimator", 8th AIAA Communications Satellite Systems Conference, Orlando, FL, April 20-24, 1980. AIAA 80-0573.
  
- [69] Herriges, Darrell Lee, *NORAD General Perturbation Theories: An Independent Analysis*, M. S. Thesis, Dept. of Aeronautics and Astronautics, MIT, January, 1988.
  
- [70] Chao, C.C., et al, "Challenges and Options for GEO Use of GPS", AAS/AIAA Astrodynamics Specialist Conference, Sun Valley, ID August 4-7, 1997. AAS 97-677.
  
- [71] Simpson, B. L., Rade, T. J., "Trends in Position Determination for Air Force Satellite Operations", AAS/AIAA Astrodynamics Specialist Conference, Sun Valley, ID, August 4-7, 1997. AAS 97-675.
  
- [72] Lichten, S. M., et al, "New Techniques for Orbit Determination of Geosynchronous, Geosynchronous-Transfer, and Other High-Altitude Earth Orbiters", AAS/AIAA Astrodynamics Specialist Conference, Sun Valley, ID, August 4-7, 1997. AAS 97-676.
  
- [73] NOAA Press Release, "Third Satellite in NOAA GOES Series Successfully Launched", point of contact: Patricia Viets, April 25, 1997. NOAA 97-23. Available on the World Wide Web as: <http://www.noaa.gov/public-affairs/pr97/apr97/noaa97-23.html>
  
- [74] Sabol, Chris, Burns, R., Wallace, S., "Analysis of the Telstar-401/GOES-10 Close Approach Using the Raven Telescope", AAS/AIAA Space Flight Mechanics Meeting, Monterey, CA, February 9-11, 1998. AAS 98-118.

- [75] Wallace, S., Sabol, C., Carter, S., "Use of the Raven Optical Sensor for Deep Space Orbit Determination", AAS/AIAA Astrodynamics Specialist Conference, Sun Valley, ID, August 4-7, 1997. AAS 97-705.
- [76] Seidelmann, P. K., Corbin, T., "The New Star Catalogs", AAS/AIAA Space Flight Mechanics Meeting, Monterey, CA, February 9-11, 1998. AAS 98-152.
- [77] Monet, David G., "The 488,006,860 Stars in the USNO-A1.0 Catalog", AAS/AIAA Space Flight Mechanics Meeting, Monterey, CA, February 9-11, 1998. AAS 98-153.
- [78] United States Air Force Scientific Advisory Board, "Report on Space Surveillance, Asteroids and Comets, and Space Debris", Volume 1: Space Surveillance, SAB-TR-96-04, June 1997. Available through the Department of the Air Force, AF/SB, Washington, DC 20330-1180.
- [79] Sharma, Jayant, "SBV Space Surveillance Performance", Proceedings of the 1998 Space Control Conference, 14-16 April 1998, MIT/Lincoln Laboratory, Lexington, MA.
- [80] Hoots, Felix R., Roehrich, Ronald L., "Models for Propagation of NORAD Element Sets", Spacetrack Report No. 3, December 1980, Aerospace Defense Command, United States Air Force. Available over the world wide web at:  
*<http://celestrak.com/NORAD/documentation/index.html>*
- [81] Karpiuk, Cindi A. (managing editor), *The Orbital Debris Quarterly News*, Vol. 3, Issue 2, April 1998. A publications of NASA Johnson Space Center, Houston, TX 77058
- [82] Slutsky, M. S., "Automation of Several Orbit Determination Tasks", AIAA/AAS Astrodynamics Conference, Williamsburg, VA, August 18-20, 1986. AIAA 86-2213-CP.

## **Appendix**

## A. GPS to Geosynchronous Visibility

In the preceding discussions, the use of a GPS receiver on board a geosynchronous satellite for orbit determination purposes was mentioned without regards to the availability of GPS signals to satellites in the geosynchronous regime. In this section, a simple approach is taken to determine the observability of the GPS constellation to the geosynchronous regime.

Figure A.1 shows the geometry of the GPS to GEO observability problem. GPS satellites broadcast their signals in a cone extending 21.4 degrees from nadir [51]. Thus, signals can be received by geosynchronous satellites when GPS satellites are transmitting from the opposite side of the Earth as long as the angle between the GPS satellite nadir and the geosynchronous satellite is less than 21.4 degrees. This is shown as Point 2 in Figure A.1. Even if the broadcast cone geometry is met, the signals may still be blocked or distorted by the Earth and atmosphere; thus, further restrictions are placed on the observability of the GPS constellation to the geosynchronous regime. This is denoted by Point 1 in Figure A.1. If the angle between the GPS satellite nadir is less than 21.4 degrees and sufficiently large enough for the signal to not be distorted by the atmosphere, the GPS signal is observable to the geosynchronous satellite. The arc between Points 1 and 2 illustrate this is Figure A.1. In 3-D, this arc rotates into an annulus of visibility.

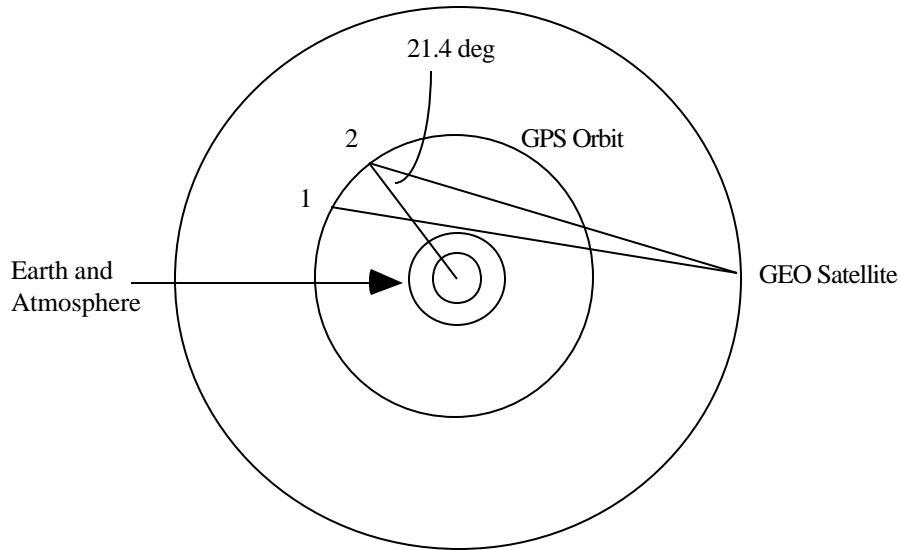


Figure A.1: GPS to GEO Observability Geometry

These constraints can be put into mathematical terms using dot products. Figure A.2 shows the GPS to GEO observability constraint geometry for Point 1.

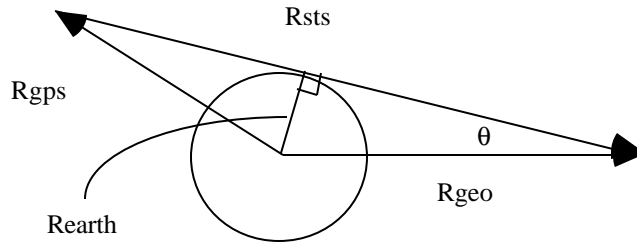
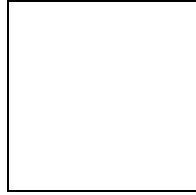


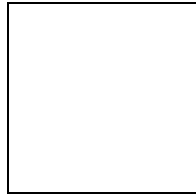
Figure A.2: GPS to GEO Observability Geometry Constraint 1

For GPS visibility we, want  $\theta$  greater than  $\theta_{\text{critical}}$  where  $\theta_{\text{critical}}$  is determined by the radius of the Earth and atmosphere:



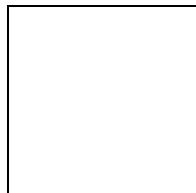
(3)

Since the extent of the atmosphere is a known or assumed quantity, we can put  $\cos(\theta)$  in terms of the GPS and geosynchronous satellite's position vectors:



(4)

If we want  $\theta$  greater than  $\theta_{\text{critical}}$ , then that means we want  $\cos(\theta)$  less than  $\cos(\theta_{\text{critical}})$  for visibility. In terms of satellite position vectors, this leads to the following constrain for GPS to GEO visibility:



(5)



The second constraint depends on the geosynchronous satellite being within 21.4 degrees of the GPS satellite nadir direction. Figure A.3 shows the observation geometry constraint represented by Point 2 in Figure A.1.

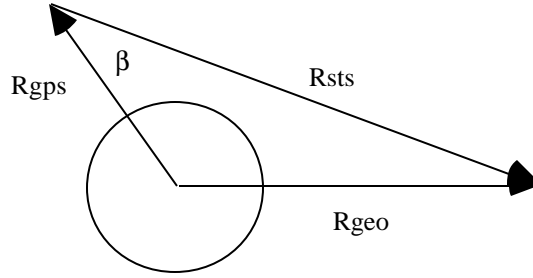


Figure A.3: GPS to GEO Observability Geometry Constraint 2

For GPS visibility we, want  $\beta$  less than  $\beta_{\text{critical}}$  where  $\beta_{\text{critical}}$  is the divergence angle of the GPS broadcast signal (21.4 degrees). If  $\beta$  is less than  $\beta_{\text{critical}}$ , then  $\cos(\beta)$  is greater than  $\cos(\beta_{\text{critical}})$ . Using the definition of a dot product,  $\cos(\beta)$  can be expressed in terms of the satellite position vectors:

$$\cos(\beta) = \frac{\mathbf{R}_{\text{gps}} \cdot \mathbf{R}_{\text{sts}}}{|\mathbf{R}_{\text{gps}}| |\mathbf{R}_{\text{sts}}|}$$

(6)

Therefore, the second observability geometry constraint can be expressed as:

$$\cos(\beta) > \cos(\beta_{\text{critical}})$$

(7)

If both equations (5) and (7) are satisfied, the geosynchronous satellite at position  $\mathbf{R}_{\text{geo}}$  is in view of the GPS satellite at position  $\mathbf{R}_{\text{gps}}$ .

If we assume a geosynchronous satellite is truly geostationary, the satellite coordinates would not change in an Earth Centered, Earth Fixed (ECEF) rotating reference frame. We can then make assumptions about the altitude of the geosynchronous satellite, the altitude of the distorting atmosphere, and use IGS Precise Orbit Ephemerides (POE's) to determine the visibility of the geostationary point to the GPS constellation over the course of a day (more information about the IGS POE's and where they are publicly available is in Appendix B).

This was done for a variety of geostationary points for August 20, 1996 with the geostationary altitude set to 42,240 km. Two atmospheric radii were used: 6,700 km and 8,000 km. The 8,000 km atmosphere radius is a conservative estimate used if only a single frequency were observed and atmospheric effects could not be differenced out. The 6,700 km atmosphere radius is a less conservative estimate aimed at dual frequency GPS signals where atmospheric effects can be eliminated through a linear combination of the two frequencies.

Table A.1 shows the average number of GPS satellites visible to various points in the geostationary ring for both values of atmospheric radius. The amount of atmospheric signal masking makes a large difference in the average number of visible satellites. Figures A.4 and A.5 plot this information.

Table A.1: Average Number of GPS satellites Visible to the Geostationary Ring

Longitude (°)	Ratm=6700 km	Ratm=8000 km
0	1.01	0.59
30	1.04	0.61
60	0.92	0.56
90	0.99	0.55
120	0.90	0.58
150	1.01	0.57
180	1.01	0.62
210	0.89	0.56
270	0.99	0.59
300	0.98	0.61
330	0.90	0.59
360	1.01	0.59
Average	0.97	0.59

Figures A.6 and A.7 show the number of GPS satellites visible to the 0 degree longitude location on the geostationary belt over one day. Figure A.6 uses an atmosphere radius of 6,700 km, and Figure A.7 uses 8,000 km. These results are consistent with those presented in References 51, 52, and 53.

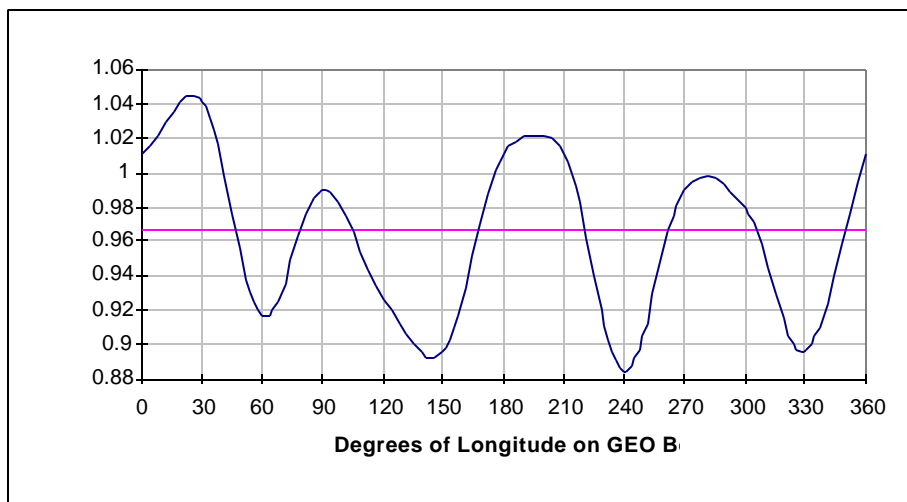


Figure A.4: Average GPS to GEO Observability for an Atmosphere Radius of 6,700 km

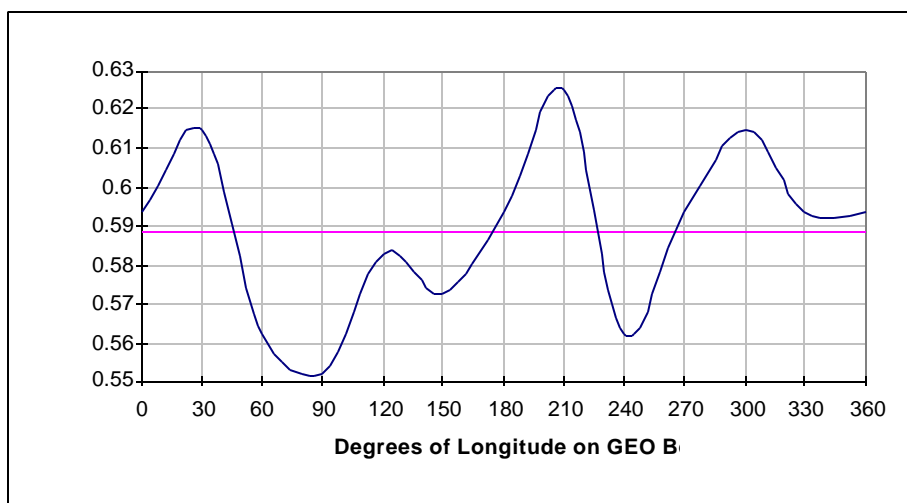


Figure A.5: Average GPS to GEO Observability for an Atmosphere Radius of 8,000 km

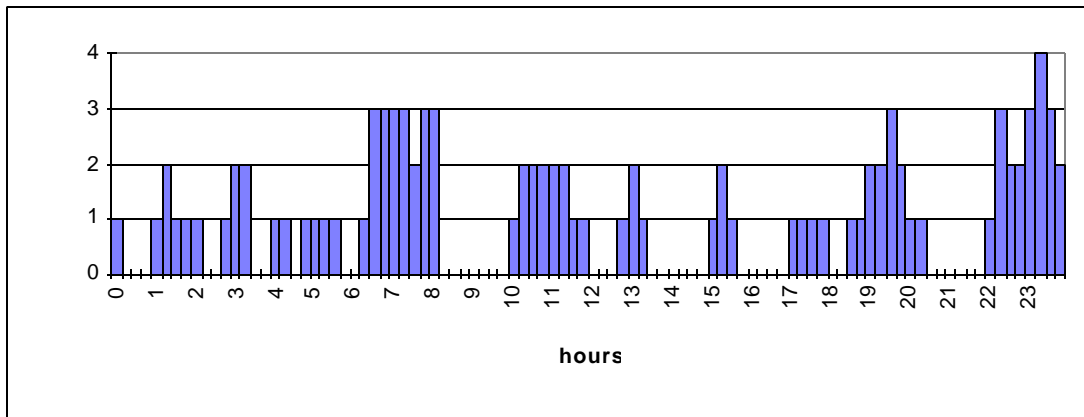


Figure A.6: GPS to 0 Degree GEO Observability for an Atmosphere Radius of 6,700 km

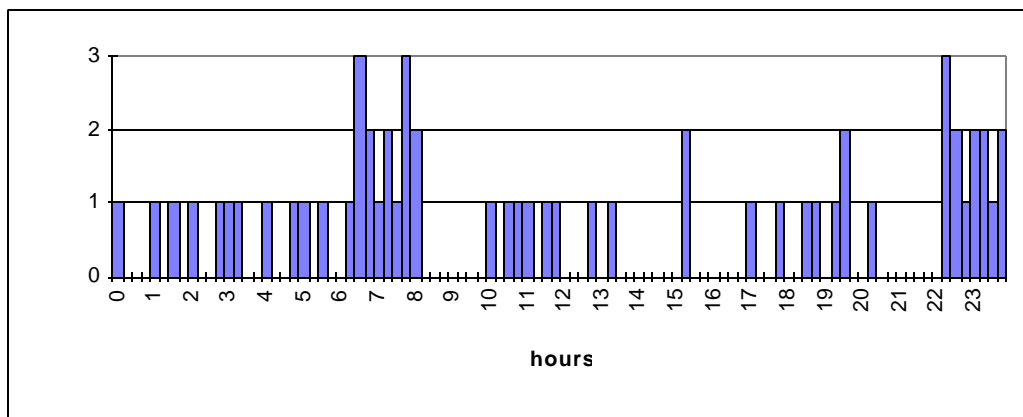


Figure A.7: GPS to 0 Degree GEO Observability for an Atmosphere Radius of 8,000 km

Even though this is a simple analysis, it can be seen that on average, the opportunity to collect GPS observables on board a geosynchronous satellite exists. While the data flow may not be continuous, it is believed that enough data will be available to perform accurate orbit determination, particularly when combined with improved angular observations.

## B. IGS GPS Precise Orbit Ephemerides

The IGS (International GPS Service for Geodynamics) has seven operational analysis centers which produce high accuracy GPS satellite orbits on a daily basis [58]. At the end of each GPS week, the results of the seven analysis centers are combined to generate the best possible orbit. These combined orbits are reported to be generally better than 20 cm 3-D RSS [59]. A summary file is also produced at the end of the week which reports the accuracy of the given orbits from each analysis center and the combined orbit. Earth rotation files are also produced to describe the body fixed ITRF (International Terrestrial Reference Frame) coordinate system the orbits are based in. The Earth rotation files are essential for the proper transformation of the orbits from the ITRF to the pseudo-body fixed coordinated system used with GTDS and to inertial coordinate systems. The combined data products are issued under the analysis center name of IGS (rapid orbits are given under the name of IGR and predicted orbits are given by IGP).

These products are made available for public distribution on a variety world wide web and ftp sites. Two useful sites are described:

- 1) JPL's IGSCB machine
- 2) Germany's IfAG GIBS web site

NASA Goddard's CDDIS site is a another option but anonymous ftp is not available.

The JPL ftp site is:

*igscb.jpl.nasa.gov*

and the directory for the precise and combined orbits is:

*igscb/product/####/*

where #### is the GPS week. Additional information regarding the JPL IGSCB site is available in the *igscb* directory.

The IfAG site contains a great deal of GPS and GLONASS information and is located at:

The data is stored in the Standard Product #3 (SP3) format. The precise orbit file naming convention is as follows:

Letters	Description
1-3	Analysis Center
4-7	GPS Week Number
8	Day of Week (0=Sunday, 1=Monday, etc.)

A '.sp3' extension follows. The summary files have 7 for the day of week and a '.sum' extension. The Earth rotation parameter files also have 7 for the day of week and a '.erp' extension; these files will be referred to as ERP files in this document.

The SP3 files contain ECEF GPS position data every 15 minutes of GPS time for all GPS satellites. The individual satellites are identified by their PRN number. The format allows for velocity data as well. The SP3 format is described by Reference 60 and the ERP file format is self explanatory with the parameters described in Reference 61. References 62 and 63 relate the satellite's PRN number to their Satellite Vehicle Number (SVN) and provides additional constellation information.

A FORTRAN utility has been created to read the SP3 data files and write the position data to a GTDS observation (OBSCARD) file; the utility is called SP32GTDS. SP32GTDS has options to write the output data in the following coordinate systems:

- 1) International Terrestrial Reference Frame (ITRF)
- 2) Pseudo-Body Fixed (polar motion applied to the body fixed ITRF)
- 3) Instantaneous True of Date (Pseudo-Body Fixed rotated about the Greenwich Hour Angle)
- 4) Mean Equator and Mean Equinox of J2000.0
- 5) Mean Equator and Mean Equinox of B1950.0

With any transformation, the appropriate leap seconds are subtracted from the GPS time tags to convert to the UTC time format used by GTDS. If needed, the position vectors are rotated through the polar motion parameters contained in the ERP file distributed with the data. The polar motion parameters are least-squares fit by a cubic polynomial to obtain a smooth history of polar motion offsets over the data span.

Additional information regarding the ITRF coordinate system, its transformations, and the rest of the International Earth Rotation Service Conventions are available in Reference 64.

To implement the IGS Precise Orbit Ephemerides into Ops GTDS, the Instantaneous True of Date option is used. To implement the IGS Precise Orbit Ephemerides into DGTDS, the Pseudo-Body Fixed option is used.

## **C. Software Modified and Developed**

To support this research, several changes were made to the DGTDS software package and several standalone FORTRAN utilities were built. These software modifications and new tools are described here.

### **C.1 DGTDS Modifications**

DGTDS was described in Section 2.2.3 and was primarily used for the Space Surveillance simulation studies. In addition to the simulation studies, DGTDS was used to produce two-line element sets that point the Raven telescope during tracking. DGTDS was also modified to support some GPS analysis that was not completed in time to be included in this work. This section gives an overview of the modifications to the code which supported this effort. More detailed information and documentation has not been published but is available through the author at the Air Force Research Lab.

#### **C.1.1 OUTTLE Card**

The Raven telescope control and pointing software, The Sky by Software Bisque, uses NORAD Two-Line Element sets (TLE's) to locate satellites. Since DGTDS supports the NORAD theories that produce TLE's, an output option was created to allow DGTDS to output TLE's. This allows the AFRL Astrodynamics Team to produce their own element sets for use with the Raven telescope. The software modifications required changes to seven subroutines and the creation of one new subroutine. The TLE output is controlled via a new GTDS input card called OUTTLE.

#### **C.1.2 Optical Data Types in Data Simulation Program**

Prior to this work, DGTDS did not support optical data types, right ascension, declination, and hour angle, in the data simulation program. This capability was required to perform the space surveillance portion of this research. Only two subroutines required modification to include the optical data types in the data simulation program.

#### **C.1.3 GPS Observation Simulation and Processing Models**

One of the original goals of this effort was to include analysis on the use of GPS observations in the geosynchronous orbit regime. The focus of the research shifted away from this goal, however, and an in depth treatment of this research area. However, plans were made to incorporate GPS observation models into the DGTDS Differential Correction, Filter, and Data



Simulation programs. This requires the development of several new subroutines and the modification of over 20 existing DGTDS routines. While the modifications were not completed, the architecture was successfully implemented in the Differential correction program and is being tested. Once the modifications are completed in follow-on work, the results will be presented in a public forum

#### **C.1.4 PHLUID4 GTDS**

PHLUID4 GTDS stands for the Phillips Lab User Interface Developed for GTDS [57]. PHLUID4 is a text-based, menu-driven user interface that controls the functions of GTDS. Prior to the development of PHLUID4, GTDS was primarily executed through the use of scripts which required manual changes to support various functions of GTDS. PHLUID4 has been developed to support both Draper GTDS in the DOS environment and Ops GTDS in the UNIX environment. The user interface makes executing the GTDS programs much easier and also helps maintain organization through file naming conventions. PHLUID4 DGTDS is comprised of over 100 files containing DOS batch files and FORTRAN utilities; PHLUID4 DGTDS also contains 71 template input decks. PHLUID4 Ops GTDS is comprised of almost 60 files containing UNIX scripts and FORTRAN utilities; PHLUID4 Ops GTDS also contains 16 template input decks. No GTDS code changes were required.

## **C.2 Stand-alone Utilities**

Several stand-alone utilities were created during the course of this research. Many were designed for format changes of observation and data files while others were designed for specialized functions or to ease repetitive processes. All utilities were written in FORTRAN 77.

### **C.2.1 CONIGS**

CONIGS stands for convert IGS and is a format conversion program designed to support the GPS architecture in DGTDS. The GPS architecture in DGTDS requires a data file containing position vectors and clock terms of the satellites in the GPS constellation. CONIGS converts the precise orbit ephemerides of the IGS in SP3 format into the DGTDS GPS constellation ephemeris data file format. CONIGS also performs a coordinate transformation from the ITRF system to the pseudo-body fixed ECEF system in GTDS by rotating through the IGS polar motion parameters.

### **C.2.2 CORNXO**

CORN XO stands for convert Rinex observations and is another format conversion program used to support the GPS architecture in DGTDS. The utility takes Rinex observation files and converts the GPS observations into GTDS OBSCARD files. GTDS OBSCARD files are used to input observations into GTDS. In addition to the change in format, the observation time-tags are changed from GPS time to UTC time by subtracting the appropriate number of leap seconds.

### **C.2.3 GEOOBS**

GEOOBS stands for geosynchronous observability and is the utility used to calculate the observability of geosynchronous satellites to the GPS constellation. This utility was used to determine the information presented in Appendix A.

#### **C.2.4 GPSCAL**

GPSCAL stands for GPS calibration and is basically a GTDS input deck builder for a specific purpose. IGS precise orbit ephemerides of the GPS constellation are used to calibrate the Raven telescope. As part of this calibration process, fits are made to the IGS ephemerides using GTDS to determine the best GTDS representation of the GPS orbits. The GTDS representation of the GPS orbit is then compared to the Raven observations. GPSCAL reads the first two position vectors from a GTDS OBSCARD file containing the IGS precise orbit ephemeride for a GPS satellite, and uses Gauss's solution to the Lambert problem to estimate the velocity at the first data point. The position and velocity are then used to construct a GTDS input deck to fit to the GTDS OBSCARD file containing the GPS precise orbit.

#### **C.2.5 GPSGUESS**

GPSGUESS is a lot like GPSCAL except that instead of building an input deck to produce the best GTDS representation of the GPS orbit, it produces an input deck designed to produce a two-line element set representing the GPS orbit. This two-line element set can then be used to point the Raven telescope.

#### **C.2.6 GPSTIME**

GPSTIME converts a time tag in calendar form (year, month, day, hour, minute, second) to GPS week, day of week, and second of week. The IGS precise orbit ephemerides of the GPS satellites are stored in terms of the GPS week and day of the GPS week. This utility makes locating the proper file much easier.

#### **C.2.7 GOA2GTDS**

GOA2GTDS stands for Gipsy-Oasis II to GTDS and is another format conversion utility. Another source of precise orbit ephemerides for the GPS constellation is the Jet Propulsion Laboratory (JPL). JPL produces precise orbits for the GPS constellation on a daily basis using the Gipsy-Oasis II orbit determination package. GOA2GTDS converts the JPL products to GTDS OBSCARD files which are used to input observations to GTDS. In addition to the format change, GOA2GTDS also rotates the position and velocity vectors from the J2000 coordinated system into the B1950 frame.

#### **C.2.8 OSCON**

OSCON is another format conversion program designed to take the geosynchronous satellite radio transponder data described in Section 2.4.1.1 and convert it to a GTDS OBSCARD file. In addition to the format changes, OSCON also performs unit conversions.

### **C.2.9 RAVROT**

RAVROT stands for Raven rotation and is used to take GTDS OBSCARD files containing right ascension and declination observations in the J2000 coordinate system and rotate them into the B1950 frame. The version of DGTDS used in this analysis does not support the J2000 system and RAVROT allows Raven observations to be processed with DGTDS.

### **C.2.10 SP32GTDS**

SP32GTDS is used to convert IGS precise orbit ephemerides in the SP3 format to GTDS OBSCARD files. GTDS OBSCARD files are used to input observations into GTDS. SP32GTDS outputs the precise orbit ephemerides in five different coordinate systems:

- 1) International Terrestrial Reference Frame (ITRF)
- 2) Pseudo-Body Fixed (polar motion applied to the body fixed ITRF)
- 3) Instantaneous True of Date (Pseudo-Body Fixed rotated about the Greenwich Hour Angle)
- 4) Mean Equator and Mean Equinox of J2000.0
- 5) Mean Equator and Mean Equinox of B1950.0

With any transformation, the appropriate leap seconds are subtracted from the GPS time tags to convert to the UTC time format used by GTDS. If needed, the position vectors are rotated through the polar motion parameters contained in the ERP file distributed with the data. The polar motion parameters are least-squares fit by a cubic polynomial to obtain a smooth history of polar motion offsets over the data span.

## DISTRIBUTION LIST

DTIC/OCP

8725 John J. Kingman Rd, Suite 0944

Ft Belvoir, VA 22060-6218 1 cy

AFRL/VSIL

Kirtland AFB, NM 87117-5776 1 cy

AFRL/VSIH

Kirtland AFB, NM 87117-5776 1 cy

**Official Record Copy**

AFRL/DEBI/DR. Chris Sabol 2 cys

AFRL/DES

Kirtland AFB, NM 87117-5776 1 cy

AFRL/DEBE

Kirtland AFB, NM 87117-5776 1 cy